SPATIAL AND TEMPORAL HABITAT USE BY BIOLUMINESCENT MARINE OSTRACODS

A Dissertation

Presented to the Faculty of the Graduate School

of Cornell University

In Partial Fulfillment of the Requirements for the Degree of

Doctor of Philosophy

by

Gretchen Anne Gerrish

May 2008

SPATIAL AND TEMPORAL HABITAT USE BY BIOLUMINESCENT MARINE OSTRACODS

Gretchen Anne Gerrish, Ph. D.

Cornell University 2008

Throughout the Caribbean, there exists a diversity of nocturnal ostracod species that conduct nightly bioluminescent courtship displays over seagrass bed and reef habitats. Identification and naming of these species began as early as 1975 and since then, researchers have focused on the chemistry and behaviors associated with their bioluminescence displays. However, minimal knowledge of their basic ecology exists in the current literature. Here, I develop the natural history of the seagrass bed inhabitant, *Vargula annecohenae.* First, I describe the three to four month life cycle of this bioluminescent marine ostracod, which consists of an initial 18.4 ± 0.52 days of embryonic development, approximately 20 day duration for each of five juvenile instars, and maximum survival of 180 days for adults. Second, I quantify the activity of each age class in relation to lunar light. The foraging behavior of juveniles does not change based on the intensity of lunar light, however adult foraging and courtship behaviors are significantly reduced by the presence of anything greater than a third of a moon illuminating the sky. Third, I use the life cycle and activity information in modeling dispersal for *V. annecohenae* across a heterogeneous 12.2 x 3.6 km portion of seagrass bed habitat. Models based on mark and recapture studies indicate males could move as far as 390 m in their lifetime meaning genetic differences across a distance of 12.2 km would be unlikely if the habitat was continuously suitable and homogenous. However, highly significant genetic differences were observed within the 12.2 km by 3.6 km region of study. Analyses of habitat variables (water velocity,

water depth, seagrass density) in a geographic information system (GIS) indicate that physical barriers to dispersal influence gene flow within this system. Finally, I asked whether habitat constraints acted upon other species of bioluminescent ostracods by measuring the spatial and temporal differentiation of courtship displays in three coexisting reef species. Despite some overlap, each species displayed in a specific microhabitat, initiated its display and peaked in display density at places and times distinct from those of the other two species.

BIOGRAPHICAL SKETCH

Gretchen Gerrish was born in West Lafayette, IN on October 22, 1976 to Steve and Anita Gerrish. During childhood, her family lived in multiple areas throughout the midwest following the employment opportunities of her father, an agricultural geneticist. She credits him with her early scientific development, having begun working in his seed corn nursery and drawing maize genealogies in her early teens. Her family finally settled in Elkhorn, Wisconsin where she finished high school. Following high school, Gretchen attended Lawrence University in Appleton, WI, from which she received her bachelor of arts in 1998. While at Lawrence, she was mentored by Dr. Bart DeStasio, who introduced her to both marine and freshwater aquatic ecosystems. During her undergraduate, she spent two summers at the University of Wisconsin, Trout Lake Field Station; first working on comparative techniques for quantifying algal densities and second studying the impacts of experimental whole lake acidification on the dormant stages of *Daphnia*. During her time at Lawrence University, she also met her future husband, Benjamin Zagorski. Gretchen continued her education at the University of Illinois, Champaign-Urbana, with Dr. Carla Cáceres, receiving her masters in Natural Resources and Environmental Science in 2001. She then headed to Cornell University to pursue her doctoral degree where she maintained her freshwater roots through interactions with the lab of Dr. Nelson Hairston Jr. and by mentoring Cornell undergraduates at Shoals Marine Laboratory. The focus of her dissertation research was conducted in the tropical reef habitats of Belize on bioluminescent ostracods, a system to which she was introduced by Dr. James Morin. In early 2007, Gretchen took a position at the University of Notre Dame as Assistant Director of UNDERC West and just prior to the completion of this dissertation, Gretchen gave birth to her first child, Luke Zagorski, on November 18, 2007.

ACKNOWLEDGEMENTS

My greatest thanks extend to my co-advisors, Dr. James Morin and Dr. Nelson Hairston. Dr. Morin excitedly shared his research system with me and demonstrated how one can maintain a youthful excitement about science through the education of others and through new discoveries. I am grateful for all his assistance in planning, executing and presenting my dissertation research. Dr. Hairston taught me to broadly apply my research and through his support of my studies, demonstrated that multiple perspectives are absolutely essential in conducting and presenting science. Additionally, Nelson is an amazing editor and I thank him for his time spent on my writings and in educating me to be a better writer. My committee consisted of Dr. Morin, Dr. Hairston and Dr. Amy McCune. I thank Dr. McCune for her perspective on the research I conducted and for her support throughout. Most of all, I thank my committee for making my time and education at Cornell an extremely enjoyable experience.

Many additional people contributed to my positive experience at Cornell. Overall, I would like to thank the people, staff, faculty and students of the EEB department for making the community one that is incredibly unique in its open and interactive nature. Specifically, I thank Colleen Kearns for all her assistance in the field and in the laboratory. I thank the Hairston and Morin Lab members for their constructive feedback on my data and project planning. I thank my office mates, Vikram Iyengar, Rulon Clark, Marie Nydam, Jamie Mandel, for their unending scientific and non-scientific education. I especially thank Krystal Rypien who spent time assisting me in the field, read manuscript drafts, discussed ideas and who is a great friend and colleague.

My greatest appreciation also extends to the people at the International Zoological Expedition facility on South Water Caye. Jennifer Hall and Jon

MacDougal provided numerous essential resources; people, equipment, emotional support, facilities, without which this research would have proved much more difficult and much less enjoyable. I also thank the staff at IZE for their support, specifically, Michael Pipersburg, Victor Escobar, and Pete Avilez who assisted me extensively in my field work.

I thank my funding sources which include, Sigma Xi, the Mario Einaudi Center for International Studies, the Orenstein Fund, Lerner Grey Fund for Marine Science, and the Andrew W. Mellon Foundation. I further thank the Belize fisheries department for their support of my research through granting annual collection and research permits.

Finally, I thank my family for their support. Thanks to my father, Steve Gerrish, for bringing out the scientist in me from a young age and continuing to share my interests as I have grown. Thanks to my mother, Anita Gerrish, for being there whenever I need her. That security is invaluable. Thanks to Jeremy, Rachel, Aaron and Parker for making home a place worth going. Thanks to Luke Zagorski for a new perspective on life. And my most heartfelt thanks to my husband, Benjamin Zagorski who has toiled with me day in and day out in the good and bad parts of all aspects of the pursuant of this degree.

TABLE OF CONTENTS

LIST OF FIGURES

LIST OF TABLES

CHAPTER 1

THE LIFE CYCLE OF A BIOLUMINESCENT MARINE OSTRACOD, VARGULA ANNECOHENAE (CYPRIDINIDAE, MYODOCOPIDA)

ABSTRACT

We present the first complete life cycle description for a marine ostracod that uses bioluminescence for courtship. The life cycle of *Vargula annecohenae* consists of five juvenile instars separated by molts and an adult instar following the terminal molt. Body size is tightly conserved within each instar; therefore, most instars can be reliably identified to instar by the length-to-height regression of carapace size. Sexual dimorphism becomes apparent in the penultimate A-I instar and remains evident through adulthood. Each juvenile instar of *V. annecohenae* lasts between 10 and 27 days, resulting in an estimated total juvenile development time of three months. Females have multiple broods and give birth to crawl-away juveniles following a 26 ± 1.6 day incubation period. Adults live up to 188 additional days, and thus *V. annecohenae* has a potential life span of up to nine months. This species is one of the large number of myodocopid ostracod species that use bioluminescence for courtship, and our description of its life cycle provides a foundation for future work on the intricate mating systems and the complex ecological interactions within this group.

KEY WORDS: bioluminescence, ostracod, life cycle, myodocopid, instar, life history

INTRODUCTION

Research into the ostracod order Myodocopida has yielded evidence for an origin of the compound eye independent from that of other arthropods (Oakley 2005). Additionally the group has provided key information regarding the evolution of

complex bioluminescent courtship behaviors (Morin 1986, Morin and Cohen 1991, Rivers and Morin in press). With over 6,000 species of described myodocopids distributed globally, this group is a diverse and abundant member of numerous marine benthic communities. However, life cycles from laboratory rearing have been published for only three species within this group, *Philomedes brenda* (Elofson 1969), *Skogsbergia lerneri* (Cohen 1983), and *Vargula hilgendorfii* (Henmi and Okamato 2003). In addition, life histories and development times of a limited number of species have been described based on seasonal field sampling and length-width regressions of multiple instars (see review in Cohen 1983). Within the Myodocopida, the Cypridinidae range in size from 0.8 mm to 3 cm and inhabit numerous diverse marine habitats ranging from the deep sea (> 5,000 m depth) (Poulsen 1962), to shallow tropical coral reefs and seagrass beds (Cohen 1983) and low to high-latitude littoral regions (Kornicker 1975). Across this diverse range of habitat, life cycles likely vary in response to seasonal changes, physical habitat constraints, and biological selection.

Here, we present the life cycle of the bioluminescent grassbed ostracod, *Vargula annecohenae* Torres and Morin (2007). Similar to *Skogsbergia lerneri*, *V. annecohenae* feeds on dead and decaying fish and invertebrates in the mieobenthos of *Thalassia*-dominated tropical seagrass beds. At times, both *S. lerneri* and *V. annecohenae* can be captured simultaneously in baited feeding traps. The most apparent difference between these two species is that males of *V. annecohenae* enter into the water column nightly to produce bioluminescent displays to attract conspecific females whereas *S. lerneri* is not luminescent (Morin and Cohen 1991, Cohen and Morin, 2003, Gerrish et al. *submitted*). Bioluminescence in ostracods has been proposed to have evolved initially as a defensive response, either as a warning to predators that the ostracod tastes bad or as part of a "burglar alarm" system (Morin

1986, Morin and Cohen 1991). Numerous *Vargula* species throughout the world, e.g. *V. hilgendorfii* in Japan (Henmi and Okamoto 2003), are capable of producing light for defense, but only in the Caribbean do *Vargula* species and other genera within the same clade also use bioluminescence as part of their intricate courtship displays. The life cycle of *V. annecohenae,* presented here, is the first reported for an ostracod that uses bioluminescence for courtship and, through comparison with other myodocopids, provides insight into whether the unique mating system of ostracods with bioluminescent courtship displays is associated with variation in basic life history characteristics.

MATERIALS AND METHODS

Vargula annecohenae Torres and Morin (2007) is a small-bodied (~2 mm) bioluminescent ostracod (Crustacea: Ostracoda: Myodocopa: Cypridinidae) that is found in high abundance (> 500 / m^2) in shallow grassbeds surrounding islands on the Belize barrier reef. Like most cypridinid ostracods, *V. annecohenae* remains primarily on or in the sea bed; however, adult males enter the water column nightly, where they produce bioluminescent displays to attract females (Morin and Cohen 1991). For the present life cycle analysis, *V. annecohenae* were collected just off the south beach of South Water Caye, Belize (N 16º48'45", W 88º04'57.5") at ~1.5 m water depth where turtle grass (*Thallasia testudinum*) dominated the substratum. To gather ostracods, live traps, which consisted of cylindrical polyvinyl chloride (PVC) tubes (7 cm long × 3.8 cm diameter) containing inverted mesh funnels of 75 μm nylon mesh, were placed at the sediment water interface. Each trap contained a piece of dead fish flesh (≈ 1 cm^3) to attract scavenging ostracods. We measured carapace length and height (Figure 1.1) of 593 live individuals to develop size classifications for all instars of *V. annecohenae*. In addition, the widest part of the pigmented portion of the eye and the

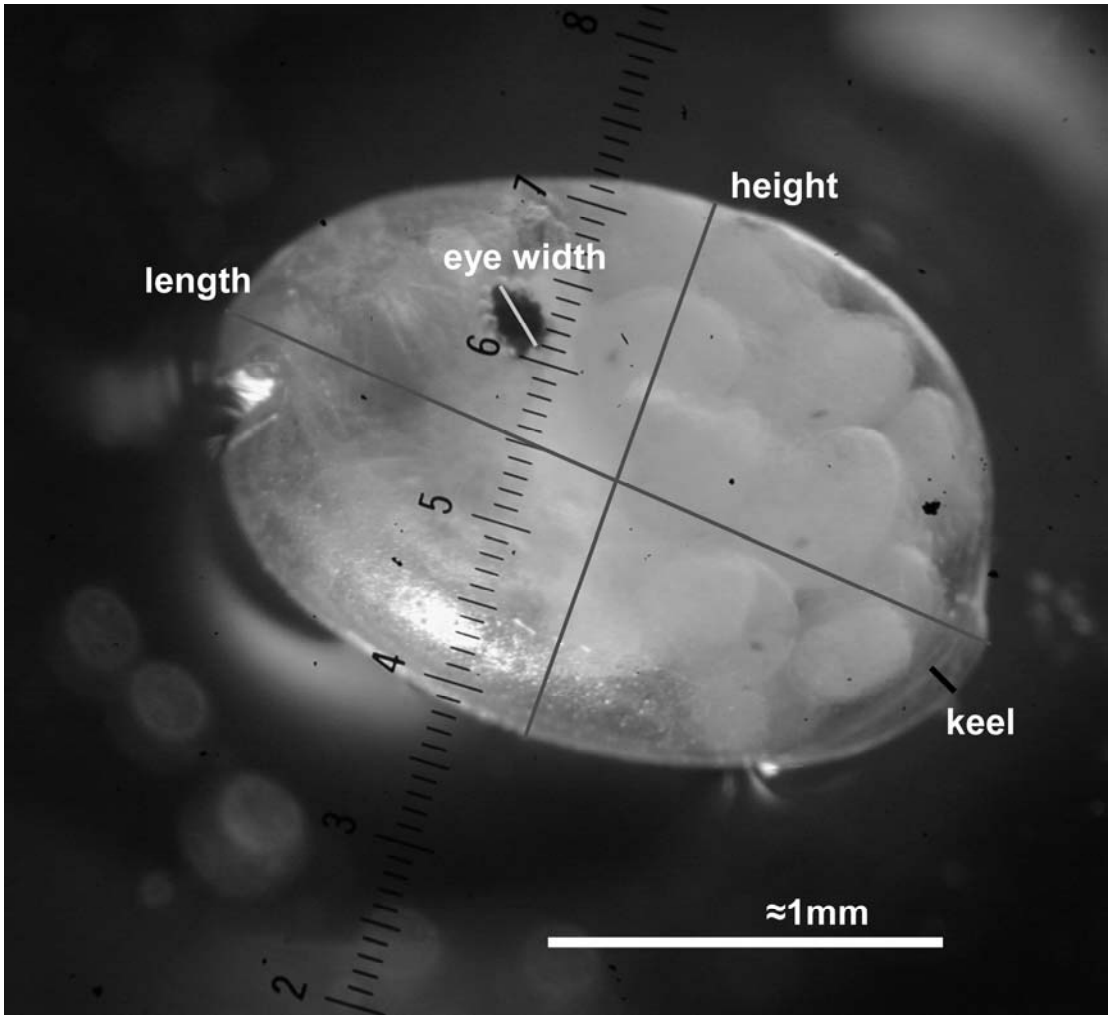

Figure 1.1. *Vargula annecohenae*, brooding female, with red lines representing axes for measurements of carapace length and height, and eye and keel width. Precise placement of axes on a given specimen was done so as to maximize their length.

widest part of the keel (Figure 1.1) were measured for some individuals of each instar. These measurements were used to characterize sexual dimorphism in A-I instars and adult individuals. Because there was some overlap in the length-to-height regression of adult male instars and sub-adult (A-1) females, we used a discriminant function analysis (DFA: SYSTAT 9.0) that included length, height, eye size, and keel width to differentiate quantitatively the males and females of the A-I and adult instars. We photographed live individuals of all instars using a Nikon Coolpix 4500 camera held to the eyepiece of a Wild M5 dissecting microscope at 25x magnification. To calculate the timing and duration of development, individuals of each size-class were placed into separate 10 ml wells of a 12-well tissue-culture tray and monitored through successive molts and reproductive stages. In January, February, and March, 2002, 20-30 individuals from each age class were monitored first for 10 days in Belize, while being fed on Tetramin fish flakes (ProCare™) every 2 days and cultured at ambient temperature (26 ± 2º C). The water was changed after every feeding. The individuals were then transported in a single day to our laboratory at Cornell University in Ithaca, New York where they were maintained in artificial seawater (Instant Ocean ® Sea Salt) at 36 g/L salinity, placed on a 12-hour light-dark cycle, kept at a constant temperature (26º C) and fed Tetramin fish flakes *ad libitum* every 2 days through the duration of their development. Similarly, from January through early March, 2003, at South Water Caye in Belize, except when low numbers of particular (early) age classes precluded doing so, 24-36 individuals of each age class were maintained in laboratory cultures using natural seawater at a constant (26º C) temperature, and fed freshly dead fish every two days. All individuals were monitored at least every other day for molting, brooding, release of offspring, and mortality. In addition, length and height were recorded pre- and post- molt for all individuals.

The duration of each instar was calculated in two ways. Field-collected individuals of a known age class were placed as a group in culture, and the time from collection to individual molt was recorded. Individuals molted constantly, creating a linear relationship between the numbers of animals molted over time for each instar. Based on this relationship, the duration of the instar was calculated as the time at which the line fitted to a plot of molt occurrence reached 100% of all individuals molted. Additionally, some individuals of each instar were maintained through multiple instars in the laboratory, and the entire duration of each instar was recorded. There was no difference in the estimates of development time between the animals cultured in Ithaca in early 2002 and those cultured in Belize in 2003; therefore, data from these studies were pooled for analysis.

Female reproductive traits such as time from mating to production of brood, time from brood production to hatching, and time between clutches and number of clutches in a lifespan were determined based on females in laboratory cultures. Gestation period was measured similarly to instar duration by using field-collected individuals with unknown impregnation times. Additionally, virgin females (which were cultured from the immature A-I stage) were impregnated by males under laboratory conditions and monitored as embryos developed. We used a Canon Digital Rebel XTI camera with 2.5x lens mounted on a Olympus model BH2-RFC dissecting microscope at 4.7x magnification to photo-document embryonic development within brooding *V. annecohenae*.

RESULTS

Vargula annecohenae has six instars and exhibits determinate growth. Each instar has a highly conserved size range (Figure 1.2; Table 1.1). Based on length-to-height regression, we can confidently identify ostracods of the first four instars (A-V,

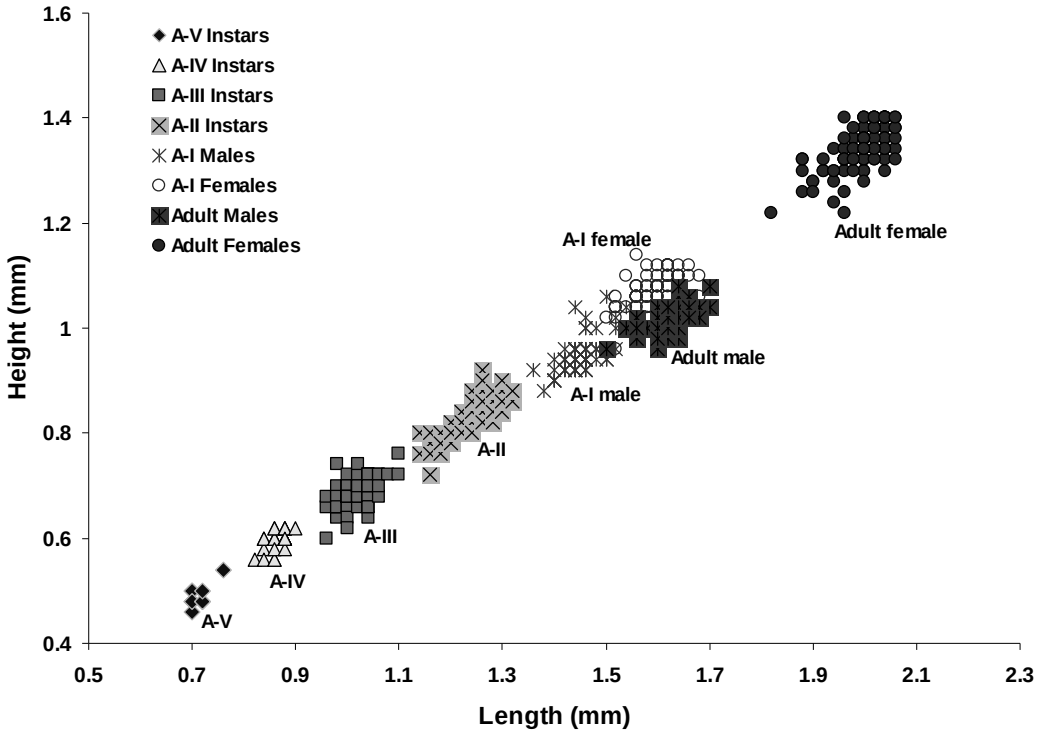

Figure 1.2. Relationship between carapace length and height for *V. annecohenae* (N=593), showing distinct groupings for early instars. Adult females and A-I males are also distinct groups but adult males and A-I females overlap somewhat in length to height ratios.

Table 1. Measurements of each instar of *Vargula annecohenae* ± 1 sd.

Instar	N carapace size	Carapace length (mm) ± sd	Carapace height (mm) ± sd	N eye & keel size	Eye width (mm) ± sd	Keel width (mm) ± sd
A-V	10	0.712 ± 0.019	0.490 ± 0.022	2	0.070 ± 0.000	0.030 ± 0.000
A-IV	24	0.865 ± 0.019	0.596 ± 0.020	2	0.085 ± 0.007	0.040 ± 0.000
A-III	84	1.017± 0.028	0.688 ± 0.026	5	0.102 ± 0.008	0.050 ± 0.010
A-II	104	1.231 ± 0.042	0.826 ± 0.037	7	0.117 ± 0.011	0.053 ± 0.010
Male A-I	74	1.449 ± 0.033	0.948 ± 0.033	8	0.166 ± 0.016	0.069 ± 0.011
Female A-1	86	1.596 ± 0.039	1.070 ± 0.032	14	0.135 ± 0.013	0.063 ± 0.009
Adult Male	105	1.624 ± 0.035	1.020 ± 0.023	17	0.222 ± 0.013	0.077 ± 0.006
Adult Female	106	1.994 ± 0.047	1.344 ± 0.042	13	0.171 ± 0.016	0.082 ± 0.012

A-IV, A-III, A-II), fifth instar males (A-I), and adult females. Some overlap occurred between adult males and sub-adult females (A-I) (Figure 1.2). This region of overlap can be resolved visually (Figure 1.3), and also by means of a discriminant function that incorporates data on eye size, keel width, and valve length and height of A-I females and adult males. Using three factors, A-I males and females, and adult males and females were always categorized correctly ($p < 0.001$). Factors 1 and 2 were primarily associated with length and height while factor 3 incorporated more influence of eye size and keel width (Table 1.2). A-1 females have a higher carapace, smaller eyes and a narrower keel than adult males (Table 1.1). The two can be readily distinguished visually with the use of a dissecting microscope (Figure 1.3). Sexual dimorphism becomes apparent in the size and shape of the fifth instar as well as in the copulatory limb in males (Torres and Morin 2007), and remains apparent throughout the adult stage (Figure 1.2 and Figure 1.3).

Inseminated females that contained eggs within their bodies were commonly captured in feeding traps, but we never captured females that had released fertilized embryos into their brood chambers. The overall development time of ostracod eggs and embryos within the females was 26 ± 1.6 days, with the interval between mating and brood deposition averaging 7.84 ± 1.06 (n=31) days, and the subsequent time to release from the brood chamber averaging 18.4 ± 0.52 (n=33) days. During development, eggs initially become visible inside the body of the female (Figure 1.4a, see arrow). Daily observations indicated that the eggs increase in size but display no other visible morphological changes while inside the mother's body. If reproduction is similar to that of other myodocopid ostracods, it is likely that fertilization occurs as the eggs move from the female's body into the marsupium (Cohen and Morin 1990). Females release fertilized embryos into the marsupium (brood chamber) as transparent, spheroidal or ovoidal masses (Figure 1.4b). After two to three days, the

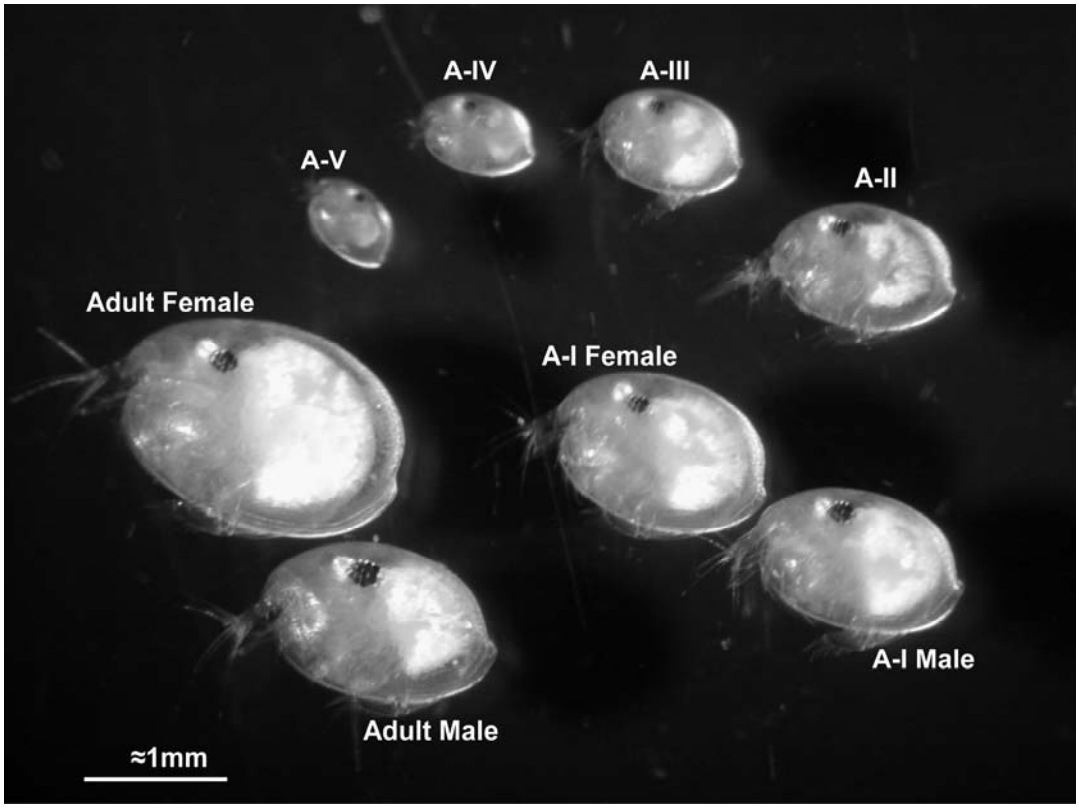

Figure 1.3. Instars of *V. annecohenae*. Photos are of live individuals with separate males and females for stage A-I and adults; sexual dimorphism is apparent.

Table 1.2. Canonical discriminant functions, standardized by within-instar size variances, were used to partition A-I males and females, and adult males and females, with 100% accuracy.

Function	1	2	3
Carapace length	0.478	0.901	0.647
Carapace height	-1.171	-0.043	-0.779
Eye width	0.888	0.267	-0.525
Keel width	-0.016	0.184	0.763

Figure 1.4. Developmental sequence for brooded embryos of *V. annecohenae*. Embryos are held in a marsupial brood pouch located in the posterior dorsal part of the carapace. a) Egg fertilization is internal and the embryos begin developing and increasing in size while inside the body of the female. One egg of this female has been released into the marsupium and the remaining four eggs are visible within the ovary of the female. b) After 7-8 days, the eggs are extruded into the marsupial brood pouch. At this time each egg consists of a large yolk mass and the cells inside are barely visible. c) By day nine in the brood pouch, cell division has created a defined, cloudy cellular mass that fills the egg. d) As the embryo develops its organs, the first apparent structures include the naupliar eye, here a red speck, and the gut. e) Just prior to release, the embryos appears as A-V instars with a large brown eye spot and a fully developed and functioning light organ. All photos are of live individuals.

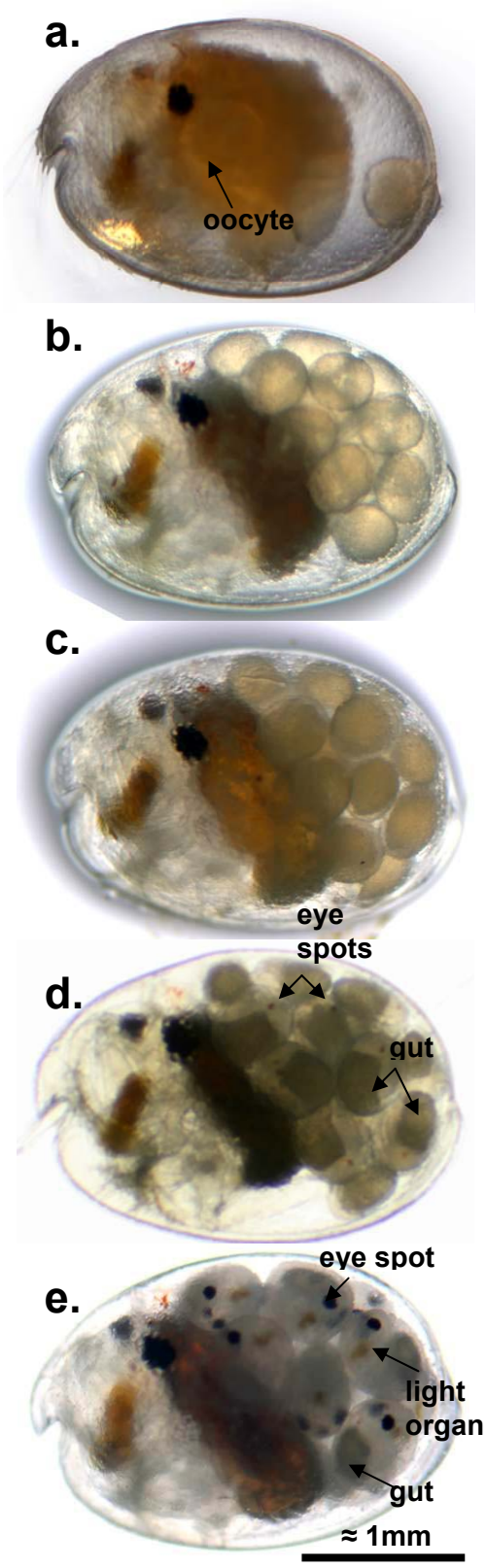
a.
oocyte
b.
c.
eye
spots
d.
gut
eye spot
e.
light
organ
gut
≈ 1mm

insides of the embryos appear cloudy compared with the fully transparent embryo initially deposited in the brood chamber. A separation of the cloudy mass, usually more dense on one side than the other, is visible by day nine (Figure 1.4c). Faint, red-pigmented eye spots begin forming by day 14 or 15 (Figure 1.4d). Eye spots develop into dark brown spots during the following two days and appear as fully formed eyes by day 17 or 18. The light organ becomes apparent after day 17 as a thin, yellowish crescent above the mouth of each embryo (Figure 1.4e, see arrow) which by this time appear to be first-instar larvae confined within the brood pouch just prior to release (19 days) (Figure 1.4e). The average number of offspring in a brood is 12.9 ± 0.43. Female *V. annecohenae* are capable of producing multiple broods without re-exposure to males, which indicates there is storage of sperm between broods. In three females, new broods were produced 15-17 days following the release of a previous cohort.

After brood release, total development time of juvenile instars (A-V through A-I) took 80 to 100 days and each instar lasted an average of 18.9 ± 0.77 days (Figure 1.5; Table 1.3). On average, 6-8 % of the individuals with the potential to molt did so each day (Figure 1.5). Adults survived up to 188 days in laboratory cultures.

DISCUSSION

Vargula annecohenae has a long life span (up to approximately 1 year), develops slowly (3 months pre-adult), has multiple broods of a few offspring (10-15), and has no free-living larval stage. While *V. annecohenae's* life span does not fall outside the range for the crustaceans reviewed in Hairston and Caceres (1996), its average reproductive life span is near the upper bound of other taxa within its size class (Figure 1.6). Other species that deviate in a similar manner include many malacostracans, which, like *V. annecohenae,* are primarily benthic. Because organisms that spend a majority of time in the benthos have a permanent refuge and

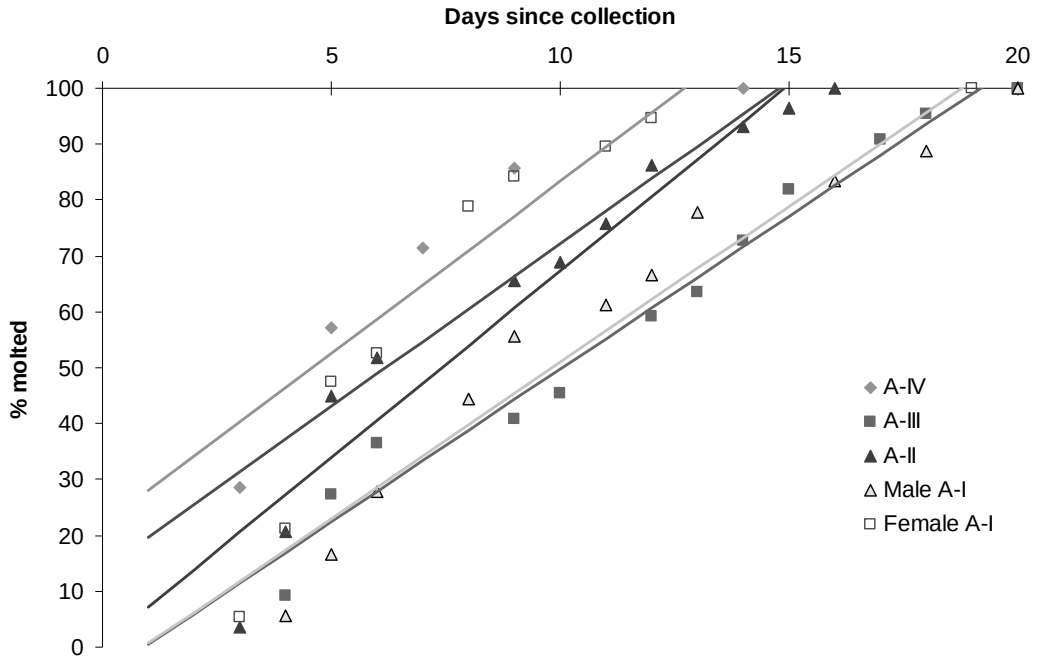

Figure 1.5. Cumulative percentage of individuals that molted per day for each instar of *V. annecohenae* collected in the field and held in the laboratory. No data are shown for instar A-V due to low sample size.

Table 1.3. Instar durations of *V. annecohenae*: A) from animals maintained in culture for an entire instar (i.e., through at least two molts), and B) based on the x-intercept of the linear regressions in Figure 1.5.

	A.			B.	
		Duration	**Mean duration**		**Duration**
Instar	**N**	**Range (days)**	**(days ± 1 sd)**	**N**	**Estimate (days)**
A-V		**NA**	**NA**		**NA**
A-IV	**1**	**22**	**22**	**7**	**13-14**
A-III	**3**	**10 to 17**	**14.7 ± 4.04**	**22**	**19-20**
A-II	**10**	**16 to 27**	**19.7 ± 3.50**	**29**	**15-16**
A-I	**16**	**10 to 26**	**19 ± 4.05**	**39**	**15-20**
(Male A-I)		**NA**	**NA**	**18**	**19-20**
(Female A-1)		**NA**	**NA**	**19**	**15-19**
Overall	**30**	**10 to 27**	**18.9 ± 3.97**	**97**	**13-20**

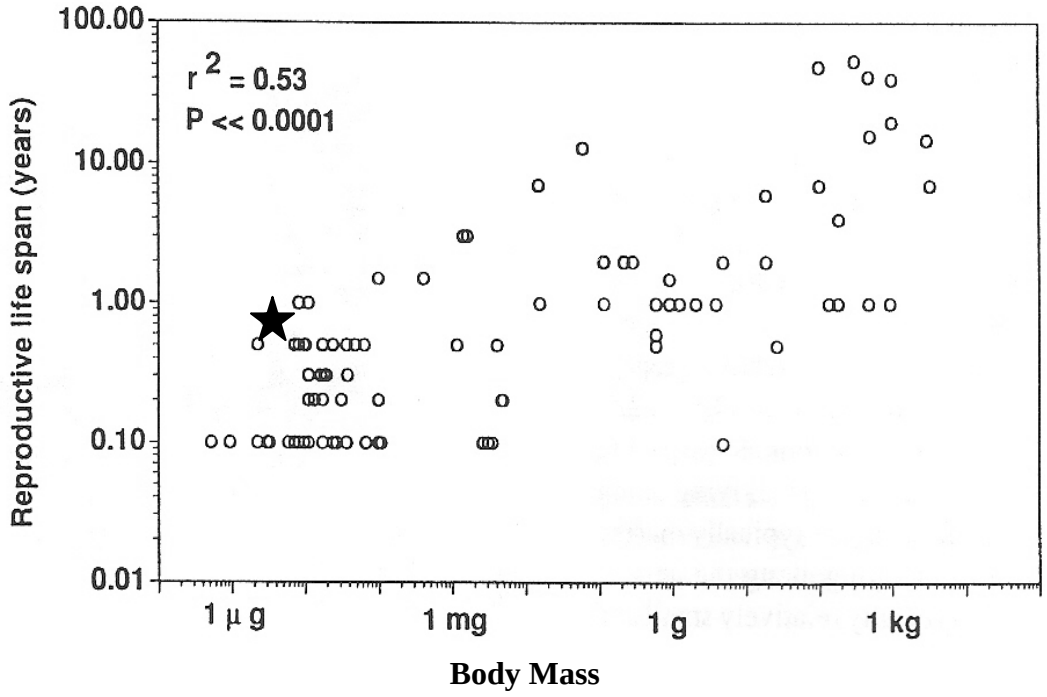

Figure 1.6. Revised from Hairston and Cáceres (1996 Fig. 2). The approximate position of *V. annecohenae* on the regression of reproductive life span vs. body size is indicated by the star and falls at the upper end of all species of its size range.

often feed on detrital matter, it is possible that their longer life span allows for a gradual accumulation of needed nutrients without selective pressure for faster maturation from the numerous predators present in the water column.

The life cycle of *V. annecohenae* is similar to those of previously described, myodocopid ostracods. As in all known myodocopids, *V. annecohenae* broods embryos and releases them as first-instar (A-V) crawl-away juveniles. The 18.4-day average duration of brooding is within the range observed for other cypridinids (10-30 days) (Cohen and Morin 1990) and similar to that of *Skogsbergia lerneri* (Cohen 1983) but slightly longer than the 16 day duration for *V. hilgendorfii* (Wakayama 2007). The stages of embryonic development also correspond to those observed in *V. hilgendorfii* (Wakayama 2007). In comparison with the eight instars of the podocopids; myodocopids, including *V. annecohenae,* exhibit a six instar life cycle. Development time through the juvenile stages varies across a range similar to that of *S. lerneri* (Cohen 1983) and is representative of the shorter development time observed for the Cypridinidae in comparison to other myodocopids, namely the Cylindroleberidae and Philomedidae (Cohen and Morin 1990). Temperature may be responsible for some of the observed developmental duration differences. Cohen (1983) and Wakayama (2007) both observed longer development times under colder conditions and the Cypridinidae that have been surveyed are from more tropical latitudes than any of the Cylindroleberidae or Philomedidae (Cohen and Morin 1990). Females of *V. annecohenae* carry an average of 13 offspring, which is less that the 20-70 observed in *Vargula hilgendorfii* (Nakamura 1954, Henmi and Okamoto 2003) and at the lower end of the 10-22 observed in *Skogsbergia* (Cohen 1983). The maximum adult lifespan observed in culture was 188 days, with 30% of the adults surviving longer than the 63-day maximum observed in *S. lerneri* (Cohen 1983).

Based on the bioluminescent mating displays conducted by males and the highly skewed sex ratio observed in mating populations of *V. annecohenae* (Morin 1986, Morin and Cohen 1991, Rivers and Morin *in press*), we predicted that differences might exist between the life histories of male and females within this species. But our data, when partitioned by sex, do not indicate clear differences between males and females in development time (Figure 1.5). More females did survive longer in culture than males. However, this pattern may be due to the fact that overall, more females were cultured. Further studies focusing specifically on the life history comparisons between the sexes may be able to tease apart sexual variation in life cycle, but our study does not indicate that clear differences exist.

Knowing the life cycle of *V. annecohenae* provides the basis for future studies of the ecology and evolution of this and other bioluminescent marine ostracods. There are numerous undescribed species of bioluminescent ostracods that share the grassbed, sand, and reef habitats throughout the Caribbean (Cohen and Morin 2003). Knowing the life cycle for this representative of the group provides a baseline for future comparative study of life histories of other members of this group and allows examination of the function and adaptive nature of the unique bioluminescent mating behavior.

ACKNOWLEDGEMENTS

We thank Nelson G. Hairston, Jr. and Amy McCune for comments on project development and this manuscript. We also are grateful for field assistance and photography assistance from Krystal Rypien, Colleen Kearns, and Anita Gerrish and support from International Zoological Expeditions on Southwater Caye. Funding sources included the Cornell University Mario Einaudi Fund. This research was completed in accordance with permits received from the Belize Department of Fisheries.

REFERENCES

Cohen A. 1983. Rearing and postembryonic development of the myodocopid ostracode *Skogsbergia lerneri* from coral reefs of Belize and the Bahamas. Journal of Crustacean Biology. 3: 235-256.

Cohen A. and J.G. Morin. 1990. Patterns of reproduction in ostracods: a review. Journal of Crustacean Biology. 10: 184-211.

Cohen A. and J.G. Morin. 2003. Sexual morphology, reproduction and the evolution of bioluminescence in Ostracoda. Paleontological Society Papers 9: 37-70.

Elofson O. 1969. Marine Ostracoda of Sweden with special consideration of the Skagerrak. – Israel Program for Scientific Translations, Ltd. Pp i-v, 1-286. [Translation from German of original 1941 publication].

Gerrish G.A., J.G. Morin, T.J. Rivers and Z. Patrawala. (*submitted*) Darkness as an ecological resource: the role of light in partitioning the nocturnal niche. Oecologia.

Hairston N.G. Jr. and C.E. Cáceres. 1996. Distribution of crustacean diapause: micro- and macroevolutionary pattern and process. Hydrobiologia. 320: 27-44.

Henmi Y. and N. Okamoto. 2002. Life history of the luminescent crustacean *Vargula hilgendorfii* and the occurrence of its crustacean ectoparasite *Onisocryptus ovalis*. Benthos Research. 57(2): 103-111.

Kornicker L.S. 1975. Antarctic Ostracoda (Myodocopina). Smithsonian Contributions in Zoology. 163: 1-720.

Morin J.G. 1986. "Firefleas" of the sea: luminescent signaling in marine ostracode crustaceans. The Florida Entomologist. 69: 105-121.

Morin J.G. and A.C. Cohen. 1991. Bioluminescent displays, courtship, and reproduction in ostracods, pp 1-16. In: R. Bauer and J. Martin (eds.), Crustacean Sexual Biology. Columbia University Press. New York.

Nakamura N. 1954. Study of the ecology of *Cypridina higendorfii*, pp 108-127. In: Japanese Society of Fisheries (ed.), General View of Fisheries. Japanese Association for Advancement of Science, Tokyo.

Oakley T. 2005. Myodocopa (Crustacea: Ostracoda) as models for evolutionary studies of light and vision: multiple origins of bioluminescence and extreme sexual dimorphism. Hydrobiologia. 538: 179-192.

Poulsen E. M. 1962. Ostracoda-Myodocopa, Part 1. Cypridiniformes-Cypridinidae. Dana Reports 57: 1-414.

Rivers T.J. and J.G. Morin (in press) Complex sexual courtship displays by luminescent male marine ostracods. Journal of Experimental Biology.

Torres E. and J.G. Morin. 2007. *Vargula annecohenae*, a new species of bioluminescent ostracode (Myodocopida: Cypridinidae) from Belize. Journal of Crustacean Biology 27:649-659.

Wakayama N. 2007. Embryonic development clarifies polyphyly in ostracod crustaceans. Journal of Zoology. 273: 406-413.

CHAPTER 2

DARKNESS AS AN ECOLOGICAL RESOURCE: THE ROLE OF LIGHT IN PARTITIONING THE NOCTURNAL NICHE

ABSTRACT

Nocturnal behaviors that vary as a function of light intensity, either from the setting sun or the moon, are typically labeled as circadian or circalunar. However, both of these terms refer to endogenous time-dependent behaviors. In contrast, the nightly reproductive and feeding behaviors of *Vargula annecohenae*, a bioluminescent ostracod (Arthropoda: Crustacea) vary in response to light intensity but the cue appears to be an exogenous, physically forced response, independent of time. We measured adult and juvenile activity of *V. annecohenae* throughout lunar cycles in January and June 2003. Overnight and nightly measurements of foraging and reproductive behavior of adult *V. annecohenae* indicated that activity was greatest when a critical 'dark threshold' was reached and that the 'dark threshold' for adult *V. annecohenae* is met when less than a third of the moon is visible or at the intensity of light two to three minutes before nautical twilight when no part of the moon is illuminated. Juvenile *V. annecohenae* were also nocturnally active but demonstrated little or no response to lunar illumination, remaining active even during brightly moonlit periods. In addition to light, water velocity influenced the behaviors of *V. annecohenae*, with fewer juveniles and adults actively foraging on nights when water velocity was high (> 25cm/s).

Our data demonstrate that the strongest environmental factor influencing adult feeding and reproductive behaviors of *V. annecohenae* is the availability of time during which illumination is below the critical 'dark threshold'. This dependence on

darkness for successful growth and reproduction allows us to classify darkness as a resource, in the same way that the term has been applied to time, space and temperature.

KEY WORDS: bioluminescence, ostracod, dark threshold, lunar

INTRODUCTION

Darkness is a resource and an environmental condition that is as important as light to almost all living organisms. In photosynthesizing plants or organisms exposed to UV radiation, periods of darkness allow time for photorepair, during which over-stimulated cells have time to recover and mend (Sutherland 1981, Mitchell and Karentz 1993, Freidberg et al. 1995). Without a period of darkness, these organisms experience reduced growth and lower reproductive success (Britt 1996, Grad et al. 2001). Additionally, because natural light and dark cycles have existed throughout evolutionary time, many organisms have evolved behaviors that are cued by or dependent upon darkness. In both terrestrial and aquatic systems the germination of seeds and hatching of eggs depend on photoperiod cues (Stross and Hill 1965, Aiken 1969, Venable and Lawlor 1980). In marine systems, timing of spawning in corals, fishes and invertebrates often corresponds to specific lunar light conditions (Taylor 1984, Babcock et. al. 1986, Lessios 1991). Nocturnal animals, such as plankton and larval fishes, exhibit increased feeding activity at night when hunting by large visual predators is inhibited (Fisher and Bellwood 2003). Bioluminescent organisms exhibit some of the most apparent adaptations to darkness. For these highly evolved organisms, darkness provides the veil under which their complex reproductive, defensive and communicative behaviors take place.

Bioluminescent organisms represent less than 10% of the fauna in littoral marine communities (Morin 1983), yet their requirement for dark conditions is representative of many of the non-bioluminescent nocturnal organisms that share this habitat. Most bioluminescent organisms use light for defense, to warn predators to stay away or to alarm nearby conspecifics (Morin 1983, Herring 1990, Hastings and Morin 1991). In many of these same species, bioluminescence is used for mate location during courtship and reproductive behaviors (Morin 1983, Herring 1990, Hastings and Morin 1991). The level of darkness required for bioluminescence to be effective depends upon a lower limit of solar, lunar, or artificial illumination (Longcore and Rich 2004, Rich and Longcore 2006). In this sense, the level of darkness acts to partition the habitat that bioluminescent organisms are able to use both temporally and spatially. The same is likely true for all organisms that are crepuscular or nocturnal.

Vargula annecohenae (Torres and Morin 2007) is a bioluminescent ostracod found in sub-tidal grassbeds of the western Caribbean and strongly depends on dark conditions for successful reproduction. During courtship, adult *V. annecohenae* males abandon their mostly benthic life style and swim up in the water column emitting packets of bioluminescent chemicals in a species-specific display pattern that attracts females (Morin and Cohen 1991). These displays are only produced and visible when the ambient light conditions in the grassbeds reach a critical 'dark threshold', which is related to the level of lunar or solar illumination and is well below the light intensities produced by a full moon (Figure 2.1a). To understand fully the role that ambient light and lunar cycling play in the life cycle of this highly abundant resident of marine grassbeds, we monitored foraging and courtship behaviors during two lunar cycles in the grassbeds surrounding South Water Caye, Belize. We proposed three alternative hypotheses to explain the potential relationship between *V. annecohenae* behavior and

Figure 2.1. (a) A general representation of the intensity of darkness each night during the lunar cycle in relation to moon rise and set. For example, on the night following full moon, the period of darkness lasts less than an hour, while on nights nearing the new moon (no visible moon) most of each night is dark. (b) The Dark Threshold Hypothesis: the highlighted area represents *V. annecohenae* activity which is expected to be similar in intensity at any time during which light levels are below the 'dark threshold'. (c) The Circalunar Burst Hypothesis: here depicted for the few days following the full moon, includes one intense burst of activity and then little to no activity for the rest of the lunar cycle. d) The Dark Threshold and Reproductive Potential Hypothesis: increased adult feeding activity and reproductive activity is expected during times when the highest number of reproductively available females is present in the population.

a) Nightly Dark Available

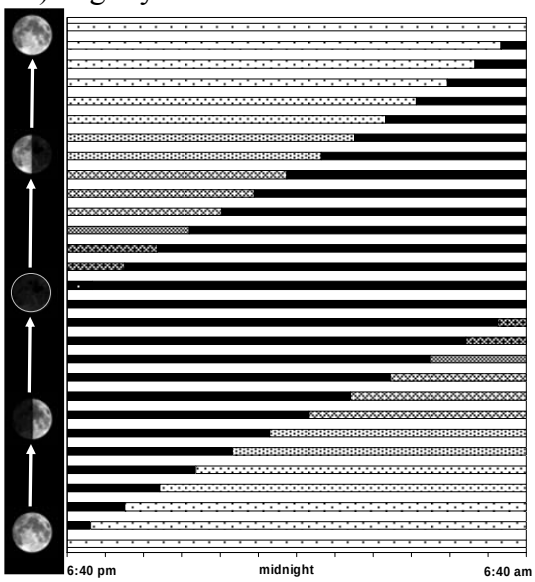

b) The Dark Threshold Hypothesis

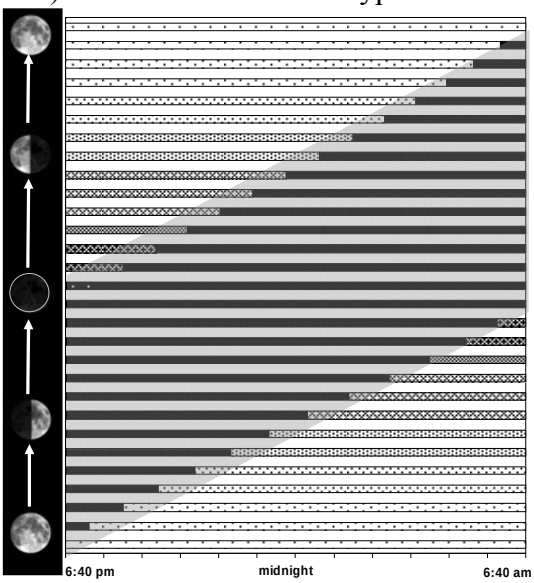

c) The Circalunar Burst

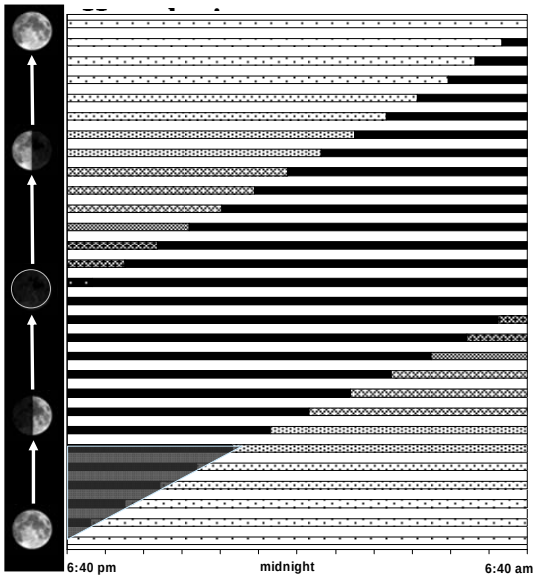

d) The Dark Threshold and Reproductive Potential Hypothesis

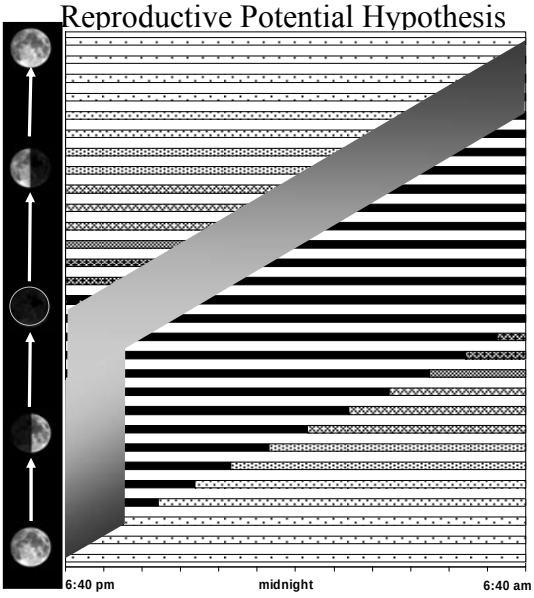

the lunar cycle. 1) The 'Dark Threshold Hypothesis' proposes that feeding and reproductive activity occurs at a constant elevated intensity whenever light levels are below a critical dark threshold (Figure 2.1b). 2) The 'Circalunar Burst Hypothesis' suggests that female *V. annecohenae* molt and become receptive cyclically due to endogenous, circalunar rhythms (e.g., at full moon) similar to other groups of crustaceans (Reaka 1976, Franke 1986), thus creating peak breeding periods under specific light and tidal conditions (Figure 2.1c). Based on the 'Circalunar Burst Hypothesis', adult reproductive behaviors should be cyclical while juvenile and adult foraging behaviors should be unaffected. 3) The 'Dark Threshold and Reproductive Potential Hypothesis' is based on our knowledge that juvenile females molt into receptive adults and adult females carrying broods of embryos release their offspring on a regular basis (Gerrish and Morin *in press*). According to this third hypothesis, during highly illuminated periods such as daytime or the nights just before the full moon, receptive females accumulate because the dark threshold, which is required for male reproductive displays, is never reached. When the dark threshold is finally crossed, we expect the activity of adults to be greatest when the highest numbers of receptive females are available or when the reproductive potential is greatest (Figure 2.1d). Juvenile behaviors should demonstrate little to no response.

MATERIALS AND METHODS

Study System:

Vargula annecohenae is a small bodied (~2 mm) bioluminescent ostracod (Crustacea: Ostracoda: Cypridinidae) that is found in high abundances (> 500 / m^2) in grassbeds surrounding islands on the Belize barrier reef (Morin and Torres in press). Like most cypridinid ostracods, *V. annecohenae* remains primarily on or in the sea bed; however, adult *V. annecohenae* males enter the water column nightly where they

produce bioluminescent displays to attract females (Morin and Cohen 1991). Similar to other cypridinid ostracods, the life cycle of *V. annecohenae* includes five juvenile instars and one terminal adult instar (Cohen 1983, Cohen and Morin 1990, Torres and Morin 2007). All instars can be accurately identified based on the length to width ratio of their carapace (Gerrish and Morin *in press*). Sexual dimorphism becomes apparent in stage five and remains obvious through the adult stage. Based on animals collected from the field and maintained in laboratory cultures, we also know that impregnation is internal and eggs develop inside the female for approximately 8 days after which time the eggs are extruded into a 'brood pouch' located within the marsupium of the females carapace. There they develop for approximately 18 additional days before release (Gerrish and Morin *in press*). Stage one juvenile instars are released from the adult females as benthic 'crawl- away' juveniles. These characteristics and the fact that *V. annecohenae* can be captured in abundance using baited foraging traps make them a tractable system for studying demographic behaviors.

Monthly and Overnight Observation:

Sampling took place just off the south beach of South Water Caye, Belize (N 16°48'45", W 88°04'57.5") in ~1.5 m deep water where turtle grass (*Thallasia testudinum*) dominated the substrate. To measure the relative activity of juvenile and adult *V. annecohenae* across time periods, we used the number of animals captured in baited traps as an estimate of foraging activity. Traps were created out of cylindrical polyvinyl chloride (PVC) piping (7 cm long × 3.8 cm diameter), containing inverted funnels of 75um nylon mesh at both ends. Screw caps lined with plastic window screening held the funnels in place and kept out the majority of large, un-wanted carrion foragers while allowing all sizes of ostracods to pass through. A brass clip

was attached to each trap using a plastic cable tie and traps were deployed containing a piece of dead fish (≈ 1 cm^3) to attract scavenging ostracods. Three traps were set each night from January 26 – February 21, 2003 during the hour immediately following the onset of reproductive displays which often occurred within 1-2 minutes of nautical twilight. While snorkeling, traps were clipped at two meter intervals along a submerged line. All individuals captured in traps were counted and aged based on documented age-size relationships for each instar (Gerrish and Morin *in press*). The data were then corrected for the time that each trap was deployed in the water (50 - 65 minutes) to provide foraging activity estimates (number collected per hour). In January 2003, we also monitored foraging activity overnight on three occasions as the moon fell and rose in the sky. Three traps were deployed every hour throughout each night and all individuals captured were again counted and assigned to instar based on size measurements.

We characterized the environment at the time of capture by measuring water velocity and temperature. Velocity measurements were taken by releasing 10 cm^3 of florescence dye hydrated with sea water at a flagged location. Dye was released just above the top of the turtle grass and allowed to move through the water. The location of the front edge of the dye was marked with another flag after a recorded duration of time. The distance between flags represents the distance the dye moved and over a known duration of time this provided our water velocity estimate (cm/s). Temperature was recorded using a mercury thermometer held at the turtle grass - water column interface (15-10 cm from bottom).

The other environmental variable of interest is represented by percent darkness, and is an estimate of the relative level of lunar illumination throughout the lunar cycle at the time of our sampling. Although directly measuring illumination at the time of sampling would have been the most accurate means of acquiring light level

estimates, because we lacked the equipment we instead used the phase of the moon and estimated percent darkness based on the lunar photometric model of Helfenstein and Ververka (1987). This model integrates Hapke's equation, which is fit to the lunar disk-integrated visual light curve and disk-resolved data, with the reflective characteristics of varied moon surface substrates and terrains (Helfenstein and Ververka 1987). Using the lunar photometric model, we calculated whole-disk brightness for each phase angle of the moon with 0-degrees being the 'ideal' full moon and 180-degrees being the 'ideal' new moon. Next, we assumed the whole-disk brightness of the moon at 2-degrees phase angle (the smallest phase seen from Earth outside lunar eclipse) as a practical reference brightness for the full moon. The level of brightness at the full moon, 2-degrees phase, was assigned 0 percent darkness and the brightness level at the new moon, 179-degrees phase, was assigned 100 percent darkness. Using this relationship, we derived a 'phase curve' to describe the relative level of darkness (% darkness) across phase angles for the entire lunar cycle (Figure 2.2). Based on almanac data from NASA regarding the timing of full and new moon for our January and June sampling periods, we identified the phase angle and percent darkness of the moon that corresponds with our sampling period each night.

From June 3 to June 30, 2003, in addition to monitoring foraging activity and environmental conditions nightly, we also monitored ostracod display activity. Quantifying the number of displays in an area proved difficult due to the patchy nature of displays, therefore we estimated densities based on catch-per-unit effort. Since we were most interested in comparing display densities between nights, the same researcher sampled displays each night within the same general region (40 m^2) and within a homogenous habitat of similar grass density and depth. Displays were sampled using a net swept upward through a single bioluminescent display, capturing the displaying male, and we counted the number of these sweeps possible in a three

minute period. Alternatively, when displays were heavy we recorded the amount of time it took to collect 50 displays. Assuming a constant swimming, detection and collection speed by the researcher, our estimate of the number of displays captured over time is comparable from night to night. Three measures of activity were made 20 minutes apart during the first hour of displays each night to document any increase or decrease in display behavior.

During January 2004, we monitored female receptivity and female reproductive activity in field populations. If females are becoming receptive or reproducing cyclically due to intrinsic circalunar cues, we would expect that all females, regardless of the timing of collection, would closely overlap in timing of mating, brooding and birthing. To test if females become receptive and reproduce cyclically throughout the lunar cycle, we collected females for 20 consecutive nights and monitored their reproductive characteristics in the laboratory during the following month. Each night, 24 females were isolated from foraging traps. To minimize exposure of females to males in the traps and limit forced copulation during confinement, we removed traps from the field and isolated the females as soon as we could determine that 24 females had been collected. The duration of trapping varied from 5-20 minutes depending on the activity level of females each night. Captive females were placed in 12-well tissue culture plates (well = 22.6mm diameter x 20mm deep), fed fresh dead fish *ad libitum*, provided fresh seawater every two to three days, and kept under photoperiod (≈ 12 hr light: 12 hr dark) and temperature (≈ 26 C) conditions similar to those found in their natural habitat. Knowing that females hold eggs internally for an average of 8 days (Gerrish and Morin *in press*), we monitored females for 15 days following collection to quantify the proportion of females that brooded within that period. Assuming that all successfully impregnated females brood

eggs, the proportion of females brooding each night is presented as it relates to the percent of impregnated females at the time of capture.

Data Analysis:

Foraging activity and water velocity were natural log transformed for analysis**.** Using the General Linear Model procedure (proc. GLM) in SYSTAT 9.0 (SPSS Science 1999), we tested how the foraging activity of each instar of *V. annecohenae* varied among nights throughout the lunar cycle. Instar (which includes male and female classes for adults), date of sampling and age class (juveniles vs. adults) were treated as fixed variables and the number of animals captured in foraging traps was our response variable. Based on non-significant interaction terms, instars that varied similarly across dates were grouped for further analysis. Next, in proc. GLM (SPSS Science 1999), we used a three-way ANOVA to test the interactions among sampling period (January and June), ostracod stage (adults vs. juveniles) and darkness (full vs. partial). Each factor was treated as fixed and categorical. Any interactions that were significant (at $p \leq 0.05$) were further analyzed using post hoc Scheffe-corrected pairwise comparisons. Foraging data were then regressed using a mixed model in proc GLM in SYSTAT 9.0 (SPSS Science 1999) against the continuous variables percent darkness and water velocity, and with season maintained as a fixed variable in the model. Based on significant interactions observed in the fully fixed model, the mixed regression was applied separately for juveniles, adults on 100% dark nights and adults on nights when darkness varied. Water velocity and darkness were not correlated (Pearson $_{n = 40} = 0.097$) and were therefore treated as independent predictor variables. Temperature did not vary within January or June and is therefore not used as a predictor of ostracod density, but a paired t-test was used to test significant differences in temperature between January and June. Models began as fully explicit,

testing all factors and interactions. We removed interactions and then main effects in a stepwise fashion (criteria $p = 0.150$) to isolate the models that explained the most variation. Because only one measure of darkness and velocity was taken on each night, we used average ostracod density collected in the three foraging traps as the response variable in the GLM.

RESULTS

Very few individuals of the youngest *V. annecohenae* instar were captured; therefore, the youngest instar was omitted from the analysis. We also observed significant differences in the density of instars A-IV, A-III, A-II and A-I that were captured ($p < 0.001$, Table 2.1). However, the foraging activity of each of the four oldest juvenile instars of *V. annecohenae* varied in a similar direction and intensity across the dates sampled ($p = 1.000$, Table 2.1) throughout both the January and June sampling periods. The significant difference between instars was primarily due to the low density of second instars (A-IV) that were captured. Based on the non-significant interaction between day sampled and instar, we treated all juveniles cumulatively for further analysis. Adult male and female instars were also grouped for further analysis with physical and temporal variables because they did not differ in relative foraging density across dates sampled ($p =1.000$, Table 2.1). Juveniles and adults differed significantly in how their foraging densities changed across the dates sampled and were therefore analyzed separately ($p < 0.001$, Table 2.1). The numbers of juveniles captured varied during the lunar cycle but showed no consistent pattern with the lunar cycle, whereas adults were captured less frequently in foraging traps on the nights approaching the full moon when the sky is brightly lit during our sampling period (the first hour after nautical twilight each night) (Figure 2.2). Additionally, because we captured some of the highest densities of *V. annecohenae* in both January and June on

Table 2.1. ANOVA to test for differences in the number of all instar *V. annecohenae* captured over days sampled.

Source	df	MSE	F-ratio	P
Day Sampled	51	16850.818	6.756	0.000
Instar	5	36291.174	14.550	0.000
Day Sampled * Age Class	51	7672.171	3.076	0.000
Day Sampled * Instar				
Within Age Class	204	1016.645	0.408	1.000
Error	595	2494.173		

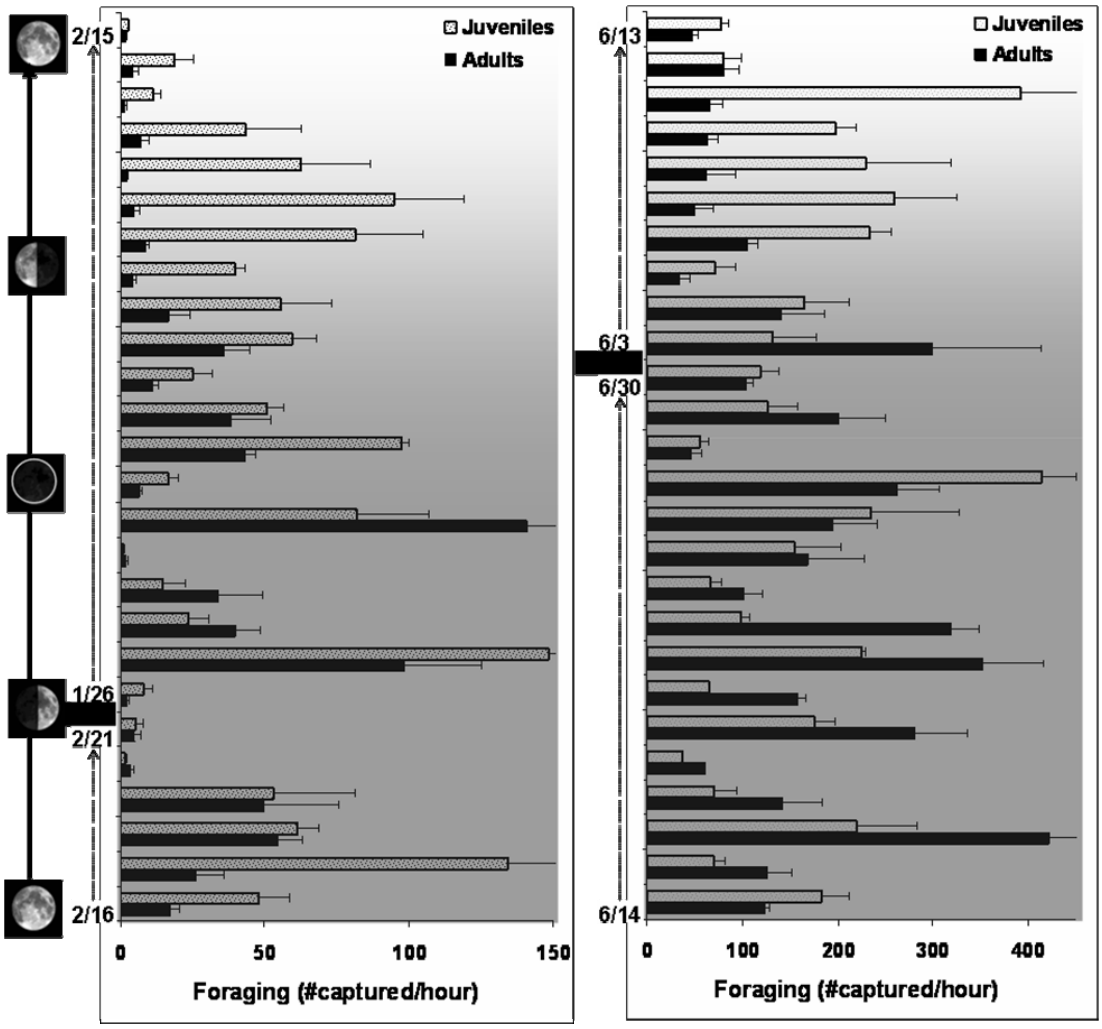

Figure 2.2. Feeding activity of adult and juvenile *V. annecohenae* during January (a) and June 2003 (b). Time in relation to the phase of the moon is presented as the y-axis moving from bottom to top with the lowest bar representing the first day after the full moon. Shading represents the % darkness available to the ostracods at the time of collection with darkest areas equal to 100% dark.

dark nights that followed many nights of previous sampling, we can assume our repeated sampling within a region did not depress ostracod capture and therefore does not bias our inferences regarding the patterns observed in foraging activity (Figure 2.2)

On half of the nights sampled, no moon was present in the sky at the time of collection, 18:30 – 19:30 (Figure 2.1a). There was a significant interaction between age class (juvenile or adult) and darkness (100% or < 100%) ($p = 0.005$, Table 2.2). In Scheffe post-hoc hypotheses tests, juveniles had no significant difference in mean activity between nights when no moon was present (= 100% darkness) and moonlit nights (< 100% darkness) (Figure 2.3, Scheffe $p = 0.863$). In contrast, adults were captured in greater densities on nights when no moon was present (Figure 2.3, Scheffe $p = 0.020$). Because there was a significant difference and because the large number of measurements at 100% darkness would heavily weight the analyses, data on adults were partitioned into two groups, nights with less than 100% darkness and nights when darkness was equal to 100% (Figure 2.4).

Temperature varied minimally within January (25.5º – 27.0ºC) and June (30.0º – 31.1º C) but did differ significantly between months ($t = 12.894$, $df = 26$, $p < 0.001$) and may have contributed to the difference in *V. annecohenae* feeding and reproductive activity between January and June. Water velocity was lower in June (4 to 21 cm/s) and varied much less than in January (5 to 75 cm/s). Because velocity varied both within and between sampling periods it was included as a variable in the analysis of both adult and juvenile feeding activities.

For juvenile activity, there was a marginally significant interaction between water velocity and sampling period (Figure 2.4a, Table 2.3, $p = 0.067$) and a significant interaction between percent darkness and sampling period (Figure 2.4b, Table 2.3, $p = 0.006$). In January, there was no relationship between darkness and

Table 2.2. ANOVA of sampling period (January and June), Darkness (= 100 % or < 100 %), and age (juvenile or adult).

Source	df	MSE	F-ratio	P
Sampling period (SP)	1	364646.657	67.480	0.000
Age	1	6417.961	1.188	0.279
Darkness	1	14812.626	2.741	0.101
SP * Age	1	762.183	0.141	0.708
SP * Darkness	1	3716.750	0.688	0.409
Age * Darkness	1	44602.585	8.254	0.005
Darkness * SP * Age	1	19915.992	3.686	0.058
Error	96	5403.768		

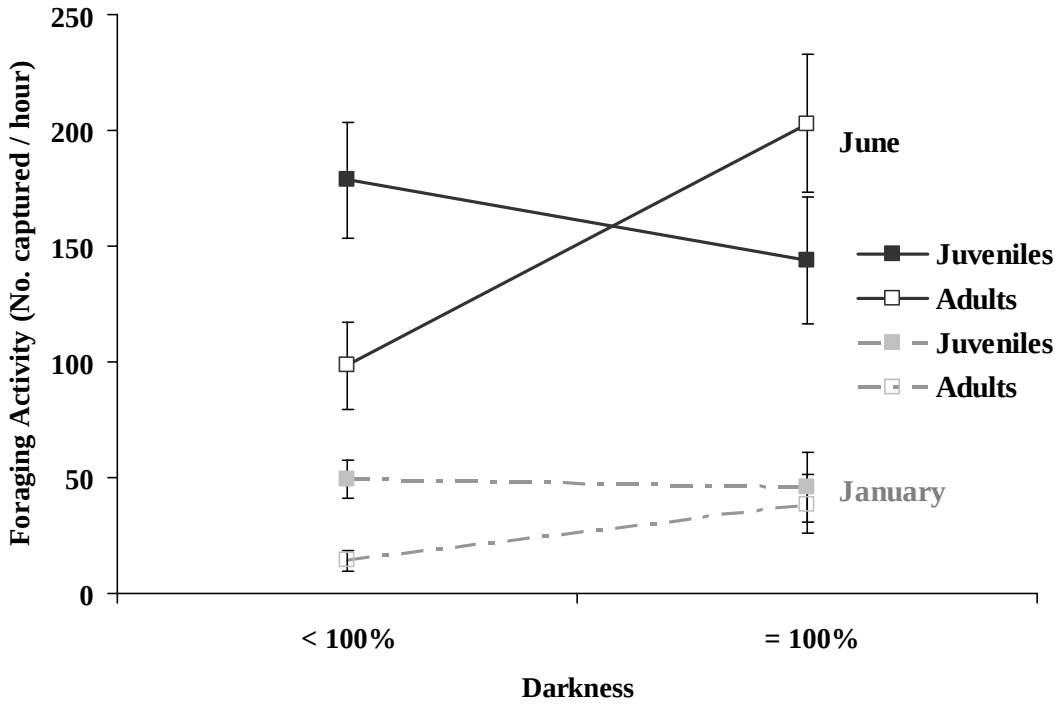

Figure 2.3. Average adult and juvenile *V. annecohenae* feeding activities during January vs. June on nights when a moon is present in the sky (darkness < 100%) or on nights when no moon is present in the sky (darkness = 100%).

Figure 2.4. *V. annecohenae* feeding activity in relation to flow and darkness. Activity and flow varied across exponential scales and therefore both variables were natural log transformed for analysis of (a) juvenile *V. annecohenae*, (c) adult *V. annecohenae* when darkness is less than 100%, and (e) adult *V. annecohenae* when darkness is equal to 100%. Because darkness did not vary on nights when darkness equals 100% the relationships between darkness and *V. annecohenae* density were only explored for (b) juveniles and (d) adult *V. annecohenae* when darkness is less than 100%,.

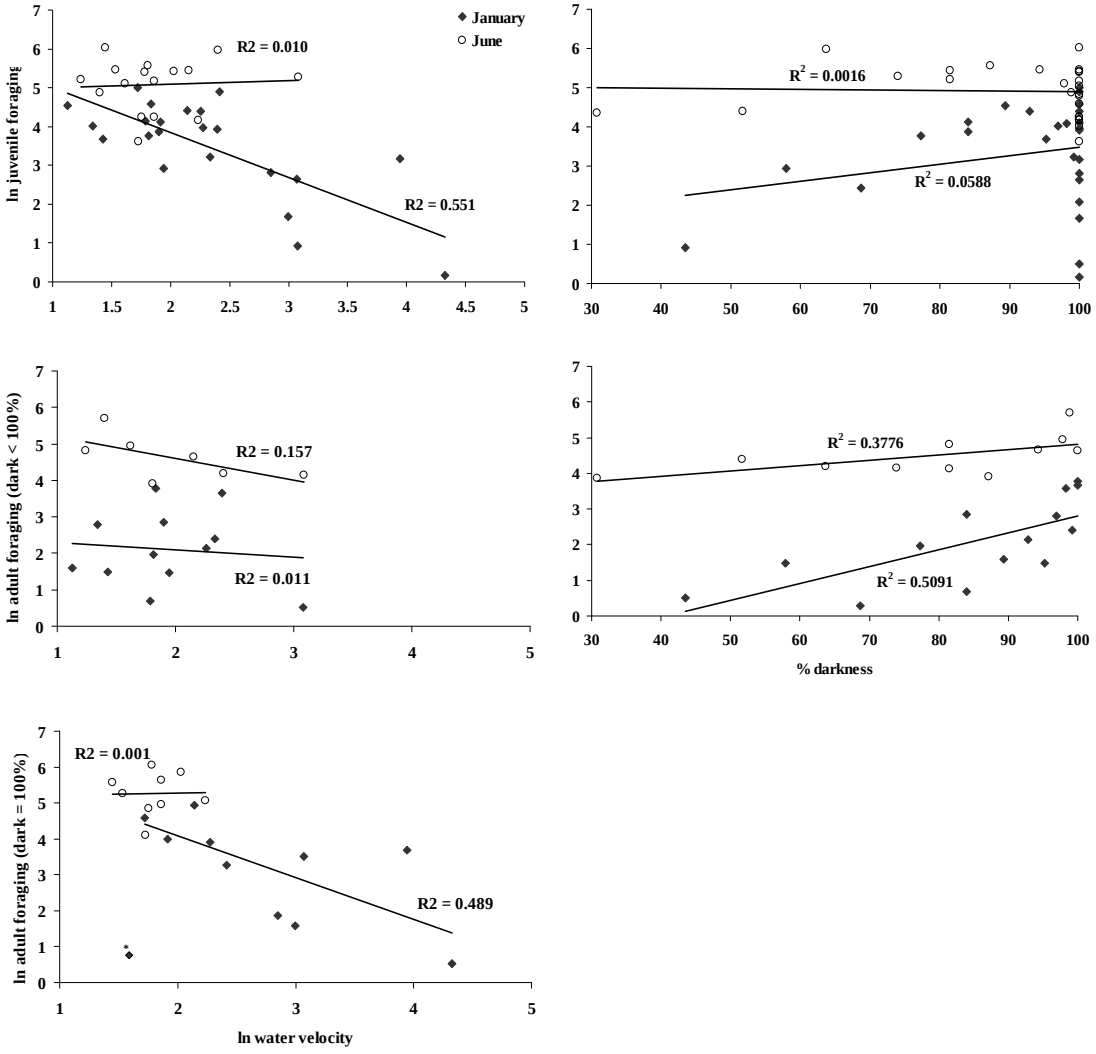
ln juvenile foraging
January
June
R2 = 0.010
R2 = 0.551
R2 = 0.0016
R2 = 0.0588
ln adult foraging (dark < 100%)
R2 = 0.157
R2 = 0.011
R2 = 0.3776
R2 = 0.5091
% darkness
ln adult foraging (dark = 100%)
R2 = 0.001
R2 = 0.489
ln water velocity

Table 2.3. Reduced General Linear Models (GLMs) for juveniles, adults when darkness is less than 100 %, and adults when darkness equals 100 %.

Source	df	MSE	F-ratio	P
Juveniles ($r^2 = 0.750$)				
Sampling Period (SP)	1	1.359	2.792	0.104
Water Velociy	1	4.164	8.553	0.006
% Dark	1	0.003	0.006	0.937
SP * % Dark	1	4.177	8.579	0.006
SP * Water Velocity	1	1.746	3.586	0.067
Error	33	0.487		
Adults when Darkness < 100% ($r^2 = 0.803$)				
SP	1	8.734	17.483	0.000
% Dark	1	7.434	14.879	0.001
SP * % Dark	1	2.595	5.194	0.033
Error	22	0.500		
Adult GLM = 100% Darkness ($r^2 = 0.691$)				
Water Velocity	1	28.511	38.02	0.000
Error	17	0.750		

juvenile ostracod activity (Figure 2.4b, $r^2 = 0.0588$, $p = 0.233$). In June, slightly fewer juvenile ostracods were captured on darker nights (Figure 2.4b, $r^2 = 0.0016$, $p = 0.848$). Yet, on very bright nights (darkness < 10%) very few juveniles were captured (Figure 2.4b). No relationship was observed between juvenile activity and water velocity in June (Figure 2.4a; $r^2 = 0.010$, $p = 0.812$), however in January; fewer juvenile *V. annecohenae* were captured on nights when velocity was high (Figure 2.4a, $r^2 = 0.551$, $p < 0.001$). The best fit model predicted 75.0% of the variation observed in juvenile activity and included sampling period, water velocity, darkness and the interactions of sampling period with water velocity and darkness.

On nights when a moon was present in the sky during sampling (darkness < 100%), water velocity, the interaction of velocity and sampling period, and the three-way interaction between water velocity, sampling period and percent darkness did not explain a significant amount of variation in adult activity, however the negative trend observed with fewer individuals captured under higher water velocity conditions was maintained (Figure 2.4c). In both June and January, increased numbers of adult *V. annecohenae* were captured in feeding traps on darker nights (Figure 2.4d; Table 2.3, $p < 0.001$). But, the strength of this interaction varied significantly between January and June (Figure 2.4d, Table 2.3, $p = 0.033$). The best fit model to predict adult *V. annecohenae* densities on moonlit nights included sampling period, darkness and their interaction ($r^2 = 0.803$).

For adults, on nights when no moon was present in the sky during sampling (darkness = 100%), a greater average number of *V. annecohenae* adults was collected overall (Figure 2.3) however, there was a large amount of variation in densities within dark nights (Figure 2.2b). Water velocity explained a significant portion of this variation and only its main effect was significant (Figure 2.4e, $p < 0.001$, $r^2 = 0.691$). In June there was very little variation in velocity and we observed less variation in

adult activity (Figure 2.4e, $r^2 = 0.001$, $p = 0.934$). However, in January when water velocity varied most, fewer adult *V. annecohenae* were captured when water velocity was high (Figure 2.4e, $r^2 = 0.489$, $p = 0.024$).

Display activity:

Reproductive display behavior by males follows a threshold response with zero displays occurring on nights when darkness is less than 95%. Higher display activity was observed on darker nights with the highest activity observed on 100% dark nights (Figure 2.5). Additionally, on nights when displays occurred, displays started 1-2 minutes before nautical twilight, peaked ($r^2 = 0.53$) and then dropped off over the following hour ($r^2 = 0.42$, linear regression $F = 7.887$, $p = 0.017$: Figure 2.6).

Overnight activity:

Hourly measures of *V. annecohenae* activity using feeding traps set throughout the night varied depending on the timing of moon rise or moonset. Juveniles were active throughout the night on 12 January and exhibited lowest activity during dark periods at which time adults peaked in activity. Adults became active as the moon set and were most active during the first hour following moonset after which time the number captured each hour decreased (Figure 2.7a). Both adult and juvenile activity remained low on 19 January after the nearly full moon rose at 19:00 (Figure 2.7b). Low numbers of both juveniles and adults were actively foraging on 25 January and no clear patterns are visible in the data, except a small burst of activity just prior to sunrise (Figure 2.7c).

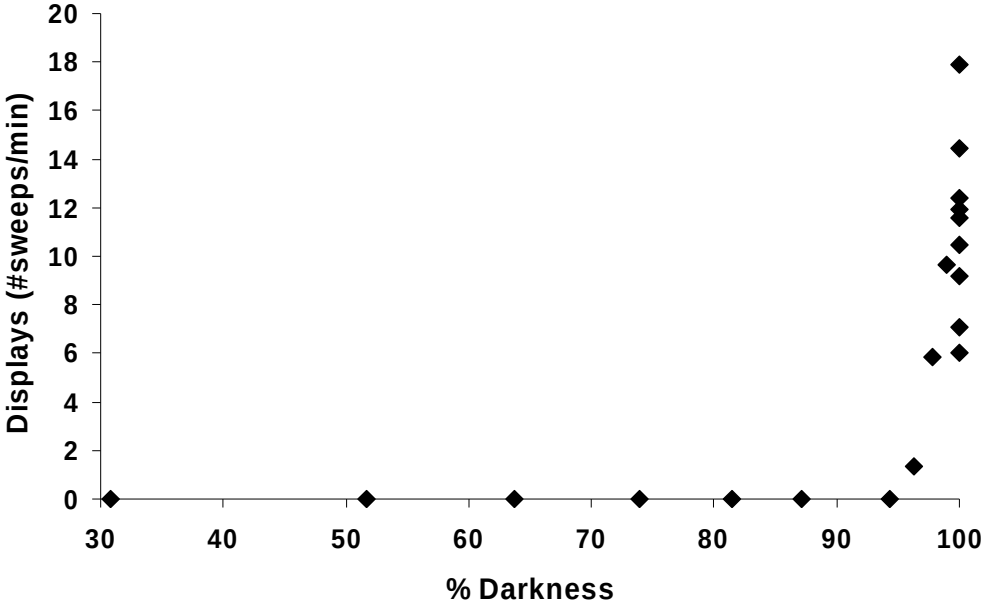

Figure 2.5. Reproductive displays throughout the June lunar cycle. Displays did not occur on nights during which darkness had not reached the 'dark threshold' which occurs somewhere between 63% and 72% darkness.

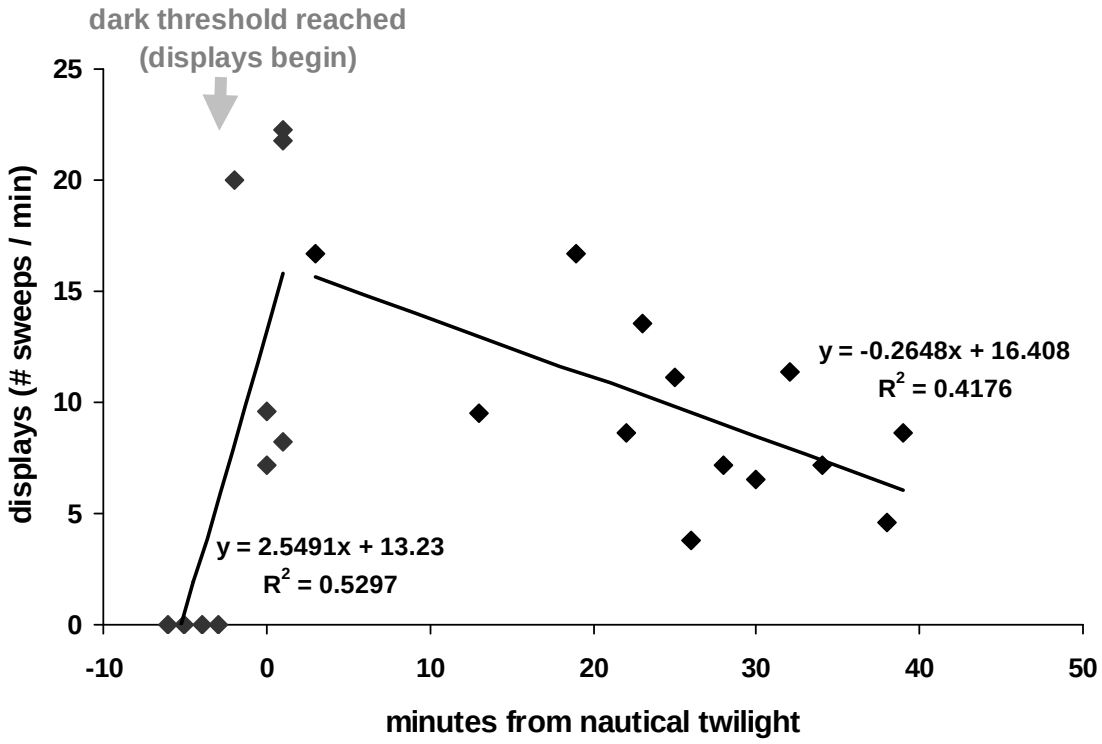

Figure 2.6. Sweep samples during the first hour indicate that displays began within 2-3 minutes of nautical twilight and quickly peaked in number, than decreased in frequency continuously over the first hour.

Figure 2.7. Overnight feeding activity of adult and juvenile *V. annecohenae*. Shading represents darkness at each hour sampled. (a) On January 12th a ¾ moon was present in the sky until it sets at 2:09 AM. (b) On January 19th, no moon is present at sunset but a nearly full moon rises one hour after sunset. c.) On January 25th no moon is present until a 1/3 moon rises at 12:57 PM.

a) January 12, 2003

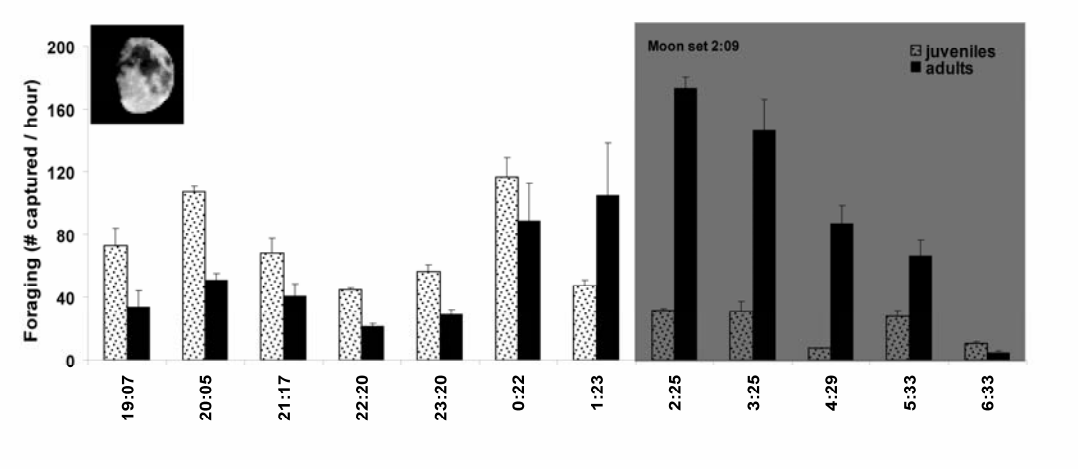

b) January 19, 2003

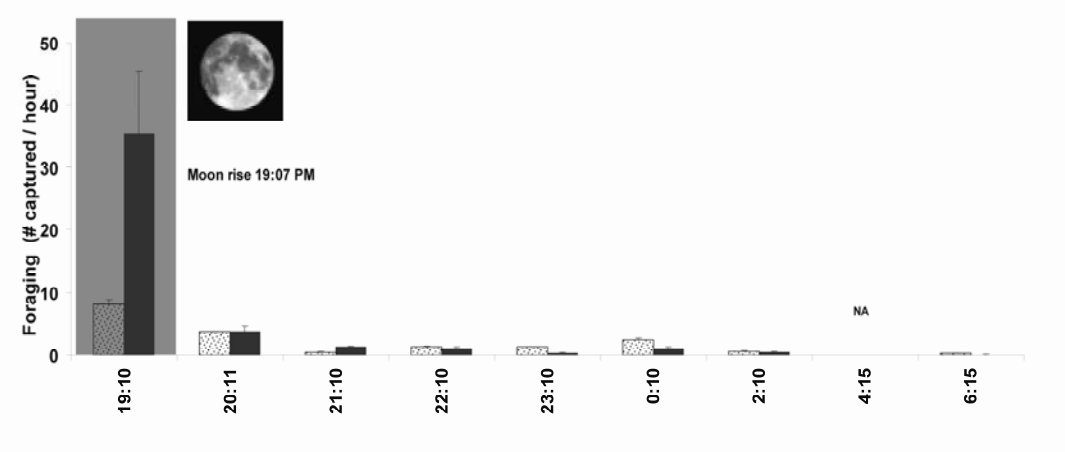

c) January 25, 2003

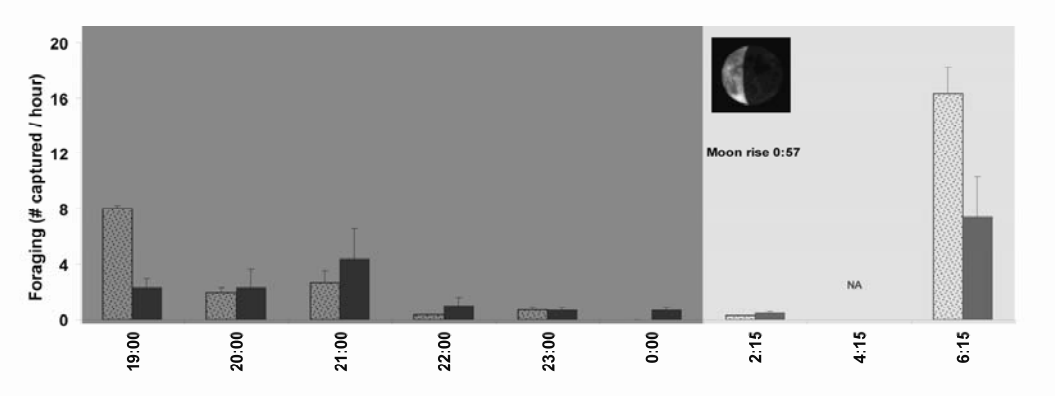

Female receptivity:

If females were fertilized by forced copulations that occurred in baited traps, we would expect most females to release eggs into the brood chamber 7-8 days following their capture. However, females brooded continuously from day 1 to day 8 after collection and we observed no evidence of higher levels of brooding on day 7 or day 8 following collection. Overall, no pattern in female receptivity or mating is discernable. On average 60% of females had already mated at the time of capture and there was no significant change throughout the lunar cycle (Figure 2.8; $p = 0.754$).

DISCUSSION

Feeding and reproductive behavior in adult *V. annecohenae* begins when the dark threshold is reached, and this threshold is roughly equivalent to when a third of a moon is present in the sky or to the intensity of light two to three minutes before nautical twilight on nights when no moon is present in the sky during sampling. The behavioral responses of *V. annecohenae* to this dark threshold are independent of timing, as indicated during overnight sampling when adults become active in the middle of the night as the moon sets. Additionally, on cloudy nights reproductive displays often begin if a partial moon is well covered and the necessary dark conditions are met (unpublished data). Furthermore, adult male *V. annecohenae* can be triggered in the laboratory to begin displaying at any time throughout a day by placing them into completely dark conditions (T.J. Rivers, personal communication). For *V. annecohenae* the exogenous cues provided by the dark threshold appear to outweigh any endogenous rhythms effecting behavior. This uncoupling of external cues and chronological rhythms occurs in multiple organisms (Danks 2005, Mathias et al. 2006), and has even been shown to have underlying genetic controls (Mathias et al. 2006). These observations bring into question the very common labeling of a light or

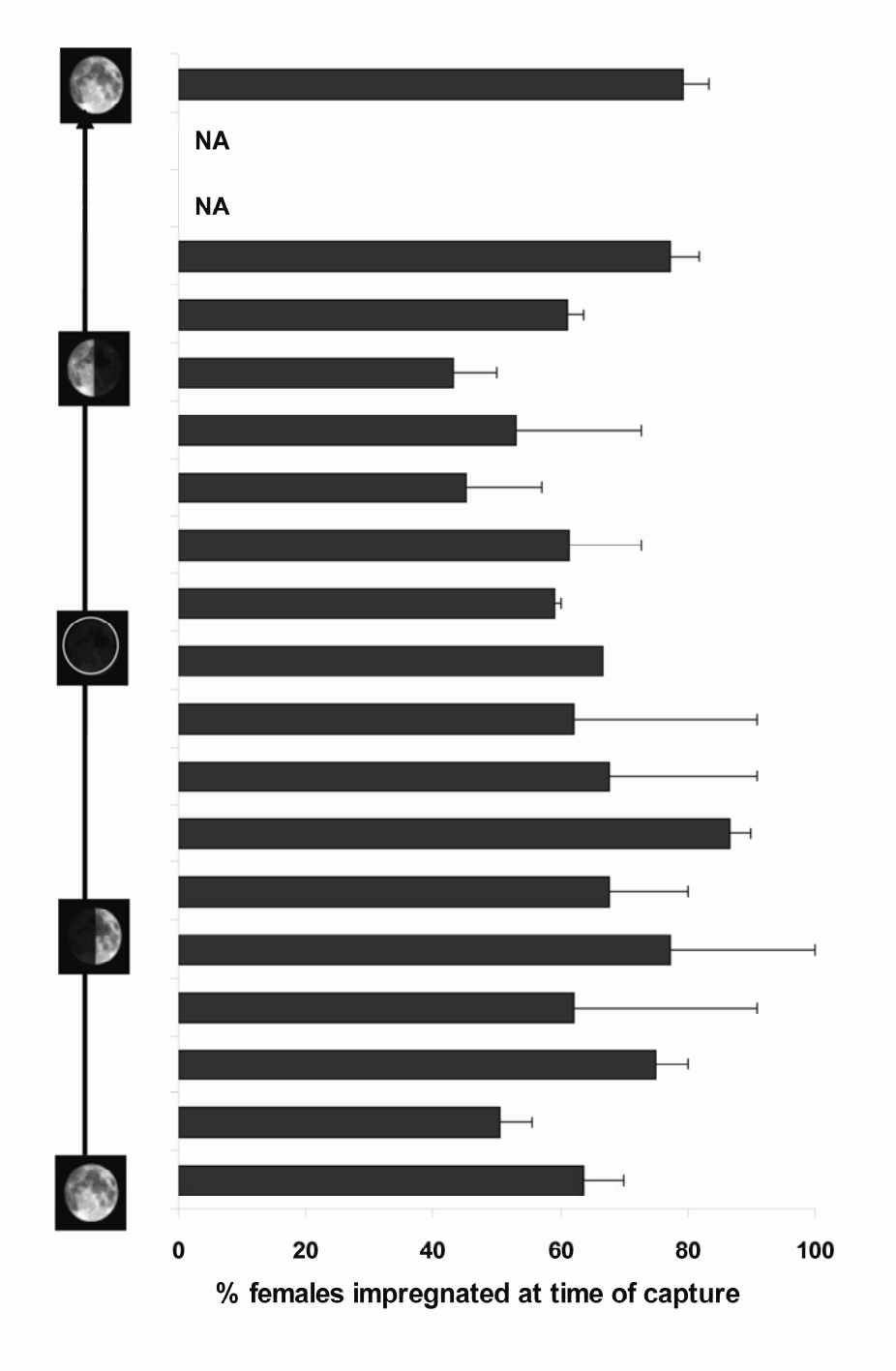

Figure 2.8. Frequency of female fertilization during the January 2004 lunar cycle.

dark condition as a Zeitgeber. Although in nature, light and dark inherently have temporal or circadian associations, they also have physiological and ecological functions which should not be overlooked or underappreciated when assigning them as temporal cues.

Peak foraging activity in adult *V. annecohenae* also appears to correspond with periods during which the maximum number of receptive females are present. This pattern supports the Dark Threshold and Reproductive Potential Hypothesis (Figure 2.1d). From life cycle studies in the laboratory, we know that fifth instar female *V. annecohenae* continuously molt into adults and that reproductive females constantly release broods over a 24 hour period regardless of light levels (Gerrish and Morin in press). If females constantly become receptive after molting or brood release, and only mate when it is dark, then during extended periods of light, reproductively available females will accumulate. Extended periods of light occur during daytime and on moonlit nights, with the longest period occurring over the two or three days near full moon when either the sun or a brightly illuminated moon is present in the sky at all times. Thus the first hour of darkness each night and the nights immediately following the full moon have the highest densities of newly receptive females. These nights also have short windows of time at the beginning of each night when the necessary 'dark threshold' is met (Figure 2.1d). Our data indicate that the peak periods of display activity occur during the first 15 minutes after the dark threshold is reached and drops off quickly, within less than an hour (Figure 2.6). Furthermore, we observed the highest display activity on the two or three nights following the full moon. This quantitative observation for June, 2003 is supported by qualitative observations over many lunar cycles (unpublished data). Whether males have adapted to display at these times to maximize fitness or are cueing off of a pheromone

produced by receptive females that stimulates reproductive behavior remains to be tested.

Additional support for the Reproductive Potential and Dark Threshold Hypothesis is provided by juvenile *V. annecohenae,* which have a much less clearly defined relationship with darkness. They are nocturnal but appear to respond to a much brighter dark threshold. It is possible that because juveniles do not actively participate in reproduction, their dependence on dark conditions and their need to detect bioluminescent displays is less important. However, all age classes and sexes of *V. annecohenae* are capable of emitting bioluminescence and it is postulated to be a means of defense against predators (Morin and Cohen 1991). Assuming that bioluminescence is important in deterring predators, its use as an alarm signal would be hindered on bright nights. One possibility is that the smaller size of juveniles makes them less susceptible to predators that orient visually in moonlit conditions, reducing their dependence on bioluminescent defense. However, stage five females, which are actually larger than adult males, show a behavioral pattern more like juveniles than adults. They actively feed on moonlit nights when adults do not, strongly indicating that the adult behaviors are due to some correspondence between reproductive and feeding or foraging behavior.

Next to darkness, water velocity is the most important variable influencing both adults and juveniles. Because *V. annecohenae* reach a maximum size of 2 mm, their swimming and grasping abilities can easily be overcome by strong currents. This is apparent when observing males attempting to display on nights when water velocity is high. The first pulse of a reproductive display occurs in or just at the top of the turtle grass where the flow is somewhat limited by the grass-water boundary. On nights when water velocity is high we observe one to three bright flashes near the grass and then one or two more flashes above the grass that move swiftly away at the

rate and in the direction that the water is moving. Under these conditions, males rarely release more than three to five pulses in a display compared to a typical display in calm conditions of 15-19 flashes (unpublished data). Like other bioluminescent ostracod species, *V. annecohenae* males cue off of and entrain on the displays of other males to begin reproductive behaviors (Rivers 2007) and this interaction does not occur on high flow nights when displays are limited to three to five flashes. Because adult feeding behavior appears to correspond with reproductive behavior, it is possible that the ostracods experience an overall lack of activity on nights when water velocity is high. However, juvenile activity is also suppressed on high flow nights. Since *V. annecohenae* spends most of its time hidden in the sediments, it is possible that it remains submerged to avoid being swept into inappropriate habitats on high flow nights. It is also possible that as a scavenger, *V. annecohenae* has difficulty detecting food sources during periods of high flow because the current carries away chemical cues for resource location.

The differences observed in feeding activity between January and June could indicate seasonal fluctuations in *V. annecohenae* densities. However, because quantitative sampling was only conducted during one January and June, we have limited ability to infer seasonal effects. Additionally, environmental conditions, such as temperature and flow varied between January and June, confounding a strict temporal inference of differences with the role of environmental drivers influencing *V. annecohenae* densities. The question remains: is seasonal variation driving actual differences in numbers, or are harsher environmental conditions during January simply limiting behaviors? Based on figures 2.4a and 2.4e, we may expect that *V. annecohenae* activity is simply limited by environmental factors as similar densities of adults are captured in January on the few nights when flow is extremely low.

In addition to the larger, measured variables influencing *V. annecohenae* densities that were the focus of this study, microhabitat variation also influences *V. annecohenae*. Among the three traps set nightly, we observed high levels of variation in the number of animals captured. Although replicate trap variation is not large enough prevent our detection of the influences of flow and darkness, there is substantial residual variation. Because of their small size, *V. annecohenae* could be responding to more localized cues within the grassbed habitat. Habitat studies indicate that this species avoids even small patches of non-grass substrate and often will congregate near the roots of older and thicker *Thalassia* roots (unpublished data).

Overall, our data support the conclusion that the strongest environmental factor influencing the feeding and reproductive behaviors of *V. annecohenae* is the availability of time during which illumination is below a critical dark threshold. This dependence on darkness for successful growth and reproduction allows us to classify darkness as a resource, in the same way that others have classified time, space and temperature as resources (Magnuson et al. 1979; Tracy and Christian 1986; Kronfeld-Schor and Dayan 2003). Considering darkness as a resource alters the way we think about important physiological, biological and behavioral activities that take place after the sun goes down. Additionally, it clarifies discussion of the increasing and severe impact that artificial lights have on darkness and hence upon the organisms that depend upon this important natural resource.

ACKNOWLEDGEMENTS

We thank Nelson G. Hairston Jr. for comments on project development and this manuscript. Thank you also to Paul Helfenstein for assisting us with the lunar model. We also are grateful for field assistance from Krystal Rypien, Michael Pipersburgh and Richie Williams and support from International Zoological

Expeditions on Southwater Caye. Funding sources included Cornell Universities Mario Einaudi Fund, and S. Ann and Robert R. Morley Research Fund. This research was completed in accordance with permits received from the Belize Department of Fisheries, BZ.

REFERECENES

Aiken D.E. 1969. Photoperiod, endocrinology and the crustacean molt cycle. Science 164: 149-155.

Babcock R.C., G.D. Bull, P.L. Harrison, A.J. Heyward, J.K. Oliver, C.C. Wallace, and B.L. Willis. 1986. Synchronous spawnings of 105 scleractinian coral species on the Great Barrier Reef. Marine Biology 90: 379-394.

Britt A.B. 1996. DNA Damage and repair in plants. Annual review of plant physiology and plant molecular biology 47: 75-100.

Cohen A. 1983. Rearing and postembryonic development of the myodocopid ostracode *Skogsbergia lerneri* from coral reefs of Belize and the Bahamas. Journal of Crustacean Biology. 3: 235-256.

Cohen A. and J.G. Morin. 1990. Patterns of reproduction in ostracods: a review. Journal of Crustacean Biology. 10: 184-211.

Danks H.V. 2005. How similar are daily and seasonal biological clocks? Journal of Insect Physiology 51: 609-619.

Fisher R. and D.R. Bellwood. 2003. Undisturbed swimming behavior and nocturnal activity of coral reef fish larvae. Marine Ecology Progress Series 263: 177-188.

Franke H-D. 1986. The role of light and endogenous factors in the timing of the reproductive cycle of *Typosyllis prolifera* and some other polychaetes. American Zoologist 26: 433-445.

Friedberg E.C., G.C. Walker, and W. Siede (eds). 1995. DNA Repair and Mutagenesis. American Society of Microbiology Press, Washington D.C.,USA.

Gerrish G.A. and J.G. Morin. *In press.* The life cycle of a bioluminescent marine ostracod, *Vargula annecohenae* [Cypridinidae, Myodocopida]. Journal of Crustacean Biology

Grad G., C.E. Williamson, and D.E. Karapelou. 2001. Zooplankton survival and reproduction responses to damaging UV radiation: A test of reciprocity and photoenzymatic repair. Limnology and Oceanography 46: 584-591.

Hastings J.W. and J.G. Morin. 1991. Bioluminescence. In: Prosser CL (ed). Neural and Integrative Animal Physiology [Comparative Animal Physiology]. Wiley-Liss Inc., Wilmington Delaware, USA. pp 131-170.

Helfenstein P. and J. Veverka. 1987. Photometric properties of lunar terrains derived

from Hapke's equation. ICARUS 72: 342-357.

Herring P.J. 1990. Bioluminescent communication in the sea. In: Herrish P.J., A.K. Cambell, M. Whitfield, and L. Maddock (eds). Light and Life in the Sea. Cambridge University Press, Cambridge, UK. pp 245-264

Kronfeld-Schor N. and T. Dayan. 2003. Partitioning of time as an ecological resource. Annual Review of Ecology, Evolution and Systematics 34: 153-181.

Lessios H.A. 1991. Presence and absence of monthly reproductive rhythms among 8 Caribbean echinoids off the coast of Panama. Journal of Experimental Marine Biology and Ecology 153: 27-47

Longcore T. and C. Rich. 2004. Ecological light pollution. Frontiers in Ecology and the Environment 2: 191-198.

Magnuson J.J., L.B. Crowder, and P.A. Mevick. 1979. Temperature as an ecological resource. American Zoologist 19: 331-343.

Mathias D., L.K. Reed, W.E. Bradshaw, and C.M. Holzapfel. 2006. Evolutionary divergence of circadian and photoperiodic phenotypes in the pitcher-plant mosquito, *Wyeomyia smithii*. Journal of Biological Rhythms 21: 132-139.

Mitchell D.L. and D. Karentz. 1993. The induction and repair of DNA photodamage in the environment. In: Young A.R., L.O. Bjorn, J. Moan, and W. Nultsch (eds). Environmental UV photobiology. Plenum Press, New York, New York, USA. pp 345-377.

Morin J.G. 1983. Coastal bioluminescence: patterns and functions. Bulletin of Marine Science 33: 787-817.

Morin J.G. and A.C. Cohen. 1991. Bioluminescent Displays, Courtship, and Reproduction in Ostracodes. In: Bauer R. and J. Martin (eds). Crustacean Sexual Biology. Columbia University Press, New York, New York, USA. pp 1-16

Reaka M.L. 1976. Lunar and tidal periodicity of molting and reproduction in stomatopod crustacea: a selfish herd hypothesis. Biological Bulletin 150: 468-490.

Rich C. and T. Longcore. (eds) 2006. Ecological Consequences of Artificial Night Lighting. Island Press. Washington D.C., USA.

Rivers T.J. 2007. Bioluminescent activity in the mating and antipredatory behavior of

a marine ostracod (Crustacea, Myodocopida). Dissertation at Cornell University: Ithaca, NY.

Stross R.G. and J.C. Hill. 1965. Diapause induction in *Daphnia* requires two stimuli. Science 150: 1464-1464.

Sutherland B.M. 1981. Photoreativation. Bioscience 31: 439-444.

Taylor M.H. 1984. Lunar synchronization of fish reproduction. Transactions of the American Fisheries Society 113: 484-493.

Torres E. and J.G. Morin. 2007. *Vargula annecohenae*, a new species of bioluminescent ostracode (Myodocopida: Cypridinidae) from Belize. Journal of Crustacean Biology 27: 649-659.

Tracy C.R. and K.A. Christian. 1986. Ecological relations among space, time, and thermal niche axes. Ecology 67: 609-615.

Venable D.L and L. Lawlor. 1980. Delayed germination and dispersal in desert annuals: escape in space and time. Oecologia 46: 272-282.

CHAPTER 3

FROM GENES TO GEOGRAPHIC INFORMATION SYSTEMS: HOW LIFE HISTORY, GENETICS AND PHYSICAL HABITAT INFLUENCE THE SPATIAL STRUCTURING OF BIOLUMINESCENT MARINE OSTRACOD POPULATIONS

ABSTRACT

Knowledge of dispersal pathways, metapopulation dynamics, genetic diversity and habitat interactions are all important when planning effective conservation efforts. This information is ultimately based on the knowledge gained from the study of individual species. To better understand the bioluminescent ostracod, *Vargula annecohenae* (Crustacea: Myodocopida: Ostracoda) and its habitat needs, in this study I integrate natural history characteristics such as life cycle dispersal abilities, gene flow and age specific abundances, with the physical reef attributes commonly considered for reef conservation (water velocity, water depth, substrate). Using mark and recapture methods, I observed that dispersal distance varies between age classes with adults males moving the greatest distances (5.1 m in 24 h). Extrapolation of dispersal estimates indicates that life time dispersal could be as high as a third of a kilometer. With this estimated level of dispersal, genetic differences across multiple kilometers would be unlikely if the habitat were continuously suitable. However, highly significant genetic differences were observed between the northern and southern regions of the study site, at distances $\leq$ 12.2 km. Analyses of habitat variables (water velocity, water depth, seagrass density) in a geographic information system (GIS) indicate that physical barriers have contributed to the maintenance of geographic population structure.

KEYWORDS: *Vargula annecohenae*, bioluminescent ostracods, GIS, microsatellite DNA, mark and recapture, dispersal, gene flow

INTRODUCTION

The influences of gene flow, dispersal and habitat heterogeneity on species distributions have been studied extensively. However, researchers have struggled to integrate the techniques and information from these three areas of research. For gene flow to be occurring, an organism must disperse to, colonize and successfully reproduce within a location. Because dispersal studies often focus on only the first phase of animal movement, migration estimates based on measures of gene flow and dispersal models have often been divergent (Holt and Gomulkiewicz 1997, Bohonak 1999, Lenormand 2002). From an evolutionary perspective, movement without successful colonization or gene flow is ineffective. On the other hand, from an ecological perspective, the number of animals moving between habitats and using resources may be more important than gene flow. Because studies of dispersal and gene flow quantify different characteristics of a species, comparisons between them can yield insights into colonization mechanisms and mating success, which are often much more difficult to measure directly *in situ*. Also, by considering the landscape in which dispersal or gene flow are studied, conservation efforts and movement models can be applied at a much larger and more realistic scale.

Theoretical and review articles continually refer to the need for empirical data on multistage and demographic dispersal information in multiple habitats when planning marine reserves (Grantham et al. 2003, Lubchenco et al. 2003, Palumbi 2003, Shanks et al. 2003). For example, a review by Shanks et al. (2003) indicates that marine larvae most commonly disperse either less than 1 km or greater than ca. 20 km, suggesting that effective reserves should range from 4 to 6 km in diameter and be

distributed 20 km apart. However, theoretical predictions based on genetic distances indicate a reserve could be 'self seeding' if it is 10 to 20 km in size (Palumbi 2003). The recommendations from each of these studies differ depending on the type of information available. Since all habitats have distinctive environments and a unique suite of adapted organisms, dispersal distances and life histories will vary greatly among organisms and must be relevant for the habitat of interest (Grantham et al. 2003).

Although marine reef lagoon areas in tropical regions, including seagrass beds, include a large portion of the area within coastal reef habitats, conservation efforts and planning often focus more specificially on the more diverse, yet smaller, areas of coral habitat. One of these overlooked habitats, grassbeds, provide a nursery for a diversity of reef fishes and invertebrates (Adams and Ebersole 2002, Butler and Herrnkind 1997) and are potentially a major factor in maintaining stable nutrient dynamics (Kenworthy and Thayer 1984) for the entire reef system. As more focus is placed upon how lagoon habitats are fundamental to reef ecosystem dynamics, further information is need about the types of organisms that specifically occupy these habitats, their life cycles, how they interact with their physical environment, and what their relationships are with other organisms outside their own habitat.

In this study, I used a geographic information system (GIS) to identify habitat-level patterns of dispersal and gene flow for an abundant grassbed invertebrate, the omnivorous ostracod *Vargula annecohenae*. The GIS model was built around satellite imagery, measurements of physical habitat characteristics, and distribution values of *V. annecohenae*. Dispersal was quantified in a series of mark and recapture studies conducted across habitat boundaries for *V. annecohenae* of all age classes. Microsatellite DNA loci were developed and the data were used to quantify gene flow

across the GIS study area for comparison with habitat types and dispersal estimates from mark and recapture results.

MATERIALS AND METHODS

Vargula annecohenae:

V. annecohenae is a charismatic bioluminescent ostracod (Crustacea: Ostracoda: Cypridinidae) for which all age classes can be trapped using baited inverted funnel traps. It occurs in high abundance throughout the study area making it appropriate for use in geographic inference. It is small bodied (ca. 2 mm long) and found in grassbeds dominated by *Thalassia testudinum* surrounding islands on the Belize barrier reef (Figure 3.1, Torres and Morin 2007). *V. annecohenae* remains primarily on or in the sea bed, actively foraging and moving about only during nighttime (Gerrish and Morin *submitted*). Adult *V. annecohenae* males enter the water column nocturnally where they produce bioluminescent displays to attract females (Morin and Cohen 1991, Rivers and Morin *in press*). Similar to other cypridinid ostracods, the life cycle of *V. annecohenae* includes five juvenile instars and one terminal adult instar (Cohen 1983; Cohen and Morin 1990; Torres and Morin 2007, Gerrish and Morin *in press*). All instars can be accurately identified based on the regression of length to width of their carapace (Gerrish and Morin *in press*). Sexual dimorphism becomes apparent in stage five (i.e. just subadult) and remains obvious through the adult stage.

Study Site:

This study was carried out at a 12.2 km (north to south) by 3.6 km (east to west) portion of the Mesoamerican barrier reef and lagoon located approximately 15.5 km east of the coast of Dangriga, Stann Creek District of Belize (Figure 3.1;

16.812734º N, -88.082575º W). This area was chosen based on its abundant population of *V. annecohenae*, its proximity to laboratory facilities on South Water Caye, and the availability of satellite imagery - accessible through collaboration with G. Gaston and A. Ballas, University of Mississippi. The region includes five islands: two mangrove islands (Tobacco Range [TBR] in the north-west and Twin Caye [TB] in the south-west) and three sandy barrier reef islands (Tobacco Caye [TBC] in the north-east, South Water Caye [SWC] and Carry Bow Caye [CBC] just north and south, respectively, of the southern most reef cut in the south-east corner, Figure 3.1). The sand islands are situated just shoreward of the extensive Belize coral forereef, which is visible running north to south on the east (right) side of Figure 3.1. Just seaward of the reef to the east, the water depth drops quickly to > 500 m. Shoreward of the reef, the light penetrates adequately to make suitable imagery of the substrate and vegetation throughout the study area. High seagrass densities are seen as dark regions (Figure 3.1), coral patches are identifiable by the circular 'halos' of light sand surrounding them, and water depth can be determined from the amount of reflected light in the image (Ballas and Gaston 2006).

Mark and Recapture:

To document potential movement distances and to assess dispersal across specific habitat barriers for *V. annecohenae*, a series of mark and recapture field studies were conducted across a range of habitat types. Ostracod age classes were recorded to provide demographic dispersal estimates for use in population level dispersal modeling.

V. annecohenae individuals were collected from each mark and recapture study site (Figure 3.1) using 5-10 small funnel traps, each consisting of a cylindrical

Figure 3.1. Satellite image of the 12.2 km × 3.6 km study area on the Belize barrier reef stretching from Carry Bow Caye at the south to just north of Tobacco Caye. The islands, Carry Bow Caye, South Water Caye, and Tobacco Caye and emergent rocks, mangroves (Twin Caye, Tobacco Range) or other vegetation are represented in bright blue. East of the barrier reef, the water depth drops quickly to > 500 m [black to the right of the image]. Dark or green areas in the image are dense seagrass on the substrate; light areas are either sand or lower density seagrass. Of the 52 sites sampled for the ostracod *V. annecohenae* (Red asterisks), 15 sites were sampled for water velocity (blue stars), 3 sites were used for mark and recapture studies (closed blue circles), and 22 sites for genetic analysis (open blue circles).

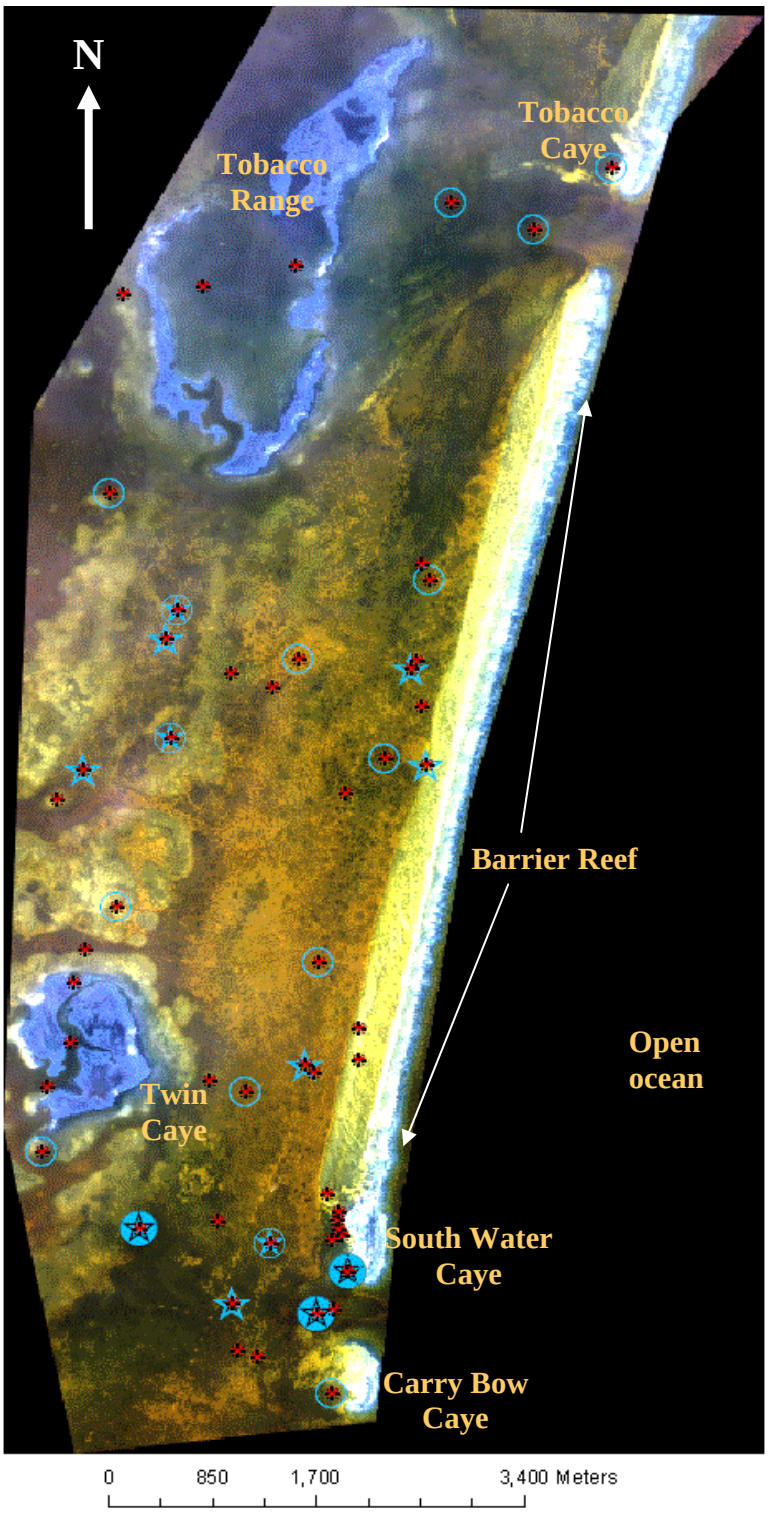

Sites sampled for:

- **density**
- **genetics**
- **flow**
- **mark and recapture (& genetics)**

polyvinyl chloride (PVC) tube (7 cm long × 3.8 cm diameter) containing inverted funnels of 75 μm nylon mesh at each end. Traps were baited with pieces of freshly dead fish (ca. 2 g) and placed at the sediment-water interface. Traps were deployed at approximately 18:30 h and remained overnight in the habitat to maximize the number of animals captured. Traps were collected in the early morning at approximately 07:00 h. All individuals captured were taken to the lab and counted and aged based on their carapace length and height, eye and keel size (Gerrish and Morin *in press*). Sex was determined for all A-1 (= 5^{th} stage) and adult (= 6^{th} stage) instars. All individuals were then marked with bright pink nail polish that contrasted with the translucent white and yellow of the ostracod body, facilitating detection of marked individuals upon recapture. To mark individuals, I briefly placed 15-20 *V. annecohenae* on a piece of 75 μm plankton mesh and allowed the water to wick away from their carapace exteriors. During drying, the ostracods pulled their valves tightly together and maintained water inside their carapace while the outside dried. Once the external carapace was dry (ca. 15 s), each individual was placed in a dry Petri dish under a dissecting microscope and, using a fine tipped probe, quickly dabbed with a small mark of nail polish on the posterior of whichever valve was facing upward. The quick-dry polish was given one minute to dry before the animals were placed into a dish of clean sea water. Marked individuals were maintained in the laboratory at ambient temperature and in freshly collected seawater from the time of collection (ca. 07:00 h) until sunset (ca. 18:00 h) at which time they were released back into the seagrass bed near the site of their capture, which was flagged and noted on GPS.

To control for mortality due to the marking process, marking failure, and molting during the experiment, one set of 238 animals was marked and kept in the laboratory in a 750 ml container of clean sea water for the duration of the study. I used the proportion of *V. annecohenae* that survived and maintained their markings in

reference group to calculate an adjusted number of individuals available for recapture in each study (Table 3.1). Note that this adjustment, based on animals held in laboratory conditions, likely underestimated the actual loss of markings on animals in the field. Therefore recapture rates during the studies, if inaccurate, would likely be conservative.

For each experiment, marked *V. annecohenae* were transported to the field in a small plastic container that had been filled with seawater so that it contained no air bubbles. The absence of air bubbles made it possible to submerse and open the container under water at the substrate with minimal disruption of the ostracods. The container was opened near the water-sediment interface, within the grassbeds. Upon release, the ostracods could be seen immediately swimming quickly downward to the base of the seagrasses. The release point was marked with a flag and its GPS position noted for easy relocation. Twenty-four hours was chosen as the duration for this study based on three preliminary trials, two in which traps were set at both 24 and 48 h after release and one in which traps were set only at 48 h after release. Because only 2.3 % ($\pm$/- 1.3 %, n = 3) of marked individuals were recaptured after 48 h, 24 h was selected as the more useful interval of study. Recapture traps were deployed at sunset of the day following release. Three 15 m transect lines were extended from the release site in equal trilateral directions with one line distributed directly into the predominant current. Traps were attached to the transect line with brass clips at 1 m, 3 m, 5 m, 10 m and 15 m, from the release site, and one trap was placed at 0 m (16 total traps). The traps were left in place overnight and collected after sunrise (ca. 07:00). Each trap was placed into a labeled Ziploc™ bag while underwater and sealed to retain any individuals that might escape the trap during transport to the laboratory. Once in the laboratory on South Water Caye, each trap was immediately emptied into a plastic

Table 3.1. The location, date and total number of animals marked and recaptured, corrected for estimated loss of ostracods (see Methods for details).

Site	Date	Total Marked	Corrected # for Recapture	Total Recaptured	% Recapture
South Beach	1/11/2004	1314	881	47	5.33
South Beach	1/14/2004	474	318	52	16.35
South Beach	1/18/2004	2070	1387	118	8.51
South Beach	6/3/2003	983	659	36	5.46
South Beach	7/14/2003	815	546	39	7.14
Twin Caye	5/5/2005	1063	713	56	7.85
Twin Caye	5/13/2005	1034	693	41	5.92
Carry Bow Cut	5/17/2005	866	581	56	9.64
Carry Bow Cut	5/19/2005	1355	908	65	7.16

dish containing freshly collected sea water and any remaining bait removed. Captured *V. annecohenae* individuals were maintained in the laboratory (max. 1 day) at ambient temperature until they could be counted, aged and sexed (if A-I or adult) under a dissecting microscope. A total of nine mark and recapture studies were conducted, five at a single location near the south beach of South Water Caye, two at a site near the south end of Twin Caye and two in the cut between South Water Caye and Carry Bow Caye (Figure 3.1, Table 3.1).

In addition, three studies were conducted at sites between the north end of South Water Caye and Twin Cayes to test dispersal across specific boundary types. In two of these studies, *V. annecohenae* were collected from an area of dense seagrass adjacent to a sand patch. In the third, *V. annecohenae* were collected in an area of distinctly reduced seagrass density. Marked individuals were released in the heavy seagrass region from which they had been collected but less than 1m from the edge of the seagrass (near a sand flat) or near a low seagrass density habitat. Recapture traps were placed along a single line that stretched in opposite directions from the point of release. One line was run further into the seagrass habitat and one line was run into the sand habitat or low seagrass density habitat, across the boundary. Again, traps were set at 0 m, 1 m, 3 m, 5 m, 10 m, and 15 m from the release site.

I used a correlated random walk in a homogenous habitat parameterized with dispersal estimates from the mark and recapture studies (Beyers 2001) to calculate minimum, average and maximum lifetime dispersal potentials. Because instars A-V and A-IV were rarely captured and there were no significant differences among the dispersal distances of the other juvenile instars, Beyers' model was run using an average dispersal value for juvenile instars A-III, A-II and A-I combined. Dispersal of adult females and males was calculated separately. Dispersal of three hundred individuals of each instar group was simulated for 30 days and the average and

maximum dispersal estimates recorded. Finally, I estimated lifetime dispersal by multiplying movement estimates by the duration of each instar (based on Gerrish and Morin *in press*), and then summing juvenile and adult dispersal estimates.

GIS map construction:

Habitat:

I constructed a GIS habitat map based on images and initial categorizations of the study area conducted by Ballas and Gaston (2006). The image stretches along the inside of the barrier reef of Belize from north of Tobacco Caye (16.898989º N, -88.061610º W) and Tobacco Range to (16.891219º N, -88.085011º W) just south of Carry Bow Caye (16.802629º N, -88.081903º W) and Twin Cayes (16.831544º N, -88.102718º W). Ballas and Gaston (2006) categorized seagrass densities throughout this region of the satellite image and point verified seagrass densities and water depth at over 250 locations. I further verified seagrass density (using the method of Ballas and Gaston 2006) and water depth using a handheld digital sonar (Hawkeye DF2200PX) at 53 additional sites. Based on the image, knowledge of the region and recorded depth measurements, I manually drew depth contours into the GIS map.

I measured water velocity at 15 sites throughout the study area using mechanical flow meters (General Oceanics: model 2030) attached to rebar rods and positioned in the water just above the top of the seagrass at each site. Meters were placed at each site for 48 hours and readings were taken each morning and evening (approximately every 12 hours from initial deployment) for a total of 5 readings from each location. The number of rotations over time was used to calculate water velocity based on factory calibrations of the meters, yielding relative water velocity rates across the 15 sampled habitats.

Distribution:

Relative densities of *V. annecohenae* across sites were estimated using the average number of animals captured in baited traps over a known period of time. Densities were inferred from the number of animals captured based on the assumption that *V. annecohenae* actively foraged equally across sites and across sampling nights. To control for variation in activity across nights, sampling took place only during the first six to seven nights following the full moon when no moon was present in the sky following sunset. The activity of *V. annecohenae* varies in response to lunar light (Gerrish et al. *submitted*) and this variation is minimized when no moon is present in the sky.

V. annecohenae density was measured at 52 sites across the study area (Figure 3.1). Sites were chosen to represent a range of seagrass densities, sand habitats, depths and water velocities. Furthermore, sites were selected at a range of distances from one another to allow spatial patterns to be analyzed. At each site, three baited inverted funnel traps (see above) were deployed for one hour during the bioluminescent display period (first 1 - 2 h of darkness each night at the end of twilight; Gerrish et al. *in press*). Three traps were deployed at four or five sites each night and sites were marked with bouys and using GPS. After one hour, we relocated the sites using GPS and retrieved the traps. Traps were placed into individually labeled, seawater filled Ziploc™ bags and transported to the laboratory. The precise duration that each trap was deployed in the field was recorded. All individuals collected in each trap were counted, aged and sexed (for A-I and adults); densities are represented by the number of *V. annecohenae* captured per hour.

GIS Cost Analysis:

'Cost' in GIS is a relative value assigned to a landscape feature (ArcGIS, ESRI 2005), such as the 2 m water depth contour area; or a continuous habitat type, such as areas with seagrass densities greater than 50 blades/m^2. Within the GIS analysis, I assigned cost to each region of the study area based on the relationships between habitat variables and *V. annecohenae* density. First, independent cost maps were built based on each of the three habitat variables; seagrass density, depth, and water velocity. To assign relative costs based on seagrass density, I first calculated average *V. annecohenae* densities for each discrete class of seagrass densities (0, 5, 10, 20, 30, and 50 blades / m^2). I then calculated the proportion of animals captured within each seagrass density and assigned the grass class with the highest density of *V. annecohenae* a value of zero. Relative costs were then assigned for each additional seagrass density based on a 0 – 10 unit scale. Costs were assigned to each depth contour (0 - 2, 2 - 4, 4 - 6, 6 - 8, and 8 - 10 m) using a similar calculation based on average *V. annecohenae* densities across depth. Flow was partitioned into three classes, 0 – 1 cm/s, 1 – 4 cm/s and > 4 cm/s, based on natural breaks within the average *V. annecohenae* densities, and then costs were assigned. Once the three independent cost landscapes were constructed and standardized using a 0 to 10 unit scale, the maps were added together using the Map Algebra function in ArcView (Environmental Systems Research Institute, USA). The costs associated with each habitat variable were weighted equally. Upon addition, each 30 m × 30 m pixel of the study region was assigned a cumulative cost value representing the accumulated costs based on each habitat factor. This level of resolution yielded a manageable landscape for least cost path analysis.

Cost path analysis in GIS uses a statistical accumulated cost model to draw the path of least costs among points throughout a landscape. I used ArcView to draw the

least cost paths between all points for which *V. annecohenae* densities were recorded and manually calculated the number of pixels in each path between locations sampled for genetic analysis. I then regressed cost distances against genetic distances for each pair of sites and tested the relationship using linear regression in SYSTAT 9.0 (Systat Software Inc.)

Population Genetics:

I developed four microsatellite DNA markers to determine if population genetic structure varied spatially for *V. annecohenae*. Microsatellites are tandem repeats (e.g. CTTCTTCTTCTTCTT) found in DNA that are non-functional and selectively neutral (Jarne and Lagoda 1996). Because of their relatively rapid rate of mutation, microsatellites are commonly used for population level genetic analyses.

My microsatellite library was built using DNA extracted from *V. annecohenae* collected just off the southern tip of South Water Caye, Belize. I used an SNX linker and ligation protocol similar to that presented by Hamilton et al. (1999) to isolate and optimize four loci. For the comparative analysis, DNA was extracted from 35-40 individuals from each site which were collected during density sampling and placed into clean 10-ml vials filled with 95% ethanol. Where fewer than 35-40 were collected, all individuals obtained were preserved. Upon preservation, the ostracods exuded their bioluminescent products which were visible in the bottom of the samples as a yellow liquid layer. To make sure these products did not degrade the DNA in preserved samples, all ethanol was replaced four to five days after preservation. Molecular analyses were conducted in the Evolutionary Genetics Core Facility (EGCF) at Cornell University. Using a Qiagen DNEasy tissue extraction kit (QIAGEN), DNA was extracted from 24 individuals (when possible) from each of 22 sites (Figure 3.1), including two distant sites outside of the satellite image area that

served as outgroups, Glovers Reef (16.771317º N, -87.783498º W), 34.6 km to the east and Pelican Cayes (16.674238º N, -88.188239º W) 19.5 km to the south. Sites were selected to represent the full range of habitats and the full spatial extent of the study area. DNA was extracted from single whole individuals using a Qiagen tissue extraction kit (QIAGEN) and eluted into 100 µl of AE buffer. In a 10µl polymerase chain reaction (PCR), reaction reagents varied slightly in ratio for each marker but consisted of approximately 7.37 µl water, 1 µl 10 × PCR buffer, 0.4 µl Magnesium (50 µm), 0.15 of each the forward and backward primer (10 µm), 0.08 µl dNTP (25 µm), 0.1 Taq, and 0.75 DNA. The PCR profile was 95°C for two minutes, 34 cycles of 95°C for 50 seconds, a loci specific annealing temperature for one minute, and finally 72°C for one minute. Upon cycle completion products were frozen at -80°C until they could be analyzed. Fragment sizes were determined using an ABI 3100 automated capillary DNA sequencer with GeneScan-500 LIZ size standard (Applied Biosystems). Allele sizes were estimated using Genemapper version 3.5 (Applied Biosystems) and were verified by eye.

I used FSTAT 2.9.3.2 (Goudet 2002) to test assumptions of heterozygosity and linkage disequilibrium between and within sites and loci. FSTAT was also used to estimate Nei's (1978) genetic distances among all sites. Genetic distance estimates were then used in regressions against geographic distances and cost distances, and to build a neighbor joining phylogentic tree in PHYLIP 3.67 (Felsenstein 2007), which was plotted using FigTree 1.0 (Rambaut 2006). Because I had no *a priori* indication of the number of populations in the dataset, I used the Bayesian method in STRUCTURE 2.2 (Pritchard et al. 2000) to define population structure. This program uses Bayesian clustering without prior information about the source of sampled individuals. Using STRUCTURE (Pritchard et al. 2000), the number of genetic clusters (K) were inferred from Markov chain Monte Carlo (MCMC) sampling

methods, with five independent MCMC runs of 80,000 steps following a 30,000 step burn-in for each K from K = one to eight. I assumed correlated allele frequencies among populations, did not use information on the population of origin, and followed an admixture model with a single value of lambda (lambda = 1.0) inferred for all populations. I estimated K based on the log likelihood score and posterior probability of K (Falush et al. 2007), as well as the rate of change in the log likelihood score (Evanno et al. 2005).

RESULTS

Mark and Recapture:

On average, 8.15 % of the *V. annecohenae* that were released were recaptured, but this number varied among sites and replicates between 5.33 % and 16.35 % (Table 3.1). There was no significant directional movement of the animals recaptured at any site (i.e., no orientation relative to current direction; Table 3.2). Since one line of traps was consistently oriented into the dominant current direction of an area and the additional two lines were consistently oriented 120º to the first line, the lack of directional effect indicates that we detected no significant influence of water current. Furthermore, there was no significant difference in the average number of animals recaptured at each of the three sites (Table 3.2).

There was a significant difference in the average distance moved among sites, with greater distances observed at the Twin Caye and Carry Bow Cut sites than at the South Beach site (Table 3.3). Because there was no significant directionality to movement (Tables 3.2 and 3.3), I grouped the number of animals moving each distance regardless of direction for each study. However, I kept sites separate based on the observed significant effect of site on distance moved (Table 3.3).

Table 3.2. ANOVA of site and directional factors influencing the number of *V. annecohenae* recaptured.

Source	SS	df	MS	F-ratio	P
Site	39.419	2	19.709	0.462	0.637
Direction	13.006	2	6.503	0.152	0.860
Site x Direction	111.348	4	27.837	0.653	0.633
Error	767.900	18	42.661		

Table 3.3. ANOVA of site and directional factors influencing the average distance moved by *V. annecohenae*.

Source	SS	df	MS	F-ratio	P
Site	46.905	2	23.453	7.198	0.005
Direction	5.901	2	2.951	0.906	0.422
Site x Direction	25.656	4	6.414	1.968	0.143
Error	58.652	18	3.258		

Bonferroni adjusted pairwise comparisons of the three sites (df = 18).

Site	p-value
South Beach vs. Twin Caye	0.012
South Beach vs. Carry Bow Cut	0.041
Carry Bow Cut vs. Twin Caye	1.000

To test for variation in distance moved by each age class among sites, I removed instars A-V (1st) and A-IV (2nd) from the statistical analysis because no individuals in either of these age classes were recaptured. This lack of recapture is likely due to overall low numbers of these instars captured in traps. Because the data were not normally distributed due to low recapture numbers for particular instars, I natural-log transformed these data prior to statistical analysis. Following transformation, both probability plots and histograms indicated that the transformed data were normal. Juvenile instars and adult females moved an average of 1.8 m and 2.6 m in 24 h respectively, while adult males moved significantly farther (Bonferroni corrected p-value = 0.004), averaging 5.1 m in 24 h (Figure 3.2). This pattern of variation between instars did not differ significantly among sites (Table 3.4).

I used Beyers (2001) model in which each progressive "step" by an individual was non-randomly influenced by the previous step, reducing the turning radius for organisms into a correlated random walk model. This pattern of movement has been found commonly in insects and other invertebrates (Beyers 2001). Applying it to *V. annecohenae* gives an estimated average lifetime movement for females of 147 m and 244 m for males, while the maximum movement distances were 233 m for females and 392 m for males (Table 3.5).

Habitat:

Depth contours, based on actual measurements and contours visible in the satellite image, show distinct shallow regions (0 m – 2 m) surrounding each of the sandy barrier islands (Figure 3.3A). Furthermore, the crest of the reef and region immediately inland of the reef are shallow flats (0 m - 1 m) that contain scattered coral heads and sparse or no seagrass. The majority of the study area is between 4 m and 5 m deep. However, between Twin Caye and Tobacco Range, and south of Twin Caye

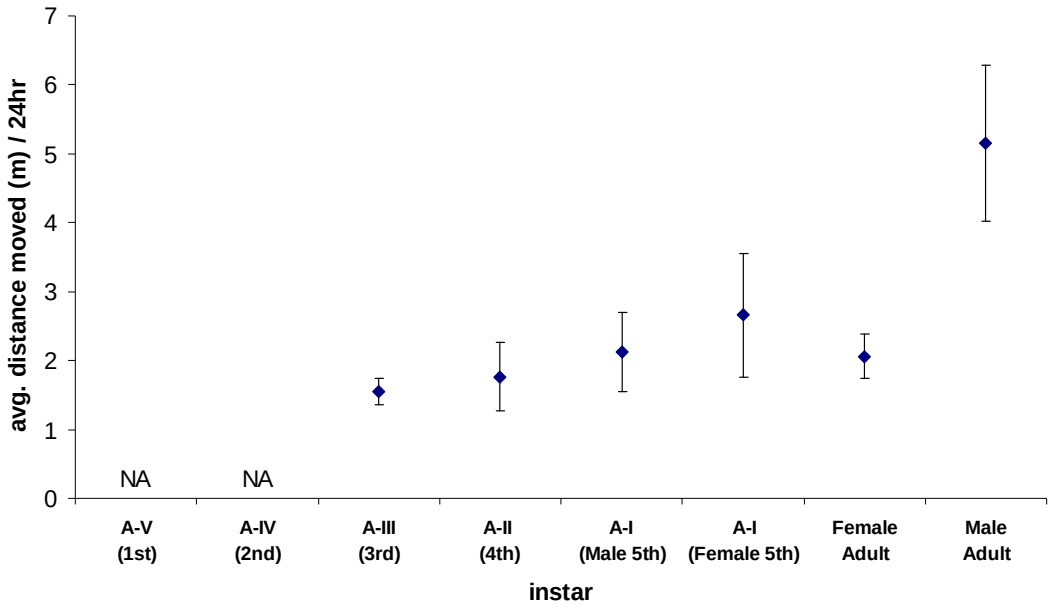

Figure 3.2. Mean (± 1 s.e.; n = 510) distance moved by each instar (at all sites) of *V. annecohenae* in 24 h mark and recapture studies.

Table 3.4. ANOVA of site and instar factors influencing the average distance moved by *V. annecohenae*.

Source	SS	df	MS	F-ratio	P
Site	0.021	2	0.010	1.104	0.342
Instar	0.226	5	0.045	4.838	0.002
Site x Instar	0.161	10	0.016	1.717	0.115
Error	0.337	36	0.009		

Table 3.5. Random walk dispersal estimates based on demographic movement measures from mark and recapture using Beyers' (2006) model.

Age/Sex	Average Instar Duration	Random Walk – 30 day Mean Dispersal	Random Walk – 30 day Max Dispersal	Avg. Dispersal Estimates for instar duration (m)	Potential Dispersal (max)(m)
Juvenile	90-100 days	17.06 ± 8.91	26.09	54.08	82.7
Adult Female	140-180 days	18.04 ± 9.61	28.29	93.27	149.94
Adult Male	120-150 days	42.21 ± 22.7	68.81	189.95	309.65

	Lifetime Dispersal (avg.)	Lifetime Dispersal (max.)
Female	147.35	232.64
Male	244.03	392.35

Figure 3.3. Habitat classification of a satellite image of the study area using GIS. A. Depth contours were drawn between 2 & 3 m, 3 & 4 m, 5 & 6 m, and 7 & 8 m based on direct field measurements, knowledge of the region, and regions apparent on the satellite imagery. B. Water velocity represented by sizes of circles. Yellow circles represent sites where flow was measured using mechanical flow meters. Orange circles represent sites where flow was estimated based on the contours of the system and the location of the reef cut. C. Seagrass densities as assigned by Ballas and Gaston (2006).

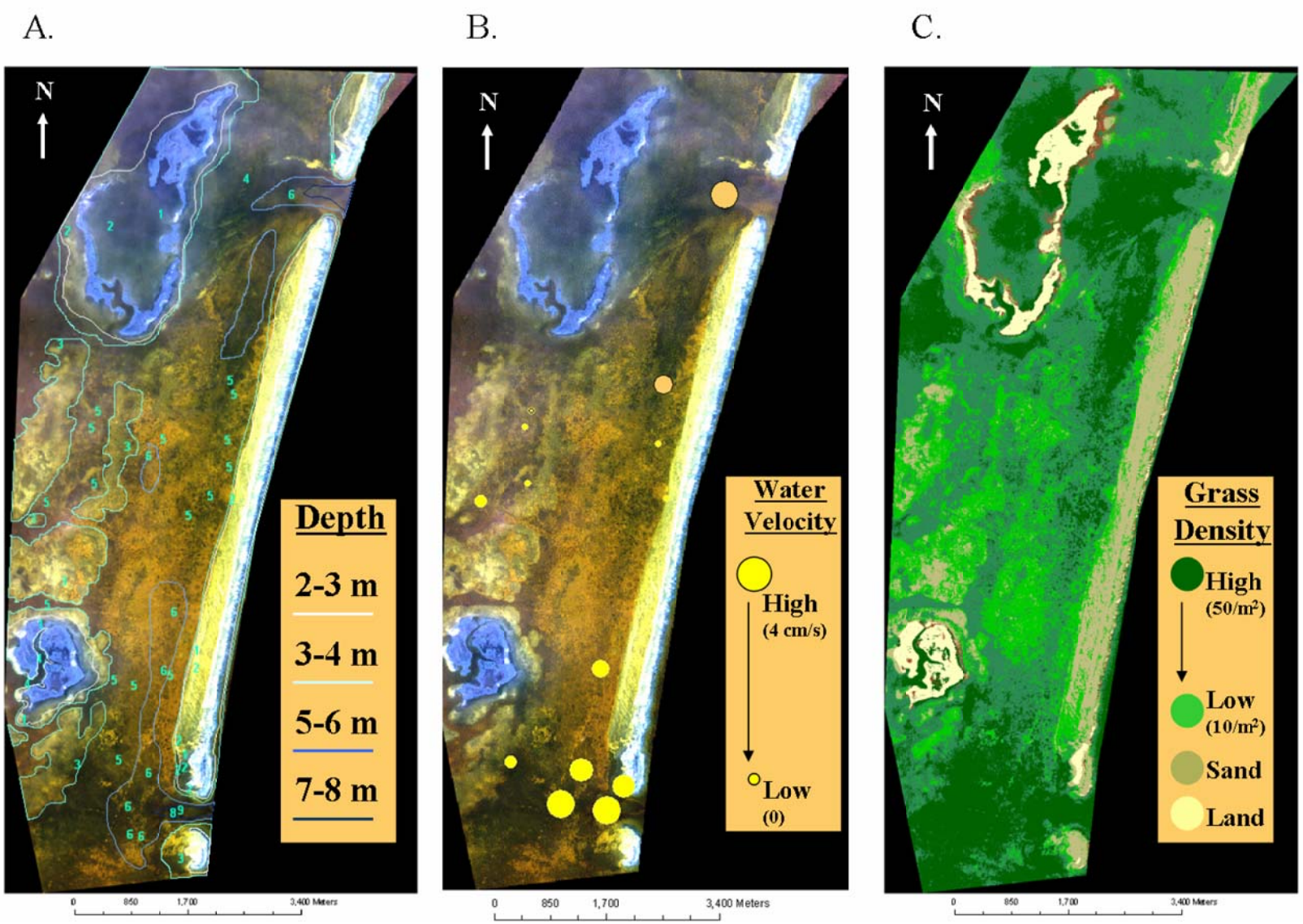
A.
B.
C.
N
Depth
2-3 m
3-4 m
5-6 m
7-8 m
Water Velocity
High (4 cm/s)
Low (0)
Grass Density
High (50/m²)
Low (10/m²)
Sand
Land
0 850 1,700 3,400 Meters

there are distinct ridges rising to within 3 m of the surface and cut by 5 m deep depressions (Figure 3.3A). The deepest areas (7 m - 9 m) occur at the two reef cuts, just south of Tobacco Caye and just south of South Water Caye.

Water velocity was highest inside and near the opening of the South Water Caye reef cut (Figure 3.3B), ranging between 0.18 cm/s and 9.2cm/s. Water velocity declined with increasing distance from this cut both west toward Twin Caye and north of South Water Caye. In sampled locations immediately behind the shallows of the reef and farther north of South Water Caye (approximately halfway between South Water Caye and Tobacco Caye), water velocity was below the minimum level detectible (0.06 cm/s) by the mechanical flow meters (Figure 3.3B). Between Twin Caye and Tobacco Range, water velocity varied between low and mid-range values (0 – 1.5 cm/s).

Ballas and Gaston (2006) provided specific protocols of seagrass habitat assignment in GIS. Overall, they identified 50 habitat classifications, including above water island habitat, coral heads, sandy substrate, and approximately 30 seagrass density classifications (Figure 3.3C).

Distribution:

V. annecohenae was captured throughout the study area wherever seagrass was present. Densities varied among sites with between 0 and 819 individuals captured/hour. The highest densities were captured in the 5 m depressions between Twin Cayes and Tobacco Range and lowest densities were captured in the shallow regions just behind the reef in low seagrass or sandy areas (Figure 3.4). The greatest densities of *V. annecohenae* were captured at intermediate depths (ca. 5 m), with

Figure 3.4. Seagrass density, water velocity and water depth maps overlaid. Red bars indicate the density of *V. annecohenae* captured per hour at each of 52 sites.

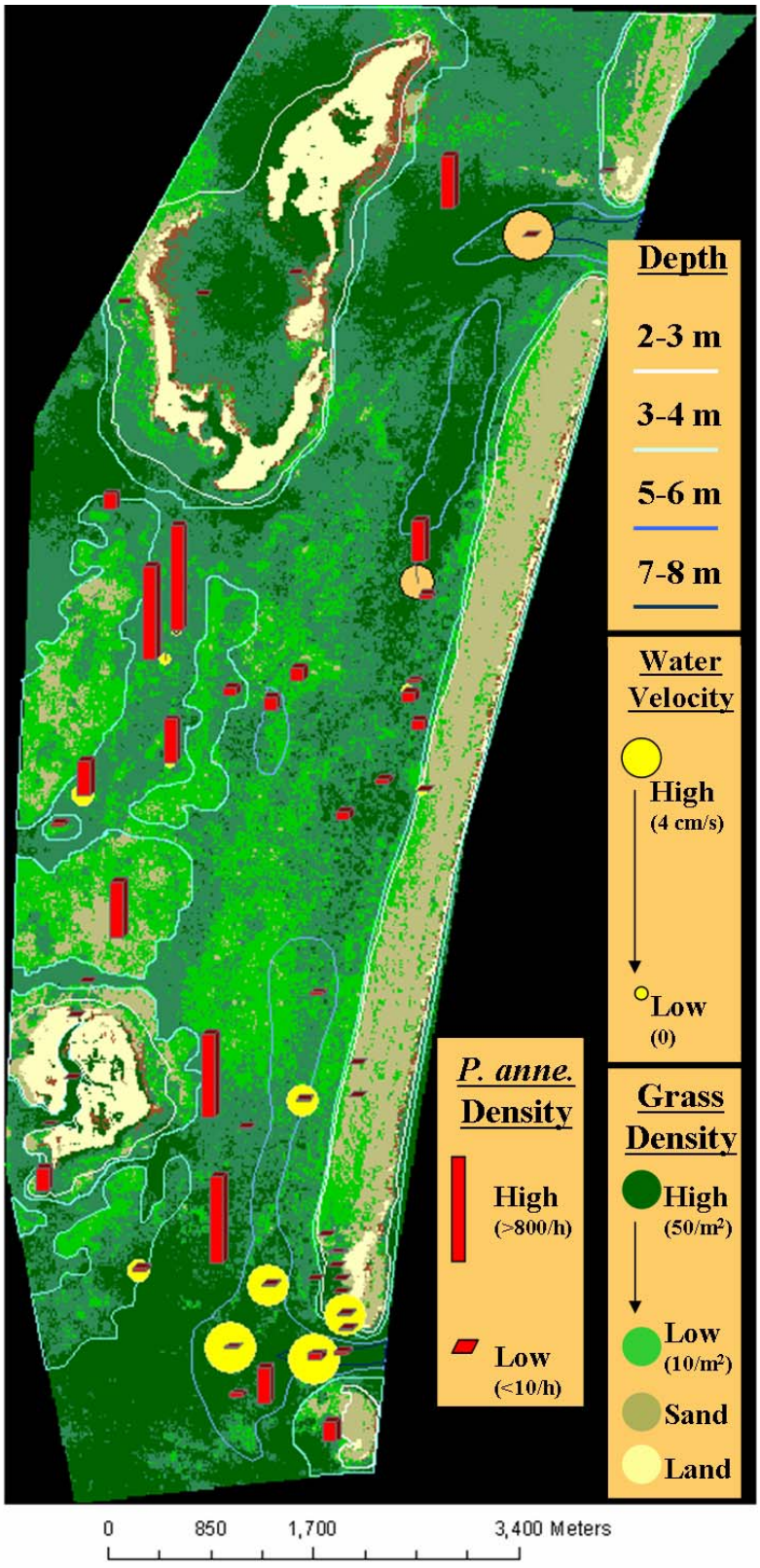
Depth
2-3 m
3-4 m
5-6 m
7-8 m
Water Velocity
High (4 cm/s)
Low (0)
P. anne. Density
High (>800/h)
Low (<10/h)
Grass Density
High (50/m²)
Low (10/m²)
Sand
Land
0
850
1,700
3,400 Meters

fewer individuals captured in water shallower that 3 m or deeper than 6 m, and very few to no individuals captured in water depths ranging from 1 m to 2 m or greater than 7 m (Figure 3.5A). The greatest densities of *V. annecohenae* were captured at sites with very low water velocity, but some animals were also captured at moderate velocities. The fewest individuals were captured at the sites with highest water velocity (> 4 cm/s; Figure 3.5B). Finally, the greatest densities of *V. annecohenae* were captured in habitats with intermediate seagrass densities (ca. 20 blades/m^2). No *V. annecohenae* were captured presumably because they or only present in extremely low densities, in regions with either very high seagrass density (> 50 blades/m^2) or very low seagrass density (0-10 blades/m^2) (Figure 3.5C).

Cost Map and Least Cost Paths:

The cumulative cost map indicates that there are low cost [=good or easiest] regions for movement throughout the habitat and they occur in habitats throughout both the north and south (Figure 3.6). Seagrass density influences the cost assignments throughout at a finer scale than either flow or depth (Figure 3.6). The impacts of depth and flow strongly influence the cost assignments near the reef cuts where > 8 m water depth and high flow are both higher cost assignments and combine to create high cost areas (Figure 3.6). Costs in relation to depth are also apparent between Twin Caye and Tobacco range where the deeper channels have zero cost assigned and the 3 m ridges received a cost assignment of seven (Figure 3.6).

Least cost paths between all pairs of sampled points illustrate the common lack of continuous low cost (good) habitat corridors between points. Instead, the pathways of lowest cost wind around in looping and hairpin turns (Figure 3.6).

Figure 3.5. The density of *V. annecohenae* captured per hour versus: (A) water depth; (B) water velocity - density was converted using natural log; (C) the number of seagrass blades per square meter - red bars indicate averages for each seagrass density. Cost values, assigned based on ostracod densities, are provided for each grass density (A), depth contour (B) and water velocity grouping (C).

A.

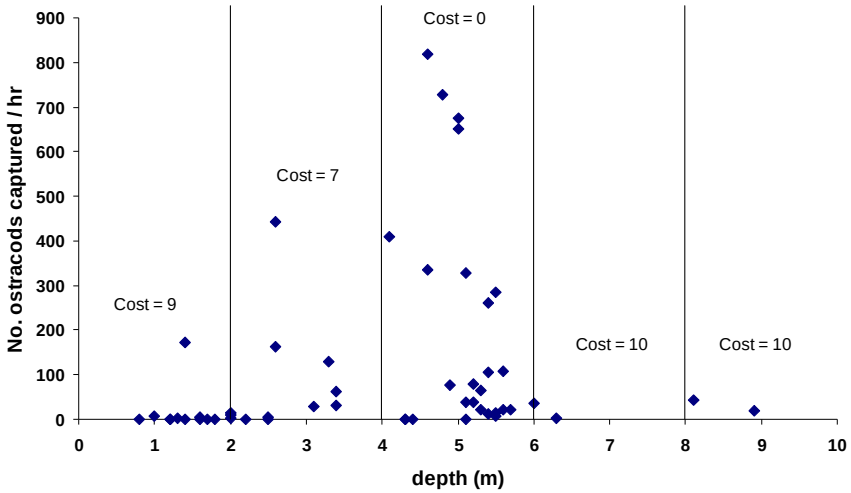
No. ostracods captured / hr
depth (m)
Cost = 9
Cost = 7
Cost = 0
Cost = 10
Cost = 10

B.

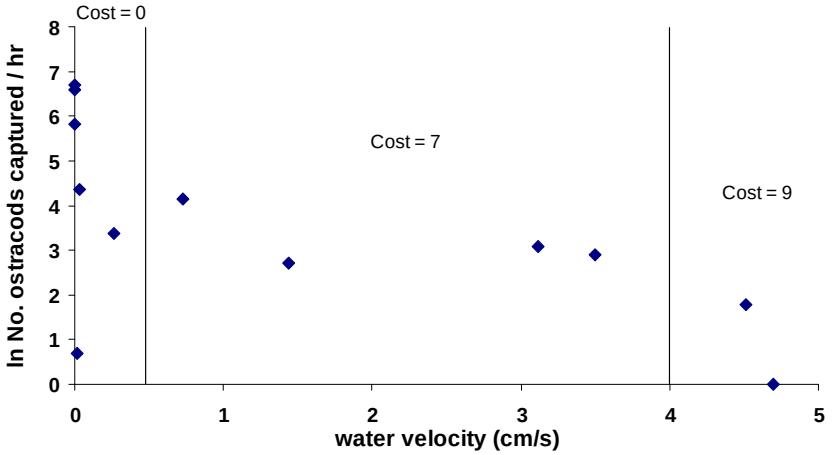
ln No. ostracods captured / hr
water velocity (cm/s)
Cost = 0
Cost = 7
Cost = 9

C.

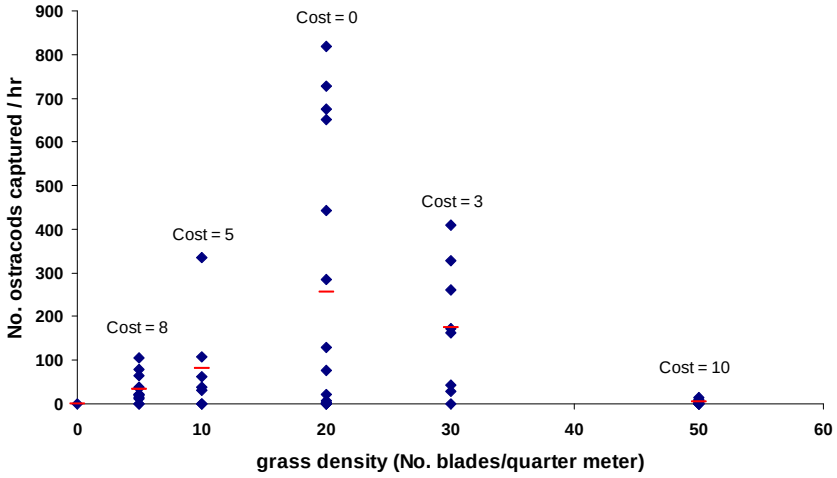
No. ostracods captured / hr
grass density (No. blades/quarter meter)
Cost = 8
Cost = 5
Cost = 0
Cost = 3
Cost = 10

Figure 3.6. Cost map and least cost paths created in the GIS, based on relationships between habitat characteristics (seagrass density, water velocity, and water depth) and the density of *V. annecohenae*. Independent cost maps for each habitat factor were added using the Map Algebra function in ArcView (Environmental Systems Research Institute, USA), which resulted in this accumulated cost map. For each 30 m × 30 m region, the cost of moving through the area is represented by its color. Light areas have zero cost and dark (black) areas have an assigned cost of ten. The least cost paths between all sampled sites were calculated in ArcView. Red indicates the paths by which the disperser will encounter habitats with lowest costs. Higher cost paths ranging from blue to green are only created when animals must cross higher cost areas to move between sites.

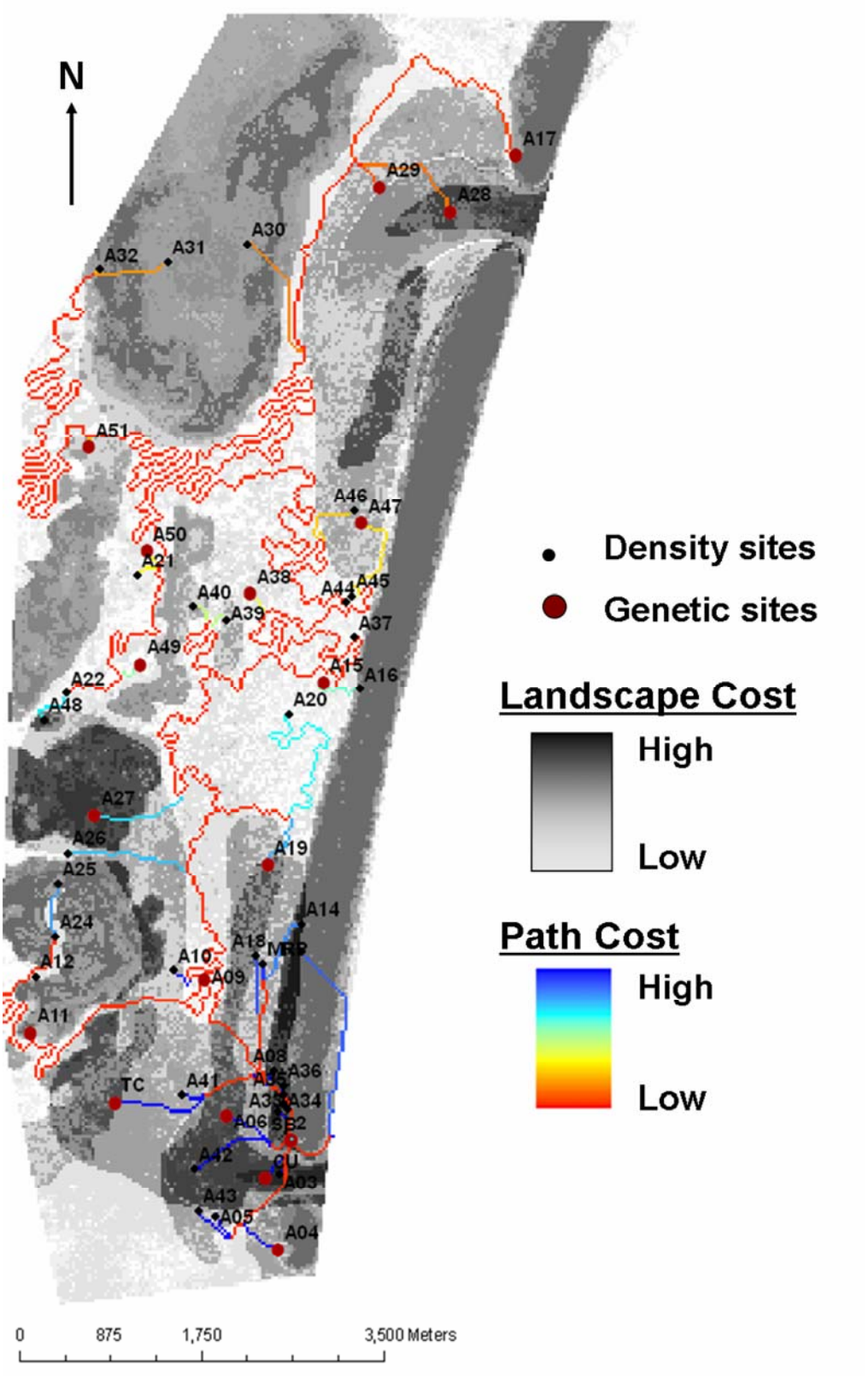
N
A17
A29
A28
A30
A32
A31
A51
A46
A47
A50
A21
A38
A40
A44
A45
A39
A37
A49
A15
A16
A22
A48
A20
A27
A26
A19
A25
A14
A24
A18
MR2
A12
A10
A09
A11
A08
A36
TC
A41
A34
A06
SB2
A42
GU
A03
A43
A05
A04
Density sites
Genetic sites
Landscape Cost
High
Low
Path Cost
High
Low
0
875
1,750
3,500 Meters

Population Genetics:

In the program STRUCTURE, the posterior probability for K (the estimated number of populations based on genetic identities), reached a plateau beyond K=2 indicating that there are two distinct populations within the data set (Pritchard 2007). This division was further supported by the rate of change in the log likelihood score based on Evanno (2005), which was over 150 times higher for K=2 than for any other potential K (1-8). Furthermore, in each STRUCTURE simulation, the same populations consistently divide into two distinct groupings.

Assumptions of Hardy Weinberg equilibrium for all loci across sites were met (Fstat version 2.9.2.2 Feb 2002) and linkage disequilibrium was not significant between any pair of loci (Table 3.6). The sites separated into genetic populations in STRUCTURE that were geographically divided into 'Northern' and 'Southern' populations (Figure 3.7). The 'Southern' population consists of all six sites south of South Water Caye and Twin Caye (Figure 3.7). Additionally, the Pelican Caye site, which is 20 km further south of Carry Bow Caye, groups within the 'Southern' population. There is only one site just north of Twin Caye that has a 'Southern' genetic signature. The 'Northern' population extends all the way from north of Tobacco Caye, down to the sites just northwest of South Water Caye and some sites between Twin Cayes and South Water Caye (Figure 3.7). The out-group from Glover's Reef, which is 35 km east the study area and separated by a trough of very deep water (> 500 m), has a genetic signature that groups it with the 'Northern' population.

A phylogenetic tree based on nearest neighbor estimation of genetic distances clearly divides the two populations that were identified by STRUCTURE (Figure 3.8). Within the 'Southern' population, the site north of Twin Caye, A27, is the most divergent and most closely related to the northern group and thus may indicate some

Table 3.6. P-value for genotypic disequilibrium based on 600 permutations in FSTAT.

Adjusted P-value for 5% nominal level is : 0.008333

Adjusted P-value for 1% nominal level is : 0.001667

Loci	P-value
10 X 32	0.01667
10 X 7	0.46167
10 X 76	0.13833
32 X 7	0.91500
32 X 76	0.93833
7 X 76	0.21833

Figure 3.7. Map of genetic populations. The six sites comprising the 'Southern' population are represented by grey squares (squares for the two sites closest to South Water Caye overlie each other). Additionally, the far south site at Pelican Cayes (outside the study area) has a 'Southern' genetic signature. Sites in the 'Northern' population are represented by circles and individuals from Glover's Reef, to the east and outside the study area, have 'Northern' genetic signatures.

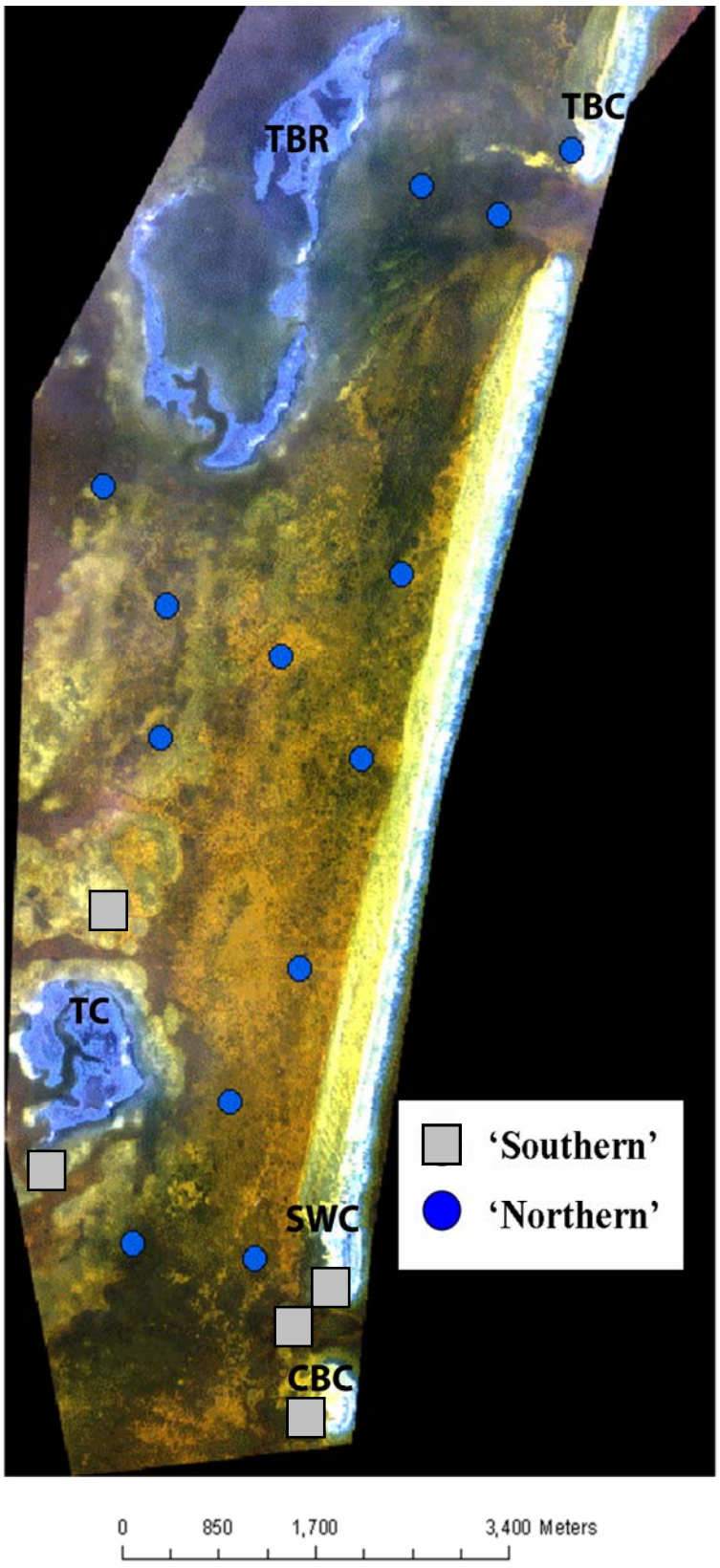
TBR
TBC
TC
SWC
CBC
'Southern'
'Northern'
0
850
1,700
3,400 Meters

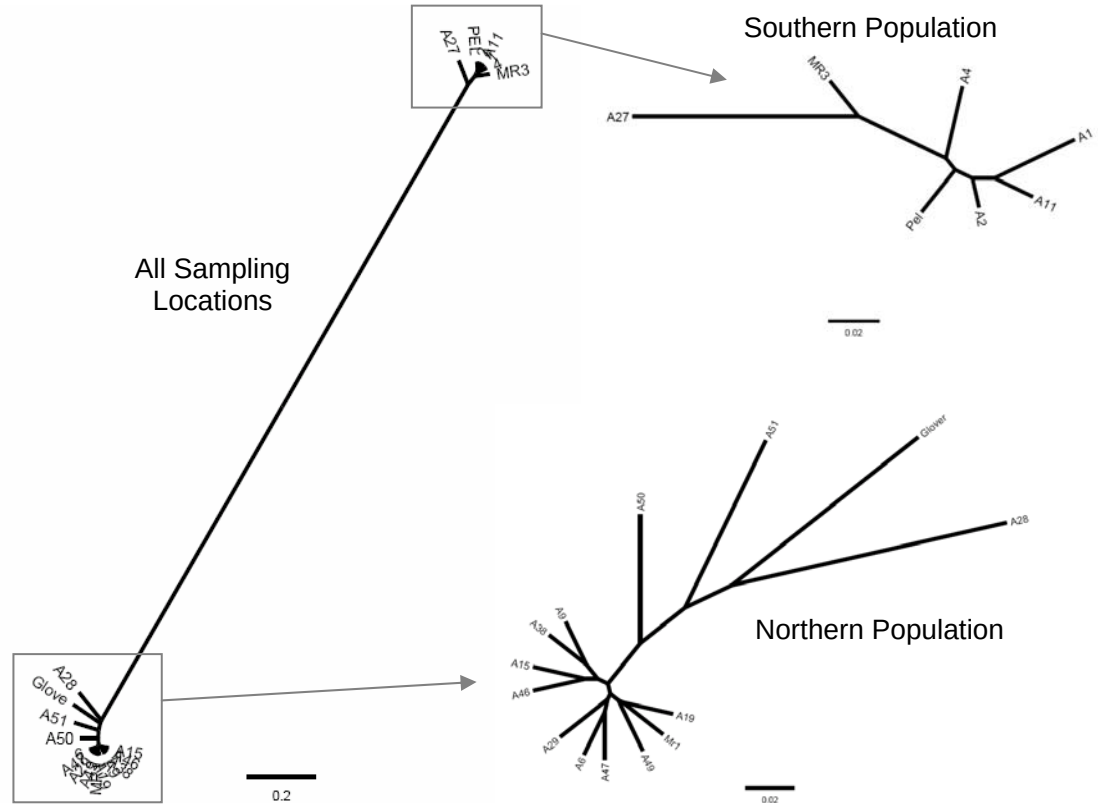

Figure 3.8. Unrooted relatedness trees created using neighbor joining in PHYLIP and plotted using FigTree. The plot of all sites (locations shown in Figure 3.6) together shows two distinct populations. Details for sites within the 'Southern' and 'Northern' populations are plotted separately.

gene flow between these two populations. However, it still strongly fits within the 'Southern' population (Figure 3.8). The least divergent sites within the 'Northern' population lie toward the north end of the study area and the three most divergent were A50 and A51, which lie between Twin Caye and Tobacco Range, and site A28, which is in the center of the study area. The outgroup site, Glover's Reef is, not surprisingly, also the most divergent from the rest of the 'Northern' population (Figure 3.8).

When comparing Nei's genetic distance (Ds) as calculated by FSTAT (Goudet 2002) and geographic distances based on GPS-UTM measurements between each site pairing (excluding the outgroups) there are higher genetic distances between 'Northern' and 'Southern' sites than there are within either population (between North and South Ds = 0.289, within North Ds = 0.018, and within South Ds = 0.017, ANOVA df = 2, $F = 611.45$, $p < 0.001$) (Figure 3.9A.). On the other hand, between these two populations or within both populations there is no significant relationship between physical distance (ln-transformed for statistics) and genetic distance (between north and south $r^2 = 0.0006$, $p = 0.792$, within north $r^2 = 0.0659$, $p = 0.862$ and within south $r^2 = 0.884$, $p = 0.842$).

Comparisons of Nei's genetic distances with GIS least cost distances indicate that in comparisons of sites between 'Northern' and 'Southern' populations, relatedness is significantly lower between sites with greater cost distances ($r^2 = 0.225$, $p < 0.001$), Figure 3.9B), indicating that the habitat variables included in this study are limiting gene flow. However, this negative relationship is not maintained in site comparisons within either the 'Northern' ($r^2 = 0.038$, $p = 0.086$) or 'Southern' populations ($r^2 = 0.099$, $p = 0.254$) (Figure 3.9B).

A.

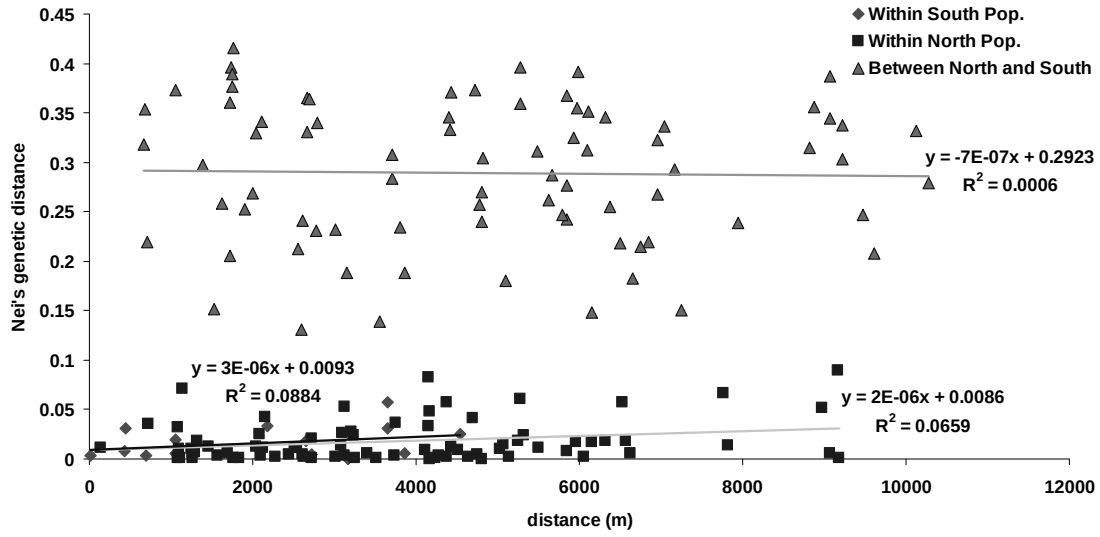

B.

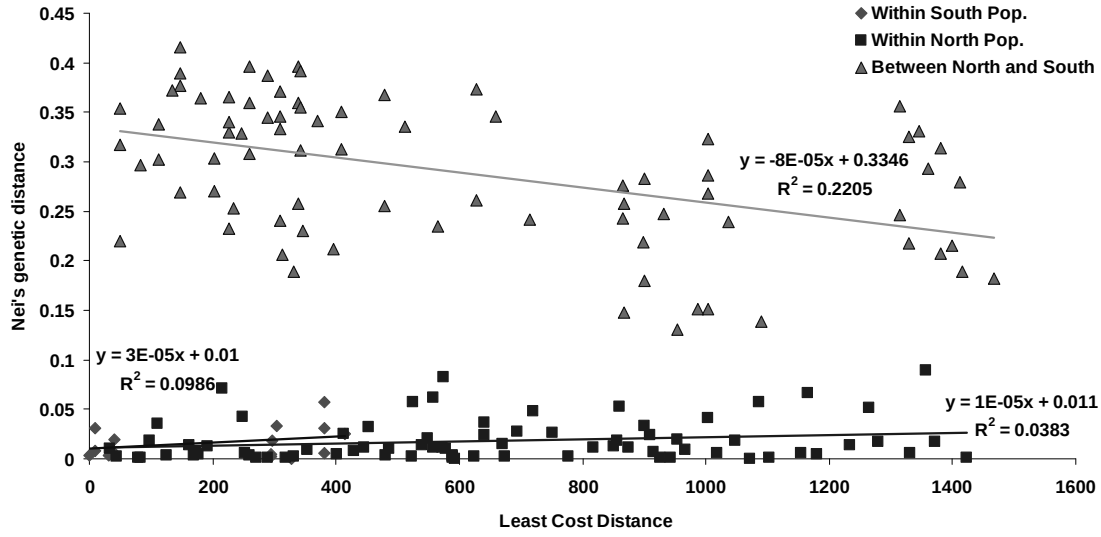

Figure 3.9. Genetic distances (Nei 1978) among all pairs of sites. Triangles: between 'northern' and 'southern' sites; squares: site pairs within the 'northern' population; diamonds: site pairs within the 'southern' population. A. Genetic distance vs. geographic distance among sites. B. Genetic distance vs. GIS least cost distance among sites.

DISCUSSION

For a predominantly benthic organism, *Vargula annecohenae* disperses large distances given a continuous seagrass habitat, with males moving over a third of a kilometer in a lifetime. This means that within 20 to 30 generations some male descendents should be able to traverse the entire study area if there were no barriers to movement. Based on this high level of dispersal, I would expect a rather homogenous genetic population throughout the region perhaps with some divergence at the extreme north and south ends. However, contrary to expectations, instead we see two clear genetic signatures (Figure 3.8) and no relationship between Nei's genetic distances and geographical distances between sampling locations (Figure 3.9A) indicating that there are, or have been physical barriers gene flow within the habitat. The impact of physical barriers on gene flow is further supported by the negative relationship between landscape cost distances and genetic distances (Figure 3.9B).

Beyers' model (2001) was chosen to estimate dispersal distances because it applies a biologically derived movement algorithm to data parameterized with actual movement estimates. Simply using distances traveled in the mark and recapture study multiplied over the life time of an individual overestimates dispersal because it assumes that the organisms move constantly in one direction. In contrast, a standard stepwise diffusion model would assume that each step was taken in a completely random direction, leading to an underestimate of the distance moved. Beyers' model (2001) is based on the observation that many species of insects and other invertebrates take each step in a direction dependent on the direction of the previous step and have a low probability of turning 360 degrees. Assuming that *V. annecohenae* behave similarly to other invertebrates, which is realistic, this model likely provides dispersal estimates that are more biologically realistic than would the other approaches.

Mark and recapture studies in marine organisms are limited because of the three dimensions of the aquatic habitat and because techniques are difficult to implement underwater. Because *V. annecohenae* is primarily benthic, comes to baited traps, and moves an average of two to five meters in 24 hrs, the mark and recapture method was successful for this species.

Gene flow, measured using molecular markers, has been used with increasing frequency in recent studies to identify patterns of dispersal in marine systems (Shanks et al. 2003). However, depending on the scale of genetic variation, local habitat variables may be overlooked as dispersal barriers because their effect is not represented by genetic divergence. In my study, genetic structure appears to be most related to water currents entering through the southern cut in the reef, across to Twin Caye. The assumption would be that water current is the factor influencing dispersal within *V. annecohenae*, but without the detail provided in this study, sandy and sparse seagrass habitats would be overlooked as barriers to dispersal.

The level of genetic isolation between the 'Northern' and 'Southern' populations is strong and very distinct considering their close proximity. The population divisions are most unexpected in regions where the sampling locations are extremely close together, within a few hundred meters. For example, individuals from the site located just south of South Water Caye, within 200 m of the shoreline, have the 'Southern' genetic signature, whereas *V. annecohenae* collected from a site only 300 m north-west have a distinct 'Northern' signatures (Figure 3.7). The two other locations that appear to be near this transition zone between genetic populations include the location just south-east of Twin Caye, which has a 'Northern' signature, and the point north of Twin Caye, which has a 'Southern' genetic signature. In each of these three cases, the neighboring sampling locations are within 300 m, yet have distinct genetic signatures. Between divergent sites near South Water Caye there is a

sandy channel only two to three meters wide created by strong currents flowing off the shallow areas between South Water Caye and the reef. It is very probable that this channel provides a large enough barrier to allow the persistence of distinct populations despite the close proximity of the two sites. The 'Southern' signature of individuals from the site just north of Twin Caye can be explained by the least cost path analysis which indicates that this site is distinctly divided by physical barriers from the nearby sites that fall out genetically in the 'Northern' population (Figure 3.6). Additional sampling and genetic analysis of *V. annecohenae* collected from sites near these boundary regions may provide additional insight into the specific barriers responsible for limiting gene flow. Analyses of more loci may also show whether or not there is some inter-population gene-exchange at bordering sites.

The negative relationship between least cost distances and genetic distances between sites in the 'Northern' and 'Southern' populations (Figure 3.9B) supports the hypothesis that the physical habitat factors of water depth, flow, and seagrass density significantly impact the dispersal of *V. annecohenae*. On the other hand, this relationship is supported by observations from the habitat-specific mark and recapture studies showing that movement is very reduced across grassbed boundaries. The least cost path analysis also provides insight into why the site immediately north of Twin Caye has a 'Southern' genetic signature and may explain why the site just to the south-east of Twin Caye (TC) has a 'Northern' signature, since it appears costly to reach from the nearby 'Southern' sites.

In addition to providing the forum for a cost analysis, the GIS analysis for this region also provides a template for overlaying habitat, distribution and genetic patterns. Having a high resolution map of my study region that is spatially referenced allowed me to locate specific sampling areas and to infer, more accurately, habitat conditions in regions that were not sampled. This type of expanded inference yields a

much better overall understanding of dispersal and gene flow at the landscape level. Of course, the resolution of verification for habitat assignment could be further augmented to yield even better classifications within the GIS analysis. However, the visualization of my data across the landscape provides a dimension that cannot be captured in genetic by geographic distance regressions or phylogenetic trees alone.

As a permanent database, this GIS analysis could be expanded in numerous ways. Spatially referenced satellite imagery of surrounding regions would extend the region of inference for this study. Distributional or genetic data collected on competitors or predators of *V. annecohenae* could be overlaid upon this database for comparative analyses. Furthermore, within this regional reef habitat, between 10 and 13 species of bioluminescent ostracods co-exist. It has been demonstrated that some, and probably all, of these species partition the reef habitat at a fine scale (Morin and Cohen 1991, Gerrish and Morin *in prep*) but their larger distributional patterns are unknown. All of the additional nine to 12 species are mainly found in specific microhabitats within reef habitats, which means that their dispersal corridors may be even more limited than those of *V. annecohenae*.

The presence of two distinct genetic populations and the clear indication of physical barriers to both gene flow and dispersal within this study area could also indicate the presence of cryptic species. And, if bioluminescent displays play a role in speciation, which we expect, there is the potential for rapid divergence due to assortative mating. A clear test to determine if the 'Northern' and 'Southern' populations are true biological species would be to attempt to mate individuals reciprocally between populations. While apparent display differences have not been observed, quantitative analyses have only been conducted on the pulse and train characteristics of the 'Southern' population (Rivers and Morin *in press*).

The integration of multiple types of data regarding *V. annecohenae* within the seagrass bed habitats of Belize has yielded crucial habitat information for conservation. It has also provided the basis for posing questions relating to speciation within bioluminescent ostracods and a foundation for future work on the genetics within these groups.

In general, management efforts have been moving towards using GIS for conducting complex spatial statistics, visualizing recommendations for conservation and integrating large data sets (Johnston 1998, Michels et al. 2001, Lourie and Vincent 2004). However, the idea of establishing a GIS analysis focused on a single species is somewhat new (Ray et al. 2002). To embrace this approach will require detailed knowledge of life cycles, genetics, habitat interactions and the physical habitat of the target species. A single-organism GIS model, like the one presented here, provides a platform for eventually building complex spatial models that integrate attributes from multiple organisms at multiple spatial scales.

ACKNOWLEDGEMENTS

Thank you to Gary Gaston and Anastasia Ballas for sharing their grassbed data and imagery. Thanks to Steve Bogdanowicz for his assistance with microsatellite development and to Kelly Zamudio, Jeanne Robertson and Krystal Rypien for assistance in genetic analysis. Colleen Kearns was instrumental in the completion of the genetics. I thank the staff at International Zoological Expeditions, my boat captains, Victor Escobar, Michael Pipersburg and Pete Avilez; and Jennifer Hall and John MacDougal. Thank you to Nelson Hairston Jr. and James Morin for comments on project development, analyses, and this manuscript. Funding for this project was provided by the Cornell University Mario Einaudi Fund, the Lerner Grey Fund for Marine Science, and the Andrew W. Mellon Foundation. All work was completed in accordance with permits obtained from the Belize Department of Fisheries.

REFERENCES

Adams A.J. and J.P. Ebersole. 2002. Use of back-reef and lagoon habitats by coral reef fishes. Marine Ecology Progress Series 228: 213-226.

Ballas A. and G.R. Gaston. 2006. Use of remote sensing to analyze *Thalassia testudinum* communities in the South Water Caye Marine Reserve, Belize, Central America. Belize National Marine Science Symposium. January 18-20, 2006. Belize City, Belize, Central America. Submitted.

Beyers J.A. 2001. Correlated random walk equations of animal dispersal resolved by simulation. Ecology 82: 1680-1690.

Bohonak A.J. 1999. Dispersal, gene flow, and population structure. The Quarterly Review of Biology 74: 21-45.

Butler M.J.IV. and W.F. Herrnkind. 1997. A test of recruitment limitation and the potential for artificial enhancement of spiny lobster (*Panulis argus*) populations in Florida. Canadian Journal of Fisheries and Aquatic Science 54: 452-463.

Cohen A.C. 1983. Rearing and postembryonic development of the myodocopid ostracode *Skogsbergia lerneri* from coral reefs of Belize and the Bahamas. Journal of Crustacean Biology 3: 235-256.

Cohen A.C. and J.G. Morin 1990. Patterns of reproduction in ostracods: a review. Journal of Crustacean Biology 10: 184-211.

Evanno G., S. Regnaut, and J. Goudet 2005. Detecting the number of clusters of individuals using software STRUCTURE: a simulation study. Molecular Biology 14: 2611-2620.

Falush D., M. Stephens, and J.K. Pritchard 2007. Inference of population structure using multilocus genotype data: dominant markers and null alleles. Molecular Ecology Notes 7: 574-578.

Felsenstein J. 2007. PHYLIP (Phylogeny Inference Package) version 3.67. Distributed by the author. Department of Genome Sciences, University of Washington, Seattle.

Gerrish G.A. and J.G. Morin. *In press*. The life cycle of a bioluminescent marine ostracod, *Vargula annecohenae* [Cypridinidae, Myodocopida]. Journal of Crustacean Biology.

Gerrish G.A. and J.G. Morin. *In prep*. Living in 'sympatry': coexistence through microhabitat and temporal niche partitioning.

Gerrish G. A., J. G. Morin, T.R. Rivers and Z. Patrawala. *submitted*. Darkness as an ecological resource: the role of light in partitioning the nocturnal niche. Oecologia.

Goudet J. 2002. FSTAT, a program to estimate and test gene diversities and fixation indices (version 2.9.3.2). Available from http://www.unil.ch/izea/softwares/fstat.html.

Grantham B.A., Eckert G.L. and A.L. Shanks 2003. Dispersal potential of marine invertebrates in diverse habitats. Ecological Applications 13 Supplement: S108-S116.

Hamilton M.B., E.L. Pincus, D.Fiore A, and R.C. Fleischer 1999. Universal linker and ligation procedures for construction of genomic DNA libraries enriched for microsatellites. Biotechniques 27: 500-2, 504-7.

Holt R.D. and R. Gomulkiewicz. 1997. How does immigration influence local adaptation? A reexamination of a familiar paradigm. American Naturalist 149: 563-572.

Jarne P. and P.J.L. Lagoda 1996. Microsatellites, from molecules to populations and back. Trends in Ecology and Evolution 11: 424-429.

Johnston C.A. (ed.) 1998. Geographic Information Systems in Ecology 1. Blackwell Science Ltd. Victoria, Australia.

Kenworthy W.J. and G.W. Thayer 1984. Production and decomposition of the roots and rhizomes of seagrasses *Zostera marina* and *Thalassia testudinum* in temperate and subtropical marine ecosystems. Bulletin of Marine Science 35: 364-379.

Lenormand T. 2002. Gene flow and the limits to natural selection. Trends in Ecology and Evolution 17: 183-189.

Lourie S.A. and A.C.J. Vincent 2004. Using biogeography to help set priorities in marine conservation. Conservation Biology 18: 1004-1020.

Lubchenco J., Palumbi S.R., Gaines S.D. and S. Andelman 2003. Plugging a hole in the ocean: the emerging science of marine reserves. Ecological Applications 13 Supplement: S3-S7.

Michels E., Cottenie K., Neys L., De Gelas K., Coppin P. and L. De Meester 2001. Geographical and genetic distances among zooplankton populations in a set of interconnected ponds: a plea for using GIS modeling of the effective geographical distance. Molecular Ecology 10: 1929-1938.

Morin J.G. and A.C. Cohen 1991. Bioluminescent displays, courtship and reproduction in ostracodes. in Crustacean Sexual Biology. (eds.) Bauer R.T and J.W. Martin. Columbia University Press, New York, NY.

Nei M. 1978. Estimation of average heterozygosity and genetic distance from a small number of individuals. Genetics 89: 583-590.

Palumbi S.R. 2003. Population genetics, demographic connectivity and the design of marine reserves. Ecological Applications 13 Supplement: S146-S158.

Pritchard J.K., M. Stephens and P. Donnelly 2000. Inference of population structure from multilocus genotype data. Genetics 155: 945-959.

Rambaut A. 2006. FigTree. Version 1.0. Available from: http://tree.bio.ed.ac.uk/software/figtree/

Ray N., A. Lehmann and R. Joly 2002. Modeling spatial distribution of amphibian populations: a GIS approach based on habitat matrix permeability. Biodiversity and Conservation 11: 2143-2165.

Rivers T.J. and J.G. Morin. *In press*. Complex sexual courtship displays by luminescent male marine ostracods. Journal of Experimental Biology.

Shanks A.L., Grantham B.A. and M.H. Carr 2003. Propagule dispersal distance and the size and spacing of marine reserves. Ecological Applications 13 Supplement: S159-S169.

Torres E. and J.G. Morin. 2007. *Vargula annecohenae*, a new species of bioluminescent ostracode (Myodocopida: Cypridinidae) from Belize. Journal of Crustacean Biology 27:649-659.

CHAPTER 4

LIVING IN 'SYMPATRY': COEXISTENCE THROUGH MICROHABITAT AND TEMPORAL NICHE PARTITIONING

ABSTRACT

Species specific mating calls or signals often vary among closely related species living in sympatry. Reproductive displays of bioluminescent ostracods inhabiting the corals reefs throughout the Caribbean are a dramatic example. Up to eight species conduct nightly reproductive displays over a single coral patch. Here we demonstrate how three of the most abundant species within a Caribbean patch reef habitat vary morphologically and in display characteristics, including, the timing of display initiation and the timing of peak display activity. Adult males of each of the three species are morphologically distinct based on carapace length and height, eye size and keel width. In addition to varying in direction, their bioluminescent displays differ in the duration of the pulses, timing between pulses and the interpulse distances. Although displays of the three species do overlap occasionally, each species seems to preferentially display in a separate microhabitat of the patch reef and initial display times and peak display times are slightly offset.

KEYWORDS: bioluminescence, ostracod, *Vargula*, niche partitioning, reproductive display

INTRODUCTION

Courtship displays, which include calling or signaling, directly influence the ecology and evolution of participating species. To maximize the visibility or audibility of visual or vocal courtship displays, organisms often move into habitats

that are used exclusively during mate attraction and copulation. For example, some frog species climb to elevated perches before calling (Höbel and Gerhardt 2003), male fireflies perform their bioluminescent displays while flying (Lloyd 1968), and lekking Bowerbirds perform their courtship behaviors in extravagant and obvious bowers, which are not used for nesting (Pruett-Jones and Pruett-Jones 1982). While these behaviors are required for successful reproduction, they also expose participating individuals to numerous ecological interactions that only occur during courtship. For example, frog-eating bats cue in on mate attraction calls by frogs (Ryan et al. 1982). If the courtship arena is shared, individuals must compete not only with conspecifics, but with related species for optimal display habitats and signal recognition. Unintended interference of courtship, due to displays by related species, may have negative effects on reproductive success (Schwartz and Wells 1983), especially in locations where closely related species co-occur. When display overlap interferes with successful mate finding in either species, the ecological boundaries in which courtship takes place are pushed to expand. Individuals courting in new locations, altering display timing, or showing a varied signal may maximize their reproductive fitness by differentiating themselves from related signaling species.

In the western Caribbean Sea, above a single coral patch, the males of as many as eight species of bioluminescent ostracods enter the water column above the reef and simultaneously perform their nocturnal courtship displays in close proximity (Morin and Cohen 1991). At first sight, the displays appear as an intermixed dynamic light show made up of rapid flashes and slow-pulsed trains of light. However, upon careful observation the unique display patterns of each species become clear and, based on the displays alone, one can identify individual species, define in which microhabitat they are likely to be found, and predict how abundant displays are likely to be at a given time. Within this system, multiple displaying species live in sympatry. Whereas each

species resides, forages and burrows primarily in the benthos, males enter the water column above the coral and accompanying interspersed sand areas to conduct bioluminescent displays. To investigate how coexisting species share this courtship arena, we focused on three bioluminescent ostracod species, documented variation in morphology, display type, and compared their locations and timing of signaling behaviors.

MATERIALS AND METHODS

Six species of displaying bioluminescent ostracods are regularly observed amid the patch reefs of the shallow back reef region immediately south of South Water Caye, Belize (16.811782° N, -88.082533° W). In the present study, we chose to focus on quantifying morphological and behavioral variation for the three most abundantly displaying species of bioluminescent ostracods within this shallow (< 4 m) patch reef area. All belong to closely related clades within the family Cypridinidae. We use the abbreviations given in Cohen and Morin (1993) for two undescribed species: 1) a slow upward displaying species (medium wide uppers = MWU) and 2) a lateral displaying species (massed shallow horizontals = MSH), both of which belong to an undescribed genus that Cohen and Morin (1993) termed *Group-H*. The third species studied, *Vargula morini* Torres and Cohen (2005) was referred to as VFF (very fast flasher) in Cohen and Morin (1993).

The three less abundant species that share this patch reef habitat are: (1) *Kornickeria hastingsi carriebowae* Cohen and Morin, (2) an un-named zig zag upward displaying species (H-Group, species ZZU), and (3) a bright slow downward displaying species (H-Group, species BSD) (Cohen and Morin 1993). *K. hastingsi carriebowae* is moderately abundant and conducts nocturnal displays consisting of rapid upward trains of closely spaced light pulses in the very shallow crests of the

coral (Cohen and Morin 1993, unpublished data). Its displays commence close to the substrate and are most abundant over the shallowest patches of coral and near the crest of the forereef (unpublished data). ZZU displays are rare in the study area, occurring on the deeper sloping areas of the coral. Their displays extend from the substrate upward 1 – 2 m into the water column with rapid, closely spaced pulses (unpublished data). BSD are the last to begin displaying on the reef and can occur in moderate densities but seem to vary in abundance among nights. They produce a downward pulsing display among the upper coral heads and sloping regions of the reef. They peak in abundance as most of the other species' displays decrease (unpublished data).

Specimens of the three focal species, MWU, MSH, and *V. morini* were collected by sweeping a net (150 μm mesh) through multiple bioluminescent displays of each single type. Separate nets were used to collect each species and because the three species co-occur, occasionally, but rarely, a male from a non-focal species was caught. After collection, at least 10 captured individuals of each focal species were measured for carapace length and height, eye size (measured as the pigmented portion of the eye at maximum width), and keel width (Figure 4.1A) using a dissecting microscope (Wild M5) equipped with an ocular micrometer, at 50× magnification. Twenty additional males of each species were measured for carapace length and height. Photomicrographs were then taken of live representatives of each species using the dissecting microscope and a Nikon Coolpix 4500. All individuals measured from each species were preserved in 95% ethanol and labeled as reference specimens for this study and for future descriptions of the undescribed species.

The bioluminescent displays of each species were recorded using a VHS camcorder (Panasonic PV-100) with night vision detection (Night Invader 3000, B.E. Meyers & Co., Inc.) housed in an underwater casing (Sea-Recorder, JayMar, Inc.).

Figure 4.1. Three common male cypridinid ostracods from Belize. A. MWU is a large bodied *H-Group* species with a wide keel. Its carapace looks slightly red in color. Labels indicate the locations of the lateral eye, gut, light organ and keel. B. MSH is another *H-Group* species that is much smaller than either MWU or *V. morini.* Its body has much lower height relative to its length. C. *V. morini* is large bodied with a round shape, very clear and non-pigmented carapace, and a more pointed keel.

A.

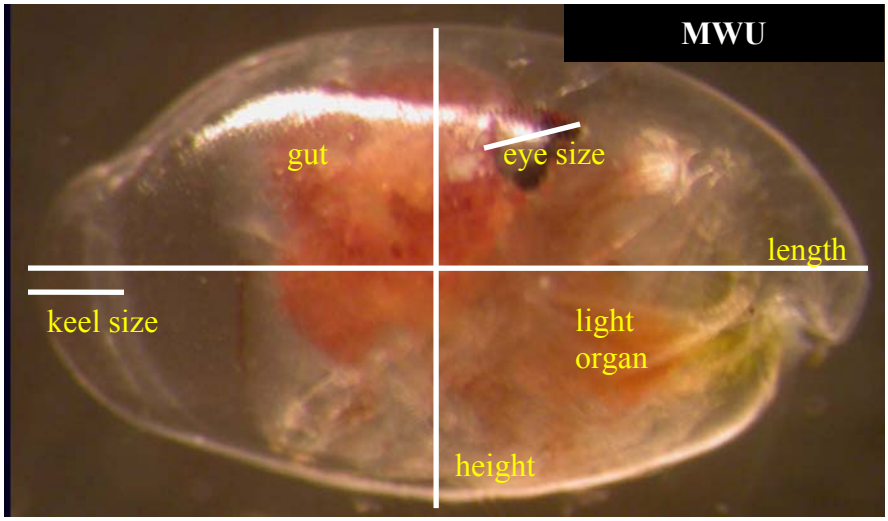
MWU
gut
eye size
length
keel size
light
organ
height

B.

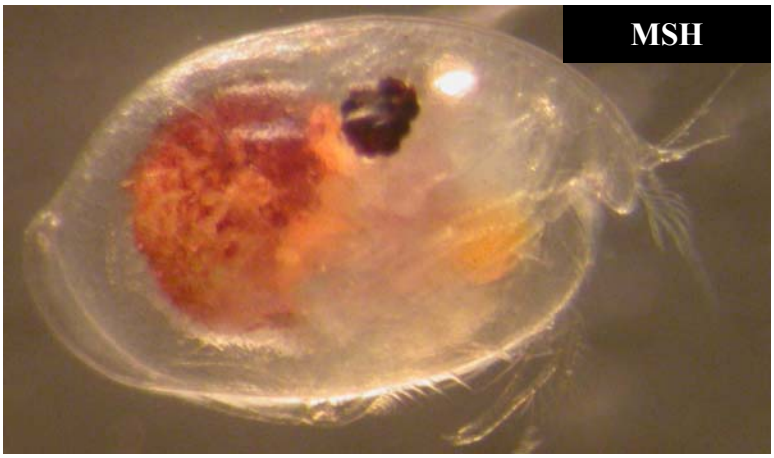
MSH

C.

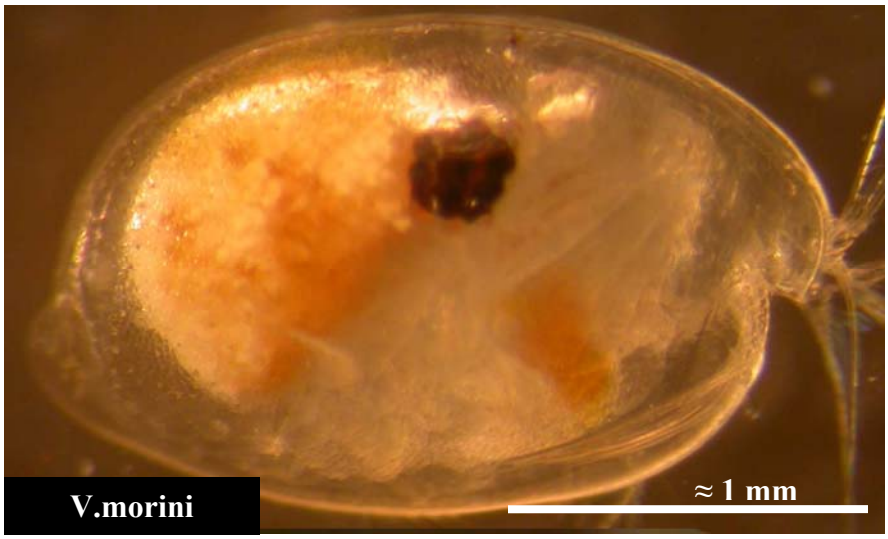
V.morini
≈ 1 mm

Displays of individuals of each species were recorded on either a patch reef area south of South Water Caye or on the nearby patch reefs just north of Carrie Bow Caye. Frame by frame analysis was used to measure the number of bioluminescent pulses, pulse duration, interpulse interval, and interpulse distances for each species' display.

The number of displays per unit time within an area for each species was estimated in two ways. First, to obtain an estimate of the number of displays per square meter, a series of counts were conducted on two consecutive nights, at three reef positions, during three time periods each night. To estimate display density, we counted the number of displays of each species that crossed any portion of a quarter meter quadrat (set upon the substrate) within a two minute period. First, a display count was conducted upon the shallow region of the of the patch reef (1-2 m water depth). Then, the quadrat was moved to the slope of the patch reef (2-3 m depth) and another two-minute count was conducted. Finally, the quadrat was placed in a sandy channel between corals (3-4 m depth) and again, displays were counted for two minutes. All observations were made by a single observer. After completion of counts in all three regions, the quadrat was moved back to the shallow region and the series was repeated; a total of three sets of consecutive counts were made. This procedure encompassed ca. 50 minutes each night and took place on 17 and 18 January, 2007. Because the density of displays changed over the course of the evening, the three sets of counts were compared as three separate time periods: early, middle and late in the evening display period. Display density values were averaged for each of the three species across the two nights. This technique, although it provided good estimates of the relative densities of each species in the three habitats sampled, only gave an approximate estimate of true densities because it did not adequately account for the highly patchy distribution of displays throughout the reef habitat.

Our second method of collection focused on documenting how display densities of the three focal species (MWU, MSH, and *V. morini*) changed over time within the display period. To estimate both density and patchiness of displays quantitatively, three observers moved (by snorkeling) constantly above the coral microhabitats and 'captured' displays as each swam through a localized sampling area (ca. 15m × 15m). Sampling included both a search element and a capture element. Observers swam at the surface, searching for displays in contiguous habitats where displays might be expected. When a display was observed, we dove down to 'capture' the display by passing an open corrugated plastic ring through the water so that the bioluminescent display passed through the ring; however, because there was no net, no males or females were caught. The males' displays may have been interrupted momentarily by being 'captured' in this way, but the male remained in the water column to contribute future displays; therefore sampling did not involve removal. This procedure did not affect the rate of signaling. We quantified the number of displays 'captured' in a two minute period and then rested at the sea surface approximately three minutes before starting the next collection. This procedure resulted in a two minute sample approximately once every five minutes and continued for ca. 95 minutes of the display period (ca. 19 samples/night/species). To minimize the effect of observer bias, each observer rotated to collect a different one of the three focal species during each of the three nights of sampling, 5 January through 7 January, 2007. We chose our sampling nights to begin two days following the full moon so that during the sampling period (20:00 - 22:00) the moon would be absent from the sky. Therefore, the start time for displays was dictated by dark conditions following the setting of the sun and not moonset. The timing of first display for each of the three focal species was recorded and two-minute sampling intervals were initiated immediately after the first display of the first species was observed.

RESULTS

The three focal species are clearly differentiated by morphological features including carapace length and height, eye diameter and keel width (Figures 4.1 and 4.2). MSH is much smaller than either MWU or *V. morini* and, on the length-to-height regression, is tightly clumped far from the other two species (Figure 4.2A). MWU and *V. morini* overlap slightly in carapace length and height, however, *V. morini* is slightly smaller than MWU (Figure 4.2A). When length, height, eye size, and keel width were evaluated using a discriminant function analysis, each species was quantitatively differentiated based on two factors (Figure 4.2B). Length made up most of factor one while keel size dominated factor two (Table 4.1). *V. morini* is rounder in shape with a very small keel at the postero-ventral of its carapace while MWU is boxier in appearance with a large, wide keel (Figure 4.1C).

The displays clearly varied among species in train pattern and train direction, pulse duration and intensity, interpulse intervals and interpulse distances (Figure 4.3, Table 4.2). Each species' display included features similar to those of already described bioluminescent ostracod species. Characteristics include an initial rapidly changing series of pulses and a terminal series of more similar pulses (referred to as the initial or shortening phase and the trill phase respectively by Morin [1986] and Morin and Cohen [1991]). Within this context there is a tendency, especially in the first few pulses (initial phase), for 1) the pulse duration to become progressively shorter within the train of pulses, 2) a progressive decrease in the both interpulse interval and interpulse distance, 3) the brightness of successive pulses to decrease. The terminal trill phase almost always shows a more consistent pattern of pulse duration, interpulse interval and distance, intensity and linear direction, which is demonstrated by a close correspondence to a particular linear regression equation (Figure 4.3). The slow vertical upward display of the medium wide upper (MWU)

A.

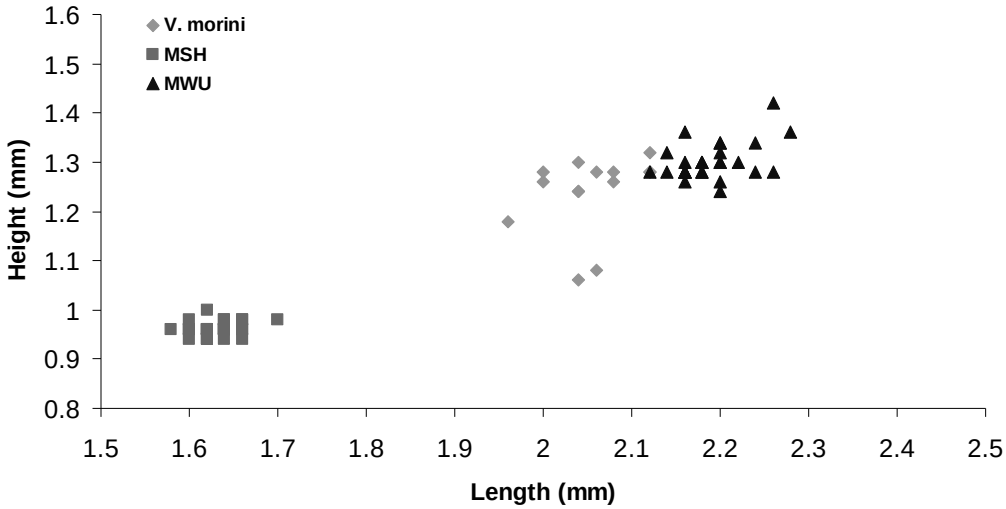

B.

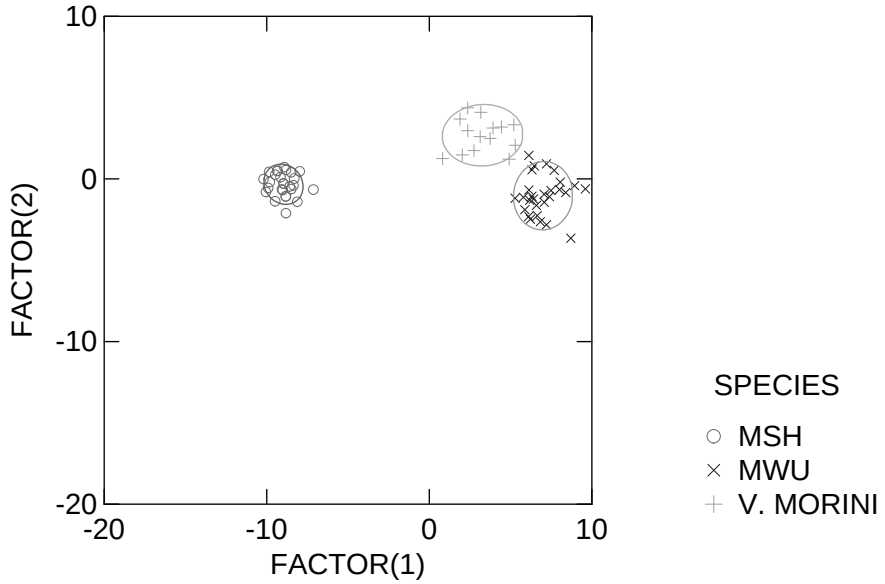

Figure 4.2. A. Length to height regression of MWU, MSH, and *V. morini*. B. Principle components canonical scores for MWU, MSH and *V. morini* based on length, height, eye size, and keel width.

Table 4.1. Average sizes and standard deviation of measurements for each species. And loadings for factors one and two in the discriminant function analysis. Need to give N

	V. morini	MSH	MWU	Factor 1	Factor 2
Length (mm)	2.054 ± 0.048	1.631 ± 0.026	2.19 ± 0.039	0.949	0.106
Height (mm)	1.239 ± 0.079	0.961 ± 0.016	1.302 ± 0.037	0.300	0.523
Eye (mm)	0.217 ± 0.023	0.184 ± 0.016	0.176 ± 0.026	-0.204	0.428
Keel (mm)	0.104 ± 0.022	0.069 ± 0.013	0.17 ± 0.017	-0.160	-1.036
Canonical					
Group Means					
Factor 1	3.287	-8.967	7.004		
Factor 2	2.689	-0.324	-1.032		

Figure 4.3. Time-distance relationships of a single representative bioluminescent display train from MWU, MSH and *V. morini*. Arrows represent the orientation in the water column of each species' display. Since light producing chemicals are secreted from the male and hang motionless at a discrete depth in the water column, they are represented by bars that extend over time but do not move in distance. Regions where the bars (= pulses) occur at the same time within a species' train indicate that multiple pulses overlap temporally as the males swim up through the water column. Each linear regression equation represents the 'apparent' swimming speed (cm/s) for the trill phase of each species. Regression coefficients indicate that the 'apparent' swimming speed did not vary through the trill phase.

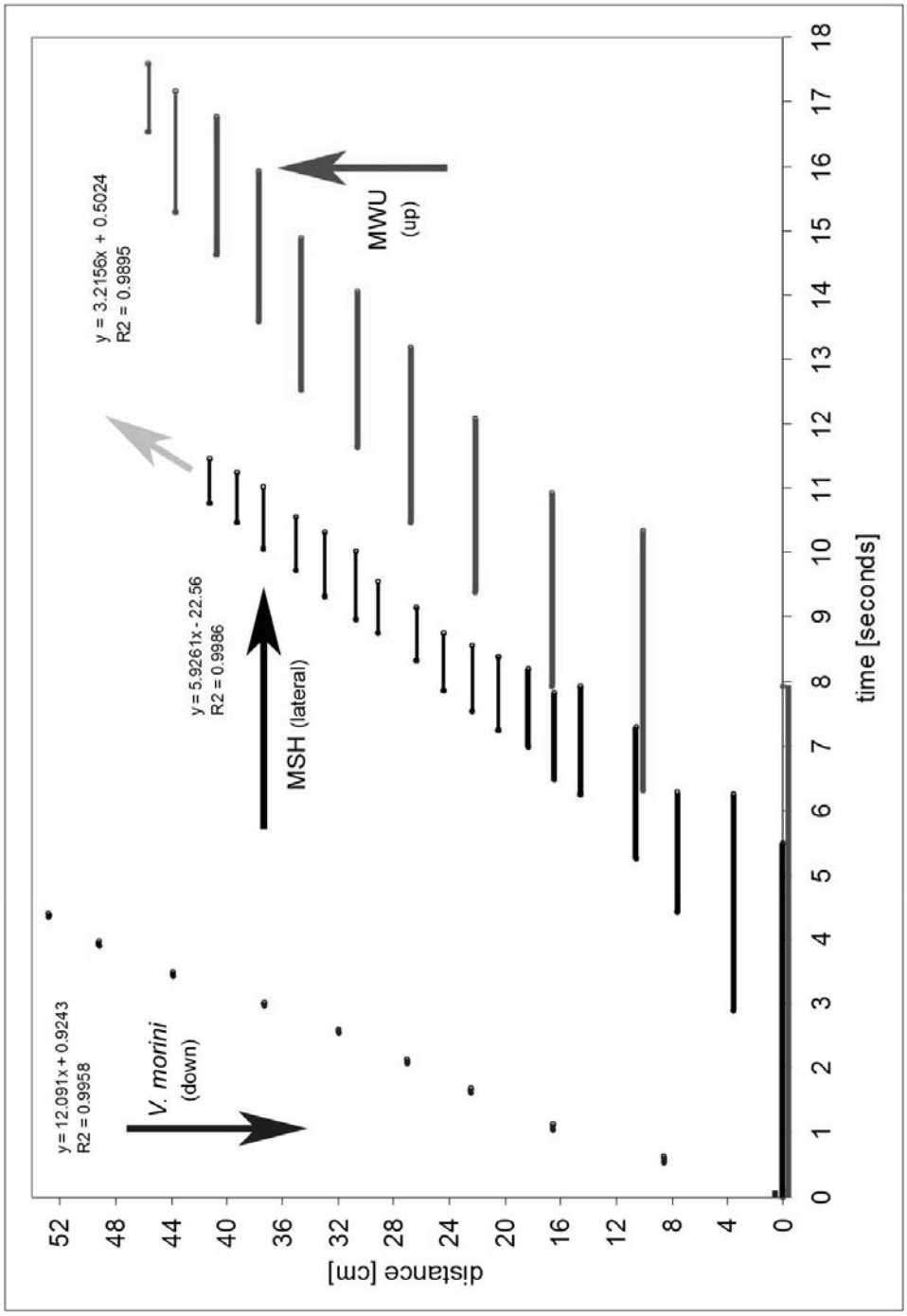
y = 12.091x + 0.9243
R2 = 0.9958
V. morini
(down)
y = 5.9261x - 22.56
R2 = 0.9986
MSH (lateral)
y = 3.2156x + 0.5024
R2 = 0.9895
MWU
(up)
distance [cm]
time [seconds]
0
4
8
12
16
20
24
28
32
36
40
44
48
52
0 1 2 3 4 5 6 7 8 9 10 11 12 13 14 15 16 17 18

Table 4.2. Display characteristics of three sympatric species of luminescent signaling ostracodes from Belize

Characteristic \ species	MWU		MSH		*V. morini*	
descriptive name	medium wide up		massed shallow horizontal		very fast flashers	
Train characteristics						
train pattern	bright, widely spaced pulses		many closely spaced, medium-bright pulses		rapid, bright, strobe-like pulses	
train direction	Up		horizontal		down	
train duration	10-25 sec		10-20 sec		~5 sec	
train length	75-100 cm		~1-2+ m		~50-60 cm	
no. pulses per train	10-20		dozens		10-20	
initial vs trill	initial phase dominates		trill dominates		trill dominates	
Pulse characteristics						
	initial phase	terminal phase [=trill]	initial phase	terminal phase [=trill]	initial phase	terminal phase [=trill]
pulse intensity*	very bright	bright	medium bright	medium bright	bright	bright
pulse duration	2.5-10 sec	1-2.5 sec	2-6 sec	1-2 sec	100-150 msec	67-100 msec
interpulse interval	1-8 sec	1-1.5 sec	0.8-3 sec	200-500 msec	400-700 msec	400-700 msec
interpulse distance	5-20 cm	1-2 cm*	2-4 cm	1.5-2.5 cm	5-10 cm?	3-5 cm
apparent swimming speed		3.2 cm/sec		~6 cm/sec		~12 cm/sec

* = relative

* = if present

species is especially characterized by long lasting and very bright pulses (up to10 sec), and long duration displays, up to ca. 25 seconds which are moderate in length (up to 1 m). The first pulses continue glowing in the water column even as the second, third and sometimes fourth pulses are secreted. The length of pulses continuously diminished; with the final pulses being much dimmer and shorter (Table 4.2). In less than about half the trains, there is a much dimmer trill of about 5-10 closely placed (ca. 1-2cm) interpulse gaps. The distance between pulses of MWU also diminished from the initial phase of the display where pulses were usually ca. 10 cm apart (Figure 4.3).

Massed shallow horizontal (MSH) displays are produced by a male swimming at an apparent swimming speed of about 6 cm/sec in a horizontal direction and the pulses of light appear much dimmer than those of MWU (personal observation, J.G. Morin personal communication). The initial phase of 2 to 4 longer pulses (2-6 sec) quickly give way to an extended trill of fairly weak pulses (1-2 sec duration) that sometimes extend for more than two meters and consists of dozens of similarly placed pulses. In comparison with the MWU, the trill display of MSH consisted of more tightly spaced (1.5 to 2.5 cm) pulses over a similar distance. With a pulse duration of nearly 1-2 seconds, the trills may have 3 to 4 (but up to about 6) bioluminescent pulses visible in the display at a given time. They give the appearance of miniature jet airline condensation trails traveling through the water. Multiple males usually entrain on the initial male so that 2 to 8 or even 10 males spread away from each other on a horizontal plane giving the appearance of rows of luminescent dotted lines splaying away from one another.

The short pulse duration of *V. morini* creates a strobe-like appearance to their display and makes them difficult to follow, especially since they often entrain with one another. The short initial phase of 2-3 pulses is not radically distinct from the trill.

Males swim downward at an apparent swimming speed of about 12 cm/sec and flash once every 5-10 cm in the beginning and 3-5 cm at the end of their display. The first pulses are a little over 100 msec duration while the later, trill pulses are fairly uniform between 67 and 100 msec. The interpulse distances of the trill range from 3 to 5 cm and the interpulse intervals are 0.4 to 0.7 sec so that, with the extremely short duration of each light pulse for *V. morini*, there are no times in which multiple pulses are simultaneously visible. Within this species, individuals have a strong tendency to entrain on one another so that a 2 m^2 area may have a rapidly "blinking," seemingly random, scintillating appearance.

Using only the fairly uniform trill portion of the displays, we calculated the 'apparent' swimming speed (Rivers and Morin *in press*) of each species during a display. This calculation accounts only for the distance between light pulses and does not take into account any swimming patterns. Rivers and Morin (*in press*) have shown that during a display, males of the nearby grassbed species *V. annecohenae* swim in a helical pattern. Therefore, the apparent swimming speed in this species is likely to be only two thirds of the actual swimming speed. Using dim red light in the field habitat, we have observed that these three species also swim in a helical pattern meaning that the actual swimming speed is higher than the speed indicated from light production alone. The 'apparent' swimming speed for *V. morini* (ca. 12 cm/sec), is two times higher than that observed for MSH (ca. 6 cm/sec) and almost four times that of MWU (ca. 3 cm/sec). In addition, for each species, the swimming trajectory during the trill was strongly linear (*V. morini*: $r^2 = 0.996$, MSH: $r^2 = 0.999$, MWU: $r^2 = 0.990$) indicating that males probably maintained not only a constant swimming speed but also a constant swimming pattern throughout the trill part of the display.

The order of appearance and location of the displays for each species on a clear calm night was highly consistent. Our quantitative sampling, which took place on

three clear calm nights in early January 2007, represents the order of appearance and timing most commonly observed by researchers starting in 1988 in Belize (personal observation, J.G. Morin, A.C. Cohen and T.J. Rivers: personal communication). The first species to display each night was MWU which began, for three successive nights from 5-7 January 2007, at 18:17 (45 min post-sunset at17:32), 18:18 (46 min post-sunset at 17:32), and 18:16 (43 min post-sunset at 17:33). MWU displays dominated the shallow areas (1 - 1.5 m) near the tops of the reefs (Figure 4.4, Figure 4.5). Few MWU displays were observed over sandy regions and those that did occur over sand areas were only in the upper part of the water column (Figure 4.4). The density of MWU displays increased rapidly within the first five minutes and continued to increase until peak densities were reached between 12 to 18 minutes after they commenced (Figure 4.6). Displays remained dense for 40 to 45 minutes and then decreased over the subsequent hour (Figure 4.6).

MSH was consistently the second species to begin their displays. They were first observed just prior to the peak in activity of MWU: 18:24 (52 min post-sunset) the first night, 18:25 (53 min post-sunset) the second night and 18:25 (52 min post-sunset) the third night. MSH displays took longer (between 20 and 25 min) than those of MWU to reach peak intensity: by 18:45 on 5 and 6 January and 18:50 on 7 January. They remained highly active for 15 - 20 min before showing a steady decline over the subsequent hour (Figure 4.6). MSH displays were only observed over regions where some sand was present (Figure 4.5). They were most abundant over the large sandy channels located between coral areas but were also found over small sand deposits that occasionally occur nestled within pockets in the coral mounds (Figure 4.4). The MSH displays occurred primarily between one and four meters in water depth, depending on the presence of a sand channel. Entrainment was persistent and pervasive in MSH. Displays regularly began at a given narrow depth horizon as a single line of light

Figure 4.4. Spatial representation of the relative positions on patch reef of displays by MWU, MSH and *V. morini* (Vm). A. Vertical view depiction in which darkly shaded regions represent coral areas close to the water surface (ca. 1 - 2 m depth), with each lighter shade representing deeper coral. The lightest shade represents a sand channel (ca. 3 - 4 m depth) running between the coral patches or ridges. B. Side view representation of display location within the water column above the substratum. The upper part of the image represents the water surface and shading again represents different depths of coral and sand.

A.

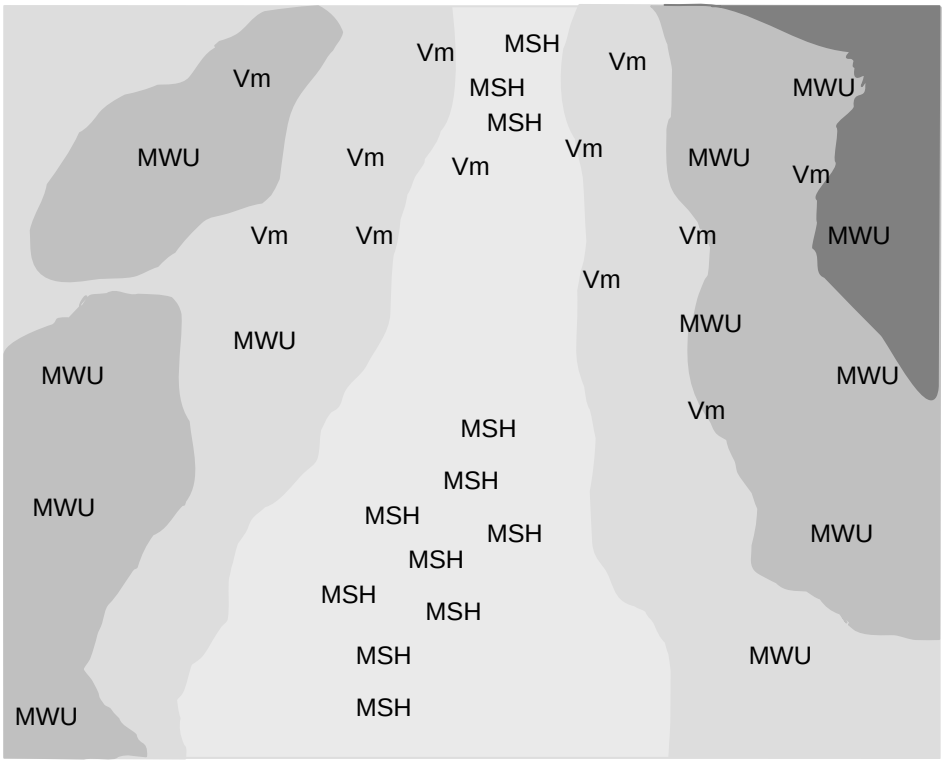
Vm
MSH
Vm
Vm
MSH
MWU
MSH
MWU
Vm
Vm
Vm
Vm
Vm
Vm
MWU
Vm
Vm
Vm
MWU
MWU
MWU
MWU
Vm
MSH
MSH
MWU
MSH
MSH
MWU
MSH
MSH
MSH
MWU
MSH
MWU

B.

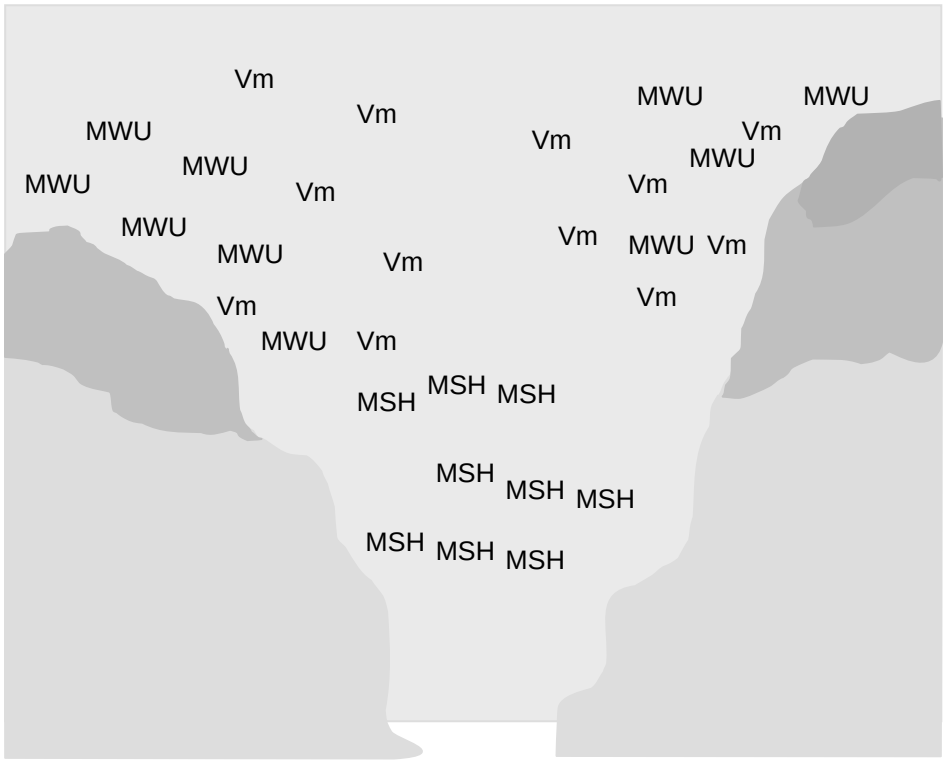
Vm
MWU
MWU
Vm
MWU
Vm
Vm
MWU
MWU
Vm
MWU
Vm
Vm
MWU
MWU
Vm
Vm
MWU
Vm
Vm
MWU
Vm
Vm
MWU
Vm
MSH
MSH
MSH
MSH
MSH
MSH
MSH
MSH

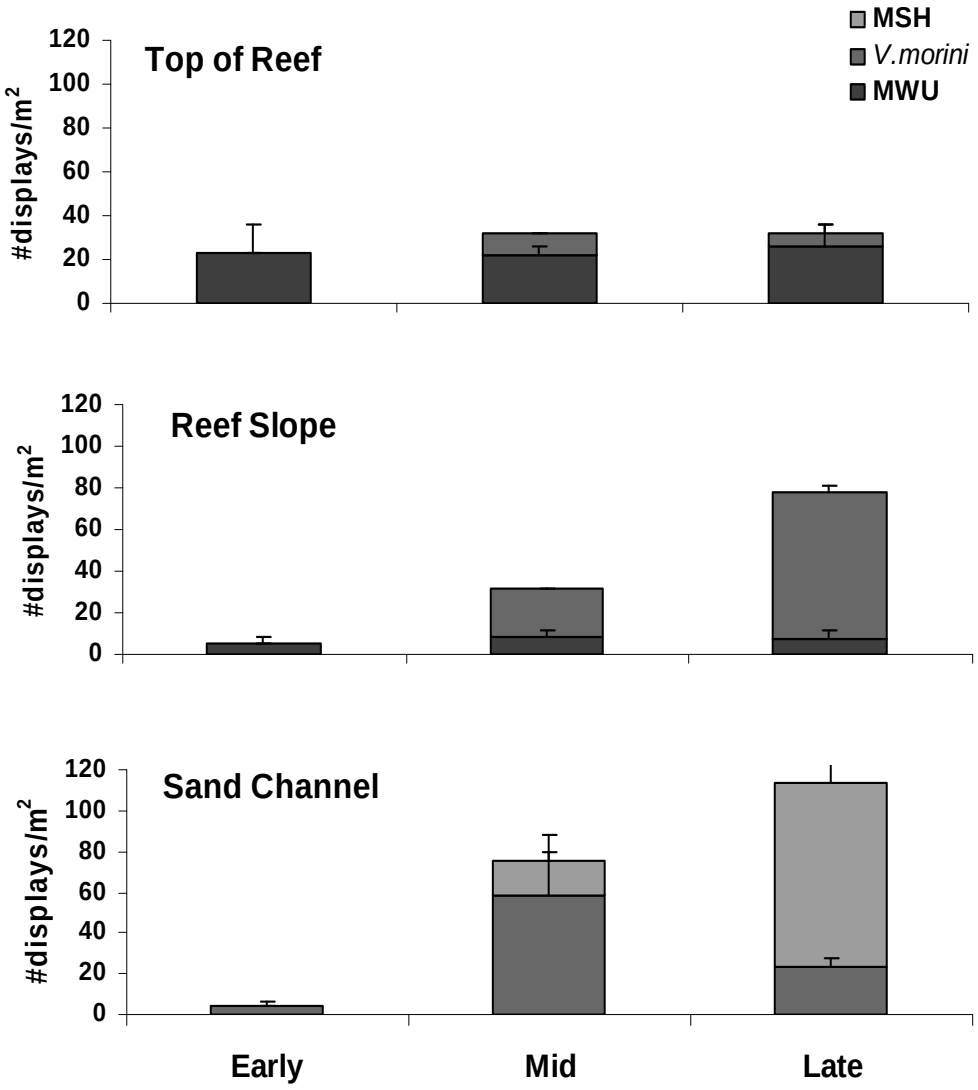

Figure 4.5. Density of displays per square meter for MWU, MSH, and *V. morini* across time periods (early = 18:38 to 18:45, mid = 18:50 to 18:55 and late = 19:00 to 19:10) and reef habitats (reef top, slope and sand channel)

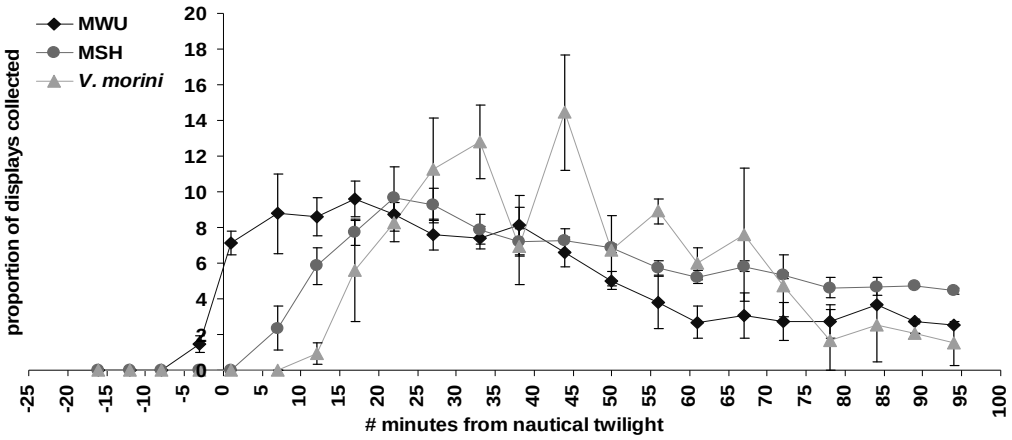

Figure 4.6. The proportion of displays occurring at a given time (out of the sum total number of displays captured in a given night). By using proportions, the variation in display density or capture rates among nights does not influence the data, providing a clear representation of changes in densities for each species throughout the display period averaged across nights.

pulses produced by one male, but was soon bifurcated or trifurcated as one or two new individuals joined to create a firework-like fan of displays as they gradually diverged and progressed through the water horizontally. Groups of entrained, displaying males would often be layered, with each group occurring 10-30 cm above or below another and their displays moving in opposing or offset directions. We often observed multiple "layers" of these displays, distributed by depth, in a single sand channel, so that they appeared overlapping when viewed from above but not from the side. Each researcher independently noted that the shallower MSH displays (1-2 meters depth) became less common later in the sampling period compared to deeper (2-3 m) displays.

V. morini was the last of the three species to begin displaying on each night. Its flashing displays were first observed over three sequential nights at 18:31 (59 min post-sunset), 18:35 (63 min post-sunset), and 18:31 (59 min post-sunset). *V. morini* also showed clear entrainment among individuals. When one display began, additional individuals commonly began displaying nearby, creating scintillating dense patches of *V. morini* displays. Because of the patchy nature of their displays and the brevity of their pulses, consistent sampling of this species was difficult. Each observer sampling *V. morini* swam a consistent route targeting the same patches of displays during each sampling period throughout the night. On the first two nights the densities sampled were comparable, but on the third night, the observer regularly sampled a high density *V. morini* patch. The occurrence of this high density patch likely reflects an overall higher abundance of *V. morini* displays on the third night. Even with this observed night to night variation, the densities measured between time points within a night still reflect consistent relative measures of activity over time. *V. morini* increased slowly in activity and maintained a moderate intensity of displays for the hour after beginning (Figure 4.6). Only on the third night did we see a slow

decline in activity during the sampling period. *V. morini* was observed in all habitats including above the corals and over the sand channels (Figure 4.5). However, it was most common on the sloping regions of the coral patches (Figure 4.4) and the depth at which its displays occurred were shallow comparable with the MWU group and above the MSH displays (Figure 4.4).

DISCUSSION

Morphological differentiation between the groups exhibiting distinct types of displays was expected based on previous observations by Cohen and Morin (1993), indicating that different display types are associated with separate species. In addition, phylogenetic data also suggest both that the *H-Group*, which includes the MSH and MWU, is a clade distinct from *Vargula,* and that there is divergence between horizontal and vertically displaying species within the *H-group* (Cohen and Morin 2003).

Bioluminescent ostracods have compound eyes capable of distinguishing both intensity of light and distance from objects (Huvard 1990). This depth of field and the fact that the displays of most ostracod species are produced from a simple luciferin-luciferase reaction that emits at a peak wavelength of 473 nm (Huvard 1990) suggests that each of these species are seeing each others' displays as they occur in overlapping or nearby reef habitats. For successful reproduction to occur, a displaying male of any one species must be seen by a con-specifc female within a water column surrounded by the displays of several other species. Termed the 'cocktail party' effect in humans (Cherry 1953), one species' courtship display is another species noise.

Each of the species' displays varied in direction, duration of pulses, interpulse intervals and distances, and 'apparent' swimming speed. The first two to four pulses of the displays of each species differed in duration and direction of placement. The

displays of each of these three species (especially apparent in MWU and MSH) have longer duration and greater spacing in their first 2 to 4 pulses compared to the end. Morin and Rivers (*in press*) characterized this initial part of the display of *V. annecohenae* as an 'alerting phase,' used to gain the attention of females (and competing males) to a conspecific male's presence. For MWU, MSH and *V. morini*, these pulses probably similarly represent an 'alerting signal' (Rivers and Morin *in press*). Furthermore, this phase is also likely to allow females and competing males to identify conspecifics, simply based on the distinctive characteristics of the first 2-4 pulses, whether the signal producer is a conspecific male or a different species. Thus the initial phase of a display provides both a means of alerting conspecifics and also a species identification signal. The remaining portion of the display, referred to as the trill, was considered by Rivers and Morin (*in press*) to be the 'orientation phase' whereby the consistent nature and specificity of the display would allow the conspecific to approach and intercept the signaler. It probably functions similarly in the species discussed here.

The divergence in timing and location of display behavior among species (Figures 4.5 and 4.6) likely represents another mechanism by which bioluminescent ostracods have evolved to reduce the impact of non-specific displays (noise) upon courtship behaviors. Courtship calls in frogs and bioluminescent displays of fireflies are often similarly divided temporally and spatially when multiple species are found in a single location (Hödl 1977, Lloyd 1966). In some frog species, deviation in calling characteristics (duration of call, pitch of call) and the location of displays has been shown to represent character displacement, limiting the possibility of producing disadvantageous hybrids (Höbel and Gerhardt 2003). Alternatively, separation of call timing and space may be driven by selection to avoid courtship interference between species.

Bioluminescent ostracods show clear and consistent differences among species in display characteristics, including timing and location of maximum displays. Regardless of whether or not this variation arises through character displacement in evolving species or through ecological interference of displays, the presence of numerous species within a habitat is likely to constrain the potential changes possible in the characteristics of bioluminescent courtship displays.

REFERENCES

Cherry E.C. 1953. Some experiments on the recognition of speech, with one and two ears. Journal of the Acoustical Society of America 25: 975-979.

Cohen A.C. and J.G. Morin 1993. The cypridinid copulatory limb and a new genus *Kornickeria* (Ostracoda: Myodocopida) with four new species of bioluminescent ostracods from the Caribbean. Zoological Journal of the Linnean Society 108: 23-84.

Cohen A. C. and J.G. Morin 2003. Sexual morphology, reproduction and the evolution of bioluminescence in ostracoda. Paleontological Society Papers 9: 37-70.

Hödl W. 1977. Call differences and calling site segregation in anuran species from Central Amazonian floating meadows. Oecologia 28: 351-363.

Höbel G. and H.C. Gerhardt 2003. Reproductive character displacement in the acoustic communication system of green tree frogs (*Hyla cinerea*). Evolution 57: 894-904.

Huvard A. L. 1990. The ultrastructure of the compound eye of two species of marine ostracods (Crustacea: Ostracoda: Cypridinidae). Acta Zoologica (Stockholm) 71: 217-223.

Lloyd J. E. 1968. A new photinus firefly, with notes on mating behavior and a possible case of character displacement (Coleoptera: Lampyridae). The Coleopterists Bulletin 22: 1-10.

Lloyd J. E. 1966. Studies of the flash communication system in Photinus fireflies. Misc. pubs. Museum of Zoology, University of Michigan (130). Ann Arbor.

Morin J.G. 1986. “Firefleas” of the sea: luminescent signaling in marine ostracode crustaceans. The Florida Entomologist 69: 105-121.

Morin J.G. and A.C. Cohen 1991. Bioluminescent displays, courtship and reproduction in ostracodes. R. Bauer and J. Martins (eds) Crustacean Sexual Biology. Columbia University Press. pp. 1-16.

Pruett-Jones M.A. and S.G. Pruett-Jones 1982. Spacing and distribution of Bowers in Macgregor’s Bowerbird (Amblyornis macgregoriae). Behavioral Ecology and Sociobiology 11: 25-32.

Rivers T.J.and J.G. Morin. *in press*. Complex sexual courtship displays by luminescent male marine ostracods. Journal of Experimental Biology.

Ryan M.J., M. D. Tuttle, and A. S. Rand 1982. Bat predation and sexual advertisement in a Neotropical Anuran. The American Naturalist 119: 136-139.

Torres E. and A. C. Cohen 2005. *Vargula morini*, a new species of bioluminescent ostracode (Myodocopida: Cypridinidae) from Belize and an associated copepod (Copepoda: Siphonostomatoida: Nicothoidae). Journal of Crustacean Biology 25: 11-24.